# THE EFFECT OF POTASSIUM FERTILIZATION ON PSYCHROPHILIC PATHOGEN SUSCEPTIBILITY AND CARBON METABOLISM OF ANNUAL BLUEGRASS

A Dissertation

Presented to the Faculty of the Graduate School

of Cornell University

In Partial Fulfillment of the Requirements for the Degree of

Doctor of Philosophy

by

David Ramsay Moody

August 2011

## ABSTRACT

*Typhula incarnata* (GSM) and *Microdochium nivale* (PSM) are important psychrophilic pathogens of cool-season turfgrasses. Existing field data suggests that K fertilization may affect disease severity, warranting additional experimentation under controlled conditions. Overwintering carbon metabolism of perennial grasses is known to affect their performance and utility. While there is some evidence that plant K status influences winter survival, the physiological basis is unclear. The goal of this project was to determine the effect of K fertilization on carbon metabolism of overwintering annual bluegrass [Poa annua var. reptans (Hauskn) Timm.] and its relationship to psychrophilic pathogen susceptibility. In a greenhouse, annual bluegrass was seeded into 30 x 10 cm diam. sand filled columns. Nitrogen (0.5 g $m^2$), K (0.5 g $m^2$), and all other plant essential nutrients were applied weekly for 90 d. Following establishment, weekly application rates of N and other essential nutrients remained constant, yet five different K treatments (0, 0.25, 0.5, 2, 3 g $m^{-2}$) were imposed for 90 d. Columns were then moved to a refrigerated room, maintained under a photosynthetically active radiation flux of ~300 µmol $m^{-2}$ $s^{-1}$, and day/night air temperature incrementally decreased every 7 d over four weeks (10/4°C, 4/-2°C, 2/-4°C, -2/-6°C). Plants were then buried under 10 cm of snow and kept under darkness at -4°C for 28 d. After thawing at 2°C, eight replicates of each K treatment were inoculated with a 5 mm agar disc taken from GSM, PSM, or sterile cultures. Columns were incubated at 2°C (40 d) then 4°C (40 d) under periodic misting and evaluated for % necrotic turf every 10 d. Survival analysis of days to 50% infection ($LI_{50}$) was used to quantify disease progression. Tissue harvested following each experimental phase was analyzed for nonacid cations, nonstructural carbohydrates, and several organic acids using gas chromatography-mass spectrometry. The experiment was conducted twice and data was pooled.

Potassium treatment significantly affected $LI_{50}$ in GSM ($Pr>\chi2 =0.007$) but not PSM ($Pr>\chi2 =0.277$) inoculated turf. While specific mechanisms remain unclear, several biochemical parameters (K, Ca, organic acid content) associated with GSM and PSM severity were impacted by K fertilization rate. In contrast to existing literature, nonstructural carbohydrate dynamics

were not strongly correlated with disease severity. Disease recovery was significantly slower for PSM inoculated turf than GSM inoculated turf. Tissue K content and cation:anion ratios increased with K fertilization rate. Overall K fertilization had a minimal impact on non-structural carbohydrate dynamics. Tissue organic acid content, particularly malate and citrate, markedly increased at greater K fertilization rates. The results of this study suggest that K fertilization significantly increases diversion of carbon resources to organic acid synthesis due to perturbations in charge and pH homeostasis associated with disparate cation/anion uptake ratios. In addition to affecting plant utility, there is a biochemical cost associated with luxury K uptake and subsequent organic acid accumulation.

## BIOGRAPHICAL SKETCH

Dave Moody was born in Hartford, CT in 1982 but grew up in Cumberland, ME. An avid golfer, a young Dave started working as a groundsman at Val Halla Golf Course in Cumberland, ME under the tutelage of Jim Hodge. Although initially this job was simply a ticket to drive strange machinery and play free golf, turfgrass management soon became a passion. While studying Biology at St. Michael's College he worked seasonally at Portland Country Club and then full-time as the second assistant superintendent for J.B. Christie in 2004. A desire to understand the biology behind turfgrass management led him to The Pennsylvania State University in 2005 to study turfgrass science with Dr. Maxim J. Schlossberg. Here he earned a M.S. in soil science in 2007. Starting in the fall of 2007, Dave began a Ph.D.at Cornell University with Dr. Frank Rossi. Once at Cornell, his interests diversified leading him to apply to the College of Veterinary Medicine at Cornell University. He will begin veterinary school in 2011, where he hopes to merge his agronomic background with large animal veterinary medicine to improve animal welfare and farmer profitability in rural farming communities. He has been blessed with excellent mentors, family members, and friends.

## ACKNOWLEDGMENTS

I would like to acknowledge my advisor Frank Rossi for his personal and academic support during the most difficult and rewarding years of my life. I would also like to thank my academic committee members Eric Nelson, Doug Soldat, Lailiang Cheng, and Neil Mattson. Thanks to Max Schlossberg for fostering my initial development as a scientist. Thanks to my roommate Ryan Higgs, friend Bob Portmess, and other friends and colleagues for many dynamic years of fun and entertainment. A special thanks to my mother and father, who provided me with a blessed life filled with good memories and endless opportunities.

## TABLE OF CONTENTS

## LIST OF FIGURES

## LIST OF TABLES

## LIST OF ABBREVIATIONS

| | |
|---|---|
| $A_{620}$ | Absorbance at 620 ηm |
| ATP | Adenosine-5'-triphosphate |
| AUCRC | Area Under Crop Recovery Curve |
| AUDPC | Area Under the Disease Progress Curve |
| BLAST | Basic Local Alignment Search Tool |
| CAD | Cation-Anion Difference |
| CEC | Cation Exchange Capacity |
| CSTC | Computed Symptomatic Turfgrass Cover |
| DGCI | Dark Green Color Index |
| $dH_2O$ | Distilled Water |
| DP | Degree of Polymerization |
| ESF | Ethanol Soluble Low Degree of Polymerization Fructans |
| EtOH | Ethanol |
| EU(s) | Experimental Unit(s) |
| F-6-P | Fructose-6-Phosphate |
| Fru | Fructose |
| G-6-P | Glucose-6-Phosphate |
| Glu | Glucose |
| GSM | Grey Snow Mold (*Typhula incarnata* Fr.) |
| IDSM | Index of Damage by Snow Mold |
| ITS | Internal Transcribed Spacer |
| JA | Jasmonic Acid |
| KWARP | Water Agar, Kanamycin, Rifampicin, Penicillin |
| $LI_{50}$ | Days of Incubation to 50% Symptomatic Turfgrass |

| | |
|---|---|
| MSTFA | N-methyl-N-trimethylsilyl-trifluoroacetamide |
| MTT | Thiazolyl Blue Tetrazolium Bromide |
| $NAD^+$ | Nicotinamide Adenine Dinucleotide |
| NCBI | National Center for Biotechnology Information |
| NSC(s) | Non-Structural Carbohydrate(s) |
| PCR | Polymerase Chain Reaction |
| PDA | Potato Dextrose Agar |
| PDB | Potato Dextrose Broth |
| PENS | Plant Essential Nutrients |
| PGA | Phosphoglucose Isomerase |
| PMS | Phenazine Methosulfate |
| PPFD | Photosynthetic photon flux density |
| PSM | Pink Snow Mold (*Microdochium nivale* Fr.) |
| RPM | Revolutions per Minute |
| Suc | Sucrose |
| TCA | Tricarboxylic Acid Cycle |
| VSTC | Visually Symptomatic Turfgrass Cover |
| WSF | Water Soluble High Degree of Polymerization Fructans |

# CHAPTER 1: LITERATURE REVIEW

## 1.1 Introduction

As social awareness of environmental issues increases, a substantial amount of research is being directed towards reducing fertilizer and pesticide applications to agricultural and landscape crops while maintaining high productivity. Because potassium (K) does not have the same stipulations attached as nitrogen (N) and phosphorus (P) regarding plant performance and environmental impact, many turfgrass managers perceive abundant K application as harmless to the plant and the environment. Although N and P have the highest potential for negatively impacting fresh water and marine ecosystems, gratuitous applications of K fertilizers may be a costly, unnecessary, and wasteful allocation of monetary and labor resources. The economic burden of K fertilization may become more significant in the future, as potash costs have increased by ~300% in the past decade (USDA, 2010).

On sand-based turfgrass sites, reference textbooks such as Carrow et al. (2001) suggests that annual K requirements can be approximated by following an N:K ratio of 1:1.45 or 1:0.83 when N is applied at rates of <167 kg $ha^{-1}$ $yr^{-1}$ or between 168 and 342 kg $ha^{-1}$ $yr^{-1}$, respectively. These annual N application rates are common in highly managed turfgrass systems; accordingly, K is applied at a rate of ~150-250 kg $ha^{-1}$ to as much as 10 ha annually, leading to a total application of ~1,500-2,500 kg golf $course^{-1}$ $yr^{-1}$. This textbook is regarded as the benchmark of turfgrass nutrient management and is utilized extensively in university turfgrass education programs. Interestingly, a recent national survey of golf courses (in press) indicates turfgrass managers utilize these guidelines.

Claims of potassium conferring increased drought, temperature stress, and wear tolerance (Shearman and Beard, 2002) are ubiquitous in textbooks (Carrow et al., 2001; Fry and Huang, 2004) and turfgrass publications, yet these statements are generally vague and poorly referenced. In an extensive literature review, Turner and Hummel (1992) examined the role of K in turfgrass establishment, cold/heat/wear tolerance, disease incidence, root growth, and color. In all cases results were inconsistent, and the specific impact of K on these parameters remains unclear.

Of particular interest, are the purported effects of K on conferring increased cold hardiness. Although the association between K fertility and winter survival is unclear, there is some evidence that abundant K applications to highly managed turfgrasses may actually be detrimental, leading to delayed spring greening (Waddington et al., 1972) and enhanced susceptibility to psychrophilic fungi (Webster and Ebdon, 2005; Woods et al., 2006). Furthermore, Tyler et al. (1981) observed that winter wheat (*Triticum aestivum* L.) grown in a hydroponic culture of 4:1 N:K ratio (0.358 μmol $L^{-1}$ K) were more cold hardy and developed hardiness more rapidly than plants grown in solutions with a N:K ratio of 1:1.25 (1.74 mmol $L^{-1}$ K).

**1.2 Essential Functions of Potassium**

Although some of the aforementioned 'whole plant' effects of K fertilization are less clear, the biochemical role of K in plants is more completely characterized. Potassium is highly mobile, is the most abundant ion in the cytoplasm, and is intimately associated with solute speciation and osmotic potential of cytosolic and vacuolar components of plant cells (Marschner, 1995). Specifically within the vacuole, K has mainly a biophysical function by regulating turgor (Leigh and Jones, 1984). Under low K conditions Na salts (Wildes and Pitman, 1975), carbohydrates (Evans and Sorger, 1966; Wildes and Pitman, 1975), and other solutes may accumulate within the vacuole to maintain vacuolar osmotic pressure as vacuolar K quenches cytosolic demands. In barley (*Hordeum vulgare* L.) grown under K limiting conditions, Pitman et al. (1968) observed root dry weight concentrations of 6 g $kg^{-1}$ K and 100 g $kg^{-1}$ reducing sugars. Reducing sugars include, *inter alia*, glucose and fructose and are characterized as reducing agents possessing a carbonyl functional group (aldehyde or ketone) that upon oxidation become a carboxyl group (Wade, 1999). As K was supplied to the plants, reducing sugar content decreased as tissue K content increased. Similarly, Nowakowski et al. (1974) observed greater reducing sugar content associated with reduced tissue K in Italian ryegrass (*Lolium multiflorum* Lam.). Increased reducing sugar content was not observed in K deficient plants grown in high

concentrations of Na (Gregory and Baptiste, 1936) or Ca (Janssen and Bartholomew, 1930). These results highlight the effect of cation nutrition on the speciation of osmotic pressure generating solutes within the vacuole.

The ability of plants to maintain vacuolar osmotic pressure and turgor utilizing an array of solutes is a brilliant demonstration of their plasticity. Plants able to utilize alternative turgor-generating solutes have a competitive advantage in K-deficient soils. Still, K concentrations in the cytosol and stroma must be closely regulated to facilitate optimal enzyme activation and regulation (Evans and Sorger, 1966; Marschner, 1995). Many K-regulated enzymes require ~50-100 mmol $L^{-1}$ cytosolic K for adequate function, far below normal tissue concentrations (Epstein, 1980). In fact, plants supplied with sufficient K generally accumulate greater tissue K than the amount required to support adequate growth and cell maintenance, termed 'luxury consumption' (Hoagland and Martin, 1933; Wildes and Pitman, 1975).

Within the cytoplasm, K has been shown to activate enzymes including those involved in glycolysis (Wildes and Pitman, 1975) and partitioning of photosynthetic triose phosphates into sucrose or storage carbohydrates (Hawker et al., 1979). Wildes and Pitman (1975) observed reduced pyruvate kinase activity in low tissue K (19 μmol $g^{-1}$ fresh weight) barley seedlings and a concomitant increase in reducing sugar content. The activities of starch synthase, phosphorylase and ADP-glucose pyrophosphorylase were increased 2–2.5 fold in the presence of 100 mmol $L^{-1}$ K (Hawker et al., 1979). These studies highlight the intimate association between potassium and enzymatic control of carbohydrate storage and metabolism. Cytoplasmic K is also thought to affect protein synthesis (Wyn Jones et al., 1979), photosynthetic efficiency (Demmig and Gimmler, 1983), and maintenance of cytosolic pH and membrane potential (Marschner, 1995). Potassium concentrations within the cytosol and stroma of well-fertilized plants is generally ~100-150 mmol $L^{-1}$ (Leigh and Jones, 1984). These conditions provide the correct thermodynamic environment for optimal protein hydration, conformation, and function (Wyn Jones and Pollard, 1983).

### 1.3 Potassium Sufficiency Ranges

Methods of evaluating soil and plant tissue K sufficiency ranges remain a significant point of contention within agricultural literature. Scores of studies have demonstrated the impotence of soil testing procedures for estimating plant available K, particularly when attempting to apply levels of adequacy to soils with varying mineralogy and non-acid cation composition (Dest and Guillard, 2001; Nair, 1996; Woods et al., 2005; Woods et al., 2006). Conducting K fertility evaluations in natural soils adds to the variability observed among studies, particularly because potassium flux from soil minerals is highly dependant on soil mineralogy, organic matter, and water content (Rich, 1968; Sparks, 1987). Furthermore, plant extraction and utilization of mineral released K is highly dependent on root metabolism, fresh weight, surface area, cation exchange capacity, and length (Mengel, 1980; Mengel and Steffens, 1985). These factors can be extremely variable across a turfgrass sward/rootzone, warranting novel protocol for evaluating K uptake and sufficiency parameters.

Tissue K concentrations vary widely across turfgrass genera, cultivars, and throughout the growing season; making sufficiency ranges difficult to ascertain (Waddington and Zimmerman, 1972). Furthermore, biomass growth or yield is a common parameter utilized for evaluating plant health or response to nutrient applications. Although useful in crops where yield is paramount, a fundamentally different approach must be taken in turfgrasses, particularly regarding K dynamics. The utility of turfgrass surfaces makes excessive shoot growth unfavorable; therefore, a more complete biochemical assessment of plant health should be conducted when considering nutrient sufficiency. In a broad sense, ‘sufficiency’ ranges should be constructed according to physiologically meaningful tissue nutrient concentrations that support optimal photosynthesis, use/storage of photosynthates, and maintenance of cellular processes, while maintaining optimal utility.

Turfgrass scientists, as well as many agronomist and whole plant physiologists almost exclusively report tissue K content on a dry mass basis ($K_D$), with a generalized sufficiency range of 15-30 g $kg^{-1}$ (Carrow et al., 2001) or 10-25 g $kg^{-1}$ (Jones, 1980) for turfgrasses. This

convention may not be appropriate, particularly because K- sensitive cytosolic reactions affecting plant growth and metabolism are regulated by cytosolic K concentrations, not a dry matter : K relationship (Leigh and Jones, 1984). Therefore, K content on the basis of tissue water ($K_W$) seems a more physiologically meaningful parameter (Pitman, 1975). In fact, Leigh and Johnston (1983b) (1983a) found that differences in $K_D$ of field grown spring barley across K treatments were due to varying tissue water content. In well-fertilized plots, barley $K_W$ was ~200 mmol $L^{-1}$ compared to 50-70 mmol $L^{-1}$ in barley grown in plots that had not been fertilized with K in over 100 years. These studies also showed that $K_W$ is age-independent, whereas $K_D$ tends to decline with age (Ulrich and Hills, 1967).

Other disciplines of plant science have reported $K_W$ for ryegrass, barley, and wheat; yet to my knowledge Woods (2006) presents the only publicly available document where highly managed turfgrass tissue K content is expressed as both $K_W$ and $K_D$. In this abstract, the authors report creeping bentgrass [*Agrostis stolonifera* var. *palustris* (Huds.) Farw.] tissue $K_D$ between 5-25 g $kg^{-1}$ with corresponding $K_W$ values between 50 and 230 mmol $L^{-1}$. Furthermore, in samples with $K_D$ below 15 g $kg^{-1}$, considered to be deficient on a dry mass basis, $K_W$ was often greater than 150 mmol $L^{-1}$, a biochemically sufficient K concentration (Leigh and Jones, 1984; Marschner, 1995). Tissue $K_W$ levels beyond the broadly defined sufficiency range (>150 mmol $L^{-1}$) may also have inhibitory effects on certain enzymes, including starch synthase (Preusser et al., 1981). Clearly turfgrass scientists need to improve methods of reporting and interpreting tissue K content. Adequate K is essential for proper plant function; however, levels of 'adequacy' and the potential harmful effects of excessive K fertilization are poorly characterized; warranting reassessment of K fertilization strategies in turfgrass systems.

Accumulation of polyamines, particularly putrescine is associated with plants grown under K-deficient conditions (Aurisano et al., 1993; Reggiani et al., 1993). Synthesis of diamines is inhibited by adequate cytosolic K and stimulated by low cytosolic pH; therefore, the divalent cation presumably functions as a substitute for K in maintaining cytosolic pH and osmotic balance (Marschner, 1995). Reggiani et al. (1993) noted large differences in putrescine content

of wheat seedling exposed for 1 hour to exogenous K solutions ranging from 0-60 mmol $L^{-1}$. Investigating the association between putrescine accumulation and tissue K content ($K_W$ and $K_D$) of plants grown under varying K levels over the course of weeks rather than hours may provide a physiologically meaningful approach to characterize K deficiency as putrescine biosynthesis is regulated specifically by the activity of K in the cytosol.

The confounding responses observed in K fertility studies may be due to methodology. Data is included from Woodhouse et al. (1978) (Table 1.1) to demonstrate that adequate tissue $K_D$, as identified by Jones (1980) and Carrow et al. (2001), can be achieved by growing perennial ryegrass in solution with K concentrations in the μM range.

**Table 1.1 Data from Woodhouse et al. (1978).**

| | 7 DAG† | | 21 DAG† | |
|---|---|---|---|---|
| | 1.3 μM K | 100 μM K | 1.3 μM K | 100 μM K |
| Dry Matter (mg $plant^{-1}$) | 1.0 | 1.1 | 18.7 | 18.7 |
| Tissue K (g $kg^{-1}$) | 26 | 40 | 41 | 52 |
| Tissue K (mmol $L^{-1}$)‡ | 85 | 130 | 138 | 175 |
| Root length (cm $plant^{-1}$) | 2 | 2 | 200 | 180 |
| Root length : Fresh weight (cm $mg^{-1}$) | 0.3 | 0.3 | 2.3 | 1.8 |
| K Flux (μg $cm^{-2}$ $d^{-1}$)§ | 47 | 77 | 10 | 13 |

† DAG, Days After Germination
‡ Calculated by author
§ Root surface area basis

Note that at 7 days after germination (DAG), tissue $K_W$ of plants grown in 1.3 μM K was bordering on deficient (~80 mmol $L^{-1}$) whereas $K_D$ was well within the recognized sufficiency range. This further illustrates the impotence of using $K_D$ to determine physiological K activity. In plants supplied with 100 μM K, $K_W$ and $K_D$ were within sufficiency ranges and K influx rates were greater than those grown in 1.3 μM K, yet root/shoot growth parameters were essentially identical between the two treatments. Twenty-one DAG, plant dry matter content was independent of solution K concentration, $K_W$ and $K_D$ for plants grown under both conditions

were within sufficiency ranges, and plants grown 100 μM K solution displayed luxury K consumption. In agreement with the results of Cherney et al. (2004), root length and root:shoot ratios were also slightly elevated in plants grown under the low K conditions. Potassium influx rates also decreased dramatically from 7 to 21 DAG and were independent of solution K concentration. Interestingly, at 21 DAG, K influx rates on a root surface area basis were similar to soil K supply rates (5-25 μg $cm^{-2}$ $d^{-1}$) measured on a soil surface area basis from a calcareous sand using cation exchange resins (Woods, 2006).

### 1.4 Storage Carbohydrate Dynamics

In general, C3 plants are less efficient than C4 plants in exporting photosynthates from mesophyll cells and have developed strategies for storing nonstructural carbohydrates (NSCs) (Hull, 1992). The complete fructan biosynthetic pathway is complicated; in summary, sucrose is transported from the cytosol to vacuoles where it activates and serves as a substrate for 1-sucrose:sucrose fructosyltransferase (1-SST, EC 2.4.1.99) (Chatterton et al., 1989), which catalyses the transfer of fructose from one sucrose molecule to another, creating 1-kestose (1-kestotriose, isokestose) (Housley and Pollock, 1985; Pollock, 1984). Fructan-fructan fructosyltransferases and/or other fructosyltransferases facilitate fructan polymerization and modification in concert with specific fructan exohydrolases (FEH, EC 3.2.1.80) (Housley and Daughtry, 1987; Nagaraj et al., 2004; Pavis et al., 2001; Pontis and del Campillo, 1985). Most gramineous species synthesize β(2-6) linked fructans with β(2-1) branches (Bancal et al., 1991; Pavis et al., 2001). Storage of NSCs in the vacuole prevents cytosolic sucrose from reaching concentrations that would inhibit photosynthesis (Housley and Pollock, 1985; Pollock and Chatterton, 1988) accordingly, 1-SST activity and fructan accumulation are enhanced under conditions that inhibit growth but permit photosynthesis (Pollock, 1984). With the onset of darkness, SST activity declines and FEH activity increases, promoting the hydrolysis of fructans and transport of mono- disaccharides to the cytosol (Obenland et al., 1991; Wagner and Wiemken, 1987; Wagner et al., 1986).

The degree of fructan polymerization varies between cool season grass genera. Perennial ryegrass and red fescue (*Festuca rubra* L.), accumulate fructans that are completely soluble in 65% EtOH, suggesting that they are short chain polymers consisting of 26 fructose units or less(Smith, 1972; Smith and Grotelueschen, 1966). In contrast, fructans extracted from Kentucky bluegrass (*Poa pratensis* L.) are soluble in very dilute EtOH or water fractions, a function of the high degree of polymerization of fructose monomers (~260). Fructan polymerization is also tissue dependant, with highly polymerized fructan chains being localized more towards stem bases than leaf blades or upper internodes (Smith, 1967; Smith, 1972). The tissue/species dependence of fructan polymerization suggests that there may be some association between fructan chain length, storage location, and the susceptibility of that plant tissue to psychrophilic fungi.

Nonstructural carbohydrates provide an essential energy reserve for actively growing plants, and as mentioned previously, K mediated enzymes play a central role in the metabolism and fate of photosynthates. As much as 12-25% of photosynthetic products may be used in root respiration (Lambers et al., 1991), with as much as 36% of total ATP consumption going toward ion uptake (Marschner, 1995). Potassium uptake is an active process, and K stimulates its own transport across the membrane by activating membrane bound ATPases, rapidly enhancing ATP consumption at concentrations greater than 1mM (Fisher et al., 1970). Phloem loading of sucrose is also impacted by phloem sap K content. Specifically, phloem transport in castor oil plants (*Ricinus communis* L.) grown in a 1 mM K solution was approximately two times that of plants grown in a 0.4 mM K solution (Mengel and Haeder, 1977). Although the proposed study would not directly evaluate K uptake energy requirements, it is conceivable that the energy (photosynthate) use associated with luxury K consumption manifests in diminished NSC storage under high K fertility. The inseparable link between K and carbohydrate dynamics highlights the importance of evaluating its impacts on the synthesis and storage of NSCs during autumn and early winter, a critical period of NSC accumulation that could influence susceptibility to psychrophillic fungi infection.

### 1.5 Carbohydrate Dynamics and Psychrophilic Fungi Susceptibility

Tronsmo (1986) demonstrated that growth of psychrophilic fungi (*Microdochium nivale* Fr. and *Typhula ishikariensis* Imai.) is reduced by ~ 50% when cultured in media with a water potential of -2 MPa vs. growth at -0.6 MPa. This same study demonstrated a significant decrease in leaf water potential of timothy (*Phleum pratense* L.) and reed canary (*Phalaris arundinacea* L.) grass after 'hardening' at 1°C for two weeks. Across species, water potentials of hardened plant tissues were reduced by ~75% versus 'unhardened' tissue, and were within the range of -1.21 to -2.08 MPa. This suggests that accumulating solutes within plant tissues reduces water potential during hardening, and may function as a deterrent for psychrophilic fungal infection and growth. The intimate association between K fertility and plant tissue osmotic balance, and the potential impact on psychrophilic fungi growth warrants tissue water potential analyses in our investigation.

Turfgrasses grown in northern locales are annually subjected to conditions that favor infection by low temperature fungi. Although potentially very destructive, pink snow mold (*Microdochium nivale* Fr.) symptoms and damage tend to develop in swards lacking snow cover and can frequently be ameliorated with preventative and curative fungicide applications. Turfgrass losses from Typhula blight (*Typhula spp.*) infection can be very severe, persist for weeks or months into the growing/golfing season, and recur in the same areas annually. Typhula blight develops exclusively under snow cover, and for this reason can only be treated preventatively with fall applications of fungicides that may loose efficacy through the winter. The insulative properties of prolonged, deep snow cover may prevent soil from freezing and allow soil to thaw through geothermal heat flux, thereby maintaining soil temperatures near 0°C (Smiley et al., 2007). These conditions not only provide ideal conditions for *Typhula spp.* development, but may also increase metabolic catabolism of plant storage carbohydrates, a

critical component of low temperature fungi pathogenicity and plant cold hardiness (Gaudet et al., 1999).

The connection between cold hardiness and low temperature fungi susceptibility is unclear, although both seem inseparably related to overwintering carbohydrate dynamics. Gaudet and Kozub (1991) did not observe a direct correlation between cold hardiness and resistance to most snow mold fungi; however, low temperature stress increases plants susceptibility to snow mold and snow mold infection may reduce the plants freeze tolerance (Gaudet and Chen, 1988). Resistance to infection by pink snow mold seems to be acquired within 1-2 weeks following the onset of hardening conditions and is dependant on light (Nakajima and Abe, 1996); in contrast, cold hardiness seems to develop more slowly, over a period of 4-8 weeks (Dionne et al., 2001; Koster and Lynch, 1992; Levitt, 1980) and is light independent (Nakajima and Abe, 1996).

Reduced catabolic processes at low temperatures results in the accumulation of photosynthates in the cytoplasm (Pollock and Cairns, 1991). High polymeric sugar concentrations in autumn and winter as well as elevated fructan content in the spring are characteristic of snow mold resistant winter wheat varieties (Kiyomoto and Bruehl, 1977). Yoshida et al. (1998) related snow mold tolerance of winter wheat varieties with cold sensitivity. Interestingly, snow mold tolerant varieties accumulated higher fructan concentrations in the fall, and hydrolysed storage carbohydrates at a slower rate than cold hardy/snow mold susceptible varieties under dark conditions. In this context, an annual bluegrass ecotype isolated from an area prone to extensive snow cover was the most cold sensitive, accumulated greater concentrations of fructans, and maintained the highest concentrations of mono- and disaccharides during the winter (Dionne et al., 2001). These results imply that there may be different ecological strategies for utilizing storage carbohydrates depending on whether psychrophilic fungi or direct low temperature damage pose the greatest threat to survival. Although previous studies have monitored NSCs during acclimation and overwintering, very few have evaluated the activity of enzymes responsible for photosynthate storage and metabolism. Quantifying the activity of photosynthate mediating enzymes while simultaneously measuring NSC of plants grown under

different K fertility conditions may more definitely elucidate cold weather NSC dynamics, and determine whether K fertility impacts these processes through mediating enzyme activity.

I previously reviewed some of the basic processes involved in the utilization and storage of photosynthates, with particular focus on fructans. During the winter, fructans are metabolized by β-fuctosidases, including FEH and invertase (EC 3.2.1.26) (Olien and Clark, 1993). Hydrolytic fructan enzymes are also activated during darkness (Wagner et al., 1986), which may significantly impact fructan hydrolysis under snow cover. It appears as though some the aforementioned enzymes may play a significant role in conferring snow mold resistance. In fact, some unpublished data indicates that SST activity may be greater in snow mold resistant cultivars than more sensitive types (Gaudet et al., 1999). That being said, fructan accumulation in acclimating wheat is not entirely associated with the activity of these enzymes (Yukawa et al., 1994).

A review by Gaudet et al. (1999) examines the connections between overwintering carbohydrate dynamics and snow mold susceptibility in winter wheat. The authors suggest that exceptionally resistant varieties have the ability to accumulate high levels of storage carbohydrates during the fall, and through enzyme mediated hydrolysis of these polymeric carbohydrates maintain high concentrations of simple sugars throughout winter into spring. These simple sugars may induce the expression of plant defense resistance genes though the hexokinase signal transduction pathway (Herbers et al., 1996). Hexokinases are ‘sugar sensing’ enzymes that phosphorylate glucose and fructose to glucose-6-Phosphate and fructose-6-Phosphate during the initial steps of glycolysis.

There may also be a connection between the down regulation of photosynthesis and the accumulation of mono- and disaccharides during the onset of cold temperatures (Herbers et al., 1996). For this reason, Gaudet et al. (1999) propose that the rapid accumulation of simple sugars during cold hardening may have a dual function in down regulating photosynthetic activity and inducing plant defense systems. Plants that are able to replenish carbohydrate pools as they are metabolized and maintain high cytosolic carbohydrate concentrations into the spring may

continuously stimulate plant defense mechanisms and thus possess exceptional snow mold resistance. Several other studies note the association between high concentrations of soluble carbohydrates in the spring and reduced snow mold damage (Kiyomoto, 1987; Kiyomoto and Bruehl, 1977).

Respiration of winter wheat decreases through the fall, and the rate of respiration at 0°C is inversely related to the degree of plant hardiness and dormancy (Newton and Anderson, 1931). Therefore, it is conceivable that early snowfall may prevent grasses from completely hardening, increase the rate of respiration and utilization of storage carbohydrates at 0°C, and leave plants more susceptible to low temperature and psychrophilic fungi damage. Following this concept, any factor that may prolong the period necessary for adequate hardening may affect snow mold susceptibility.

This leads to several key points; (i) the site of fructan storage is the vacuole; therefore, if plants are grown under high K conditions, vacuolar osmotic potential will already be very low, potentially reducing the ability of the plant to store fructans and other carbohydrates during the hardening process; (ii) high concentrations of photosynthates override light regulation of photosynthesis by reducing the activity of rubisco and Calvin-cycle proteins (Smeekens and Rook, 1997); therefore, excessively high tissue K concentrations may promote the rapid dispersion of photosynthates to sink tissues allowing photosynthesis to proceed during times when downregulation and hardening would be more beneficial; (iii) although potentially a function of the aforementioned hypotheses, (Tyler et al., 1981) observed that plants grown under low K fertility were able to harden more rapidly and to a greater extent. These features suggest that the positive association between K fertilization and psychrophilic fungi damage observed by Webster and Ebdon (2005) and Woods et al. (2006) has an underlying physiological explanation involving carbohydrate storage during autumn and metabolism through the winter.

# CHAPTER 2: THE EFFECT OF POTASSIUM FERTILIZATION ON OVERWINTERING CARBOHYDRATE AND METABOLITE DYNAMICS

## 2.1 Abstract

Overwintering carbon metabolism of perennial grasses is known to affect their performance and utility. While there is some evidence that plant K status influences winter survival, the physiological basis is unclear. The goal of this experiment was to determine the effect of seasonal K fertilization on carbon metabolism of overwintering annual bluegrass [*Poa annua* var. reptans (Hauskn) Timm.]. In a greenhouse, annual bluegrass was seeded into sand filled columns. Nitrogen (0.5 g $m^{-2}$ ), K (0.5 g $m^{-2}$), and all other essential nutrients were applied weekly for 90 d. Following establishment, 5 different K treatments (0, 0.25, 0.5, 2, 3 g $m^{-2}$ $7d^{-1}$) were imposed for 90 d. Columns were moved to a refrigerated room, maintained under a photosynthetically active radiation flux of ~300 mmol $m^{-2}$ $s^{-1}$, and day/night air temperature incrementally decreased every 7 d over 28 d (10/4°C, 4/-2°C, 2/-4°C, -2/-6°C). Plants were then kept under darkness at -4°C (28 d), 2°C (40 d), then 4°C (40 d). Tissue harvested following each experimental phase was analyzed for elemental composition, nonstructural carbohydrates, and several tricarboxylic acid cycle intermediates (TCAIs). Tissue K content and cation:anion ratios increased with K fertilization rate. Overall K fertilization had a minimal impact on non-structural carbohydrate dynamics. Tissue TCAI content, particularly malate and citrate, markedly increased at greater K fertilization rates. The results of this study suggest that K fertilization significantly increases diversion of carbon resources to organic acid synthesis due to perturbations in charge and pH homeostasis associated with disparate cation/anion uptake ratios. In addition to affecting plant utility, there is a biochemical cost associated with luxury K uptake and subsequent organic acid accumulation.

## 2.2 Introduction

Nonstructural carbohydrates (NSCs) have been the focus of studies related to heat (Liu and Huang, 2000), cold (Patton and Reicher, 2007; Yoshida et al., 1998), drought (DaCosta and Huang, 2006), and wear (Han et al., 2004) tolerance of turfgrasses. Factors affecting NSC content of forage grasses used as animal fodder have also been studied extensively, as forage carbohydrates can account for ~2/3 of a production animals total dietary carbohydrate intake (Nie et al., 2009). Overwintering carbohydrate dynamics of perennial grasses are particularly important at northern latitudes. Plant storage and utilization of carbon resources is a critical determinant of winter survival (Dionne et al., 2010), spring recovery, and seasonal yield of forage and amenity grasses (Lawton and Burpee, 1990; Sanada et al., 2010).

In addition to affecting plant utility, NSCs serve as fuel for oxidative metabolism (glycolysis, tricarboxylic acid pathway) and provide carbon skeletons for a multitude of plant biosynthetic pathways. Organic acids derived from the tricarboxylic acid (TCA) metabolic pathway participate in generating osmotic gradients (e.g. stomates), maintaining charge and pH homeostasis within cellular compartments, and nitrogen assimilation. Furthermore, the majority of reducing power generated during oxidative metabolism stems from the TCA pathway. Photosynthesis, carbon partitioning, and oxidative metabolism through the TCA cycle are all reciprocally regulated in response to plant reducing power and/or ATP demands. The effect of carbohydrate storage on organic acid metabolism has been demonstrated experimentally (Wang et al., 2010). While TCA cycle intermediates participate in many other independently regulated biochemical pathways, organic acid dynamics allow some speculation as to how plants are utilizing carbon resources and their overall metabolic activity.

Claims of potassium conferring increased drought, temperature stress, and wear tolerance (Shearman and Beard, 2002) are ubiquitous in textbooks (Carrow et al., 2001; Fry and Huang, 2004) and turfgrass publications, yet supporting data are generally vague. In an extensive literature review, Turner and Hummel (1992) examined the role of K in turfgrass establishment,

cold/heat/wear tolerance, disease incidence, root growth, and color. In all cases results were inconsistent, and the specific impact of K on these parameters remains unclear. There is some evidence that abundant K applications to highly managed turfgrasses may have detrimental effects on winter hardiness, leading to delayed spring greening (Waddington et al., 1972) and enhanced susceptibility to psychrophilic fungi (Webster and Ebdon, 2005; Woods et al., 2006). Furthermore, Tyler et al. (1981) observed that winter wheat (*Triticum aestivum* L.) grown in a hydroponic culture of 4:1 N:K ratio (0.358 μM K) were more cold hardy and developed hardiness more rapidly than plants grown in solutions with a N:K ratio of 1:1.25 (1.74 mM K).

Although some of the aforementioned 'whole plant' effects of K fertilization are less clear, the biochemical role of K in plants is more completely characterized. Potassium is highly mobile, is the most abundant ion in the cytoplasm, and is intimately associated with solute speciation and osmotic potential of the cytosol and vacuole (Marschner, 1995). Specifically within the vacuole, K has mainly a biophysical function by regulating turgor (Leigh and Jones, 1984). Under low K conditions Na salts (Wildes and Pitman, 1975), carbohydrates (Evans and Sorger, 1966; Wildes and Pitman, 1975), and other solutes may accumulate within the vacuole to maintain vacuolar osmotic pressure as vacuolar K quenches cytosolic demands. An inverse relationship between tissue K and reducing sugar content has been observed in barley (*Hordeum vulgare* L.) and Italian ryegrass (*Lolium multiflorum* Lam.), demonstrating the effect of growth media cation concentrations on the speciation of osmotic pressure generating solutes within the vacuole (Nowakowski et al., 1974; Pitman et al., 1968). Within the cytoplasm, K has been shown to activate enzymes including those involved in glycolysis (Wildes and Pitman, 1975) and partitioning of photosynthetic triose phosphates into sucrose or storage carbohydrates (Hawker et al., 1979). Leaf K concentrations have also been correlated with net photosynthetic rate, stomatal conductance, phloem loading of photosynthates, and rubisco activity (Amtmann et al., 2006). These studies highlight the intimate association between potassium fertility and enzymatic control of carbohydrate storage and metabolism.

Overwintering NSC dynamics of annual bluegrass ecotypes have been characterized in several previous studies (Bertrand et al., 2011; Dionne et al., 2001; Dionne et al., 2010), but the effects of K fertilization have not been tested. In a review of the literature, organic acid metabolism of annual bluegrass has apparently never been characterized. The central importance of carbon metabolism to the utility and performance of grasses and the likely influence of K fertilization warrants research on this topic. Therefore, the goal of this study was to evaluate the effect of seasonal K fertilization on carbohydrate and metabolite dynamics of annual bluegrass during simulated winter conditions.

## 2.3 Materials and Methods

### *2.3.1 Plant Establishment and Fertility Treatments: Greenhouse*

The experiment was repeated twice between March 15, 2009 and May 15, 2010. The second experiment began 3 months after the first experiment (June 15, 2009), and was conducted identically yet independent in space and time. The following methods apply to both experimental runs.

Forty annual bluegrass [*Poa annua* L. forma *reptans* (Hausskn.) T. Koyama)] seeds (PD-24, University of Minnesota) were sown into 125 -30.5 x 10.4 cm diam. cm polyvinyl chloride (Schedule 40) columns filled with sand (Table 2.1)Each column had been previously glued to a 11.4 x 11.4 cm square polyvinyl chloride base with a 6 mm hole drilled in the center to provide drainage. Seeds were then covered in ~5 mm of sand and fertilized with 20 mL of nutrient solution (Table 2.2) fortified to contain 5.5 mM KCl, supplying K and Cl at a rate of 0.5 g $m^{-2}$.

A 12 x 12 cm square of low-density polyethylene wrap was secured over each experimental unit (EU) to retain moisture. Experimental units were placed on raised benches in a greenhouse with a 16 hr day length (Figure 2.1). Plastic covers were removed after 10 d. Starting 14 d after seeding (DAS), every 7 d seedlings were clipped to 10 mm (clippings removed),

watered from above with a hand held nozzle until liquid spontaneously drained from the base (~ 2 cm irrigation), and then fertilized with 20 mL of KCl fortified (5.5 mM) nutrient solution. At 90 DAS, EUs were randomly selected to receive the normal weekly nutrient solution fortified with KCl to apply K and Cl at a rate of 0, 0.25, 0.5, 2, or 3 g $m^{-2}$ 7 $d^{-1}$ (Table 2.3). Weekly K fertility treatments continued for a total of 90 days ('fertilization period') before EUs were moved into a low temperature growth chamber. Once entering the simulated winter phase of the experiment, no additional fertilizers were applied.

**Table 2.1 Physicochemical characteristics of the sand growing media.**

| Parameter | Mean | N | Standard Error |
|---|---|---|---|
| pH (1:1 $H_2O$) | 6.37 | 3 | - |
| Organic Matter (g $kg^{-1}$) | 0.14 | 3 | 0.02 |
| Exchangeable Ca† (mg $kg^{-1}$) | 96.7 | 3 | 2.85 |
| Exchangeable Mg† (mg $kg^{-1}$) | 27.3 | 3 | 0.88 |
| Exchangeable K† (mg $kg^{-1}$) | 6.00 | 3 | 0.00 |
| Nonexchangeable K‡ (mg $kg^{-1}$) | 95.4 | 3 | 8.11 |
| Exchangeable Na† (mg $kg^{-1}$) | 32.3 | 3 | 0.88 |
| CEC§ ($cmol_c$ $kg^{-1}$) | 0.89 | 3 | 0.02 |
| Phosphorus† (mg $kg^{-1}$) | 2.00 | 3 | 0.00 |
| Sulfur† (mg $kg^{-1}$) | 12.7 | 3 | 0.33 |

† Mehlich III Extractant.

‡ Nonexchangeable by boiling $HNO_3$ (Pratt, 1965).

§CEC, Cation Exchange Capacity by summation of cations.

**Table 2.2 Fertilizer composition and nutrient application rates.**

| Source | Concentration (mM) | Nutrient Supplied | Application Rate ($g\ m^{-2}\ 7d^{-1}$) From Source, (Total) |
|---|---|---|---|
| $NH_4H_2PO_4$ | 2 | N | 0.06, (0.60) |
| | | P | 0.15, (0.15) |
| $NH_4NO_3$ | 5.5 | N | 0.18, (0.60) |
| $Ca(NO_3)_2$ | 5.5 | Ca | 0.50, (0.50) |
| | | N | 0.36, (0.60) |
| $MgSO_4$ | 4.5 | Mg | 0.25, (0.25) |
| | | S | 0.35, (0.35) |
| Fe-EDDHA | 1 | Fe | 0.1, (0.1) |
| $H_3BO_3$ | 0.5 | B | 0.01, (0.01) |
| $MnCl_2$ | 0.5 | Mn | 0.06, (0.06) |
| | | Cl | 0.08, 0.08 |
| $ZnSO_4$ | 0.008 | Zn | 0.001, (0.001) |
| | | S | <0.01, (0.35) |
| $CuSO_4$ | 0.003 | Cu | 0.0005, (0.0005) |
| | | S | <0.01, (0.35) |
| $H_2MoO_4$ | 0.002 | Mo | 0.0005, (0.0005) |

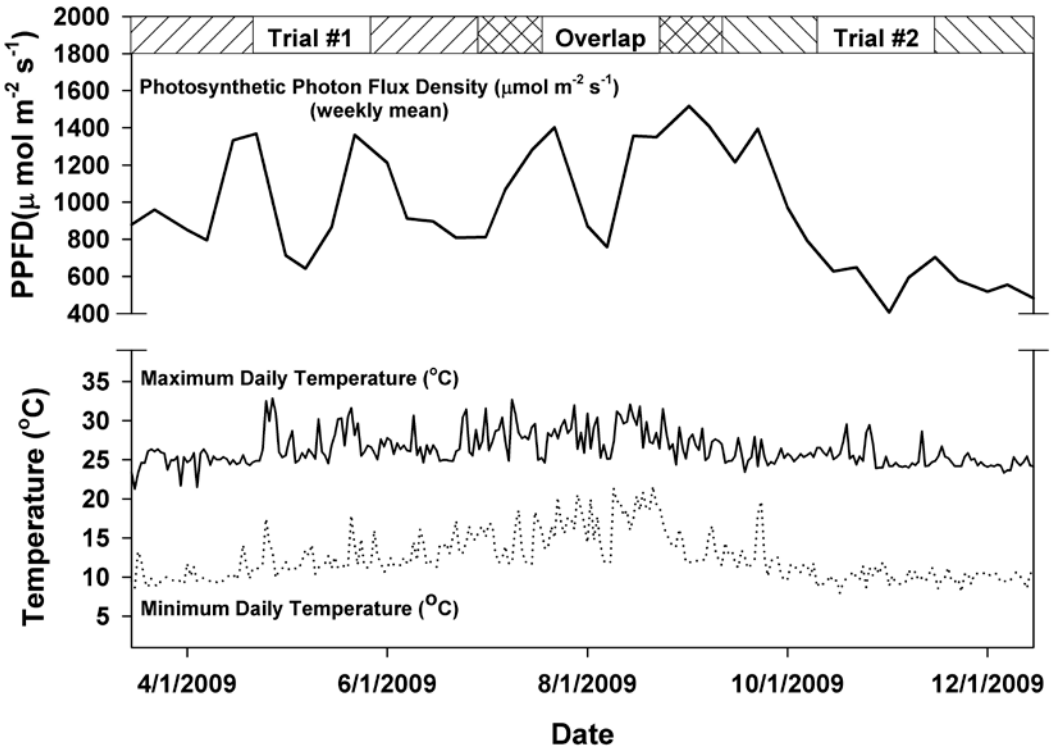


**Figure 2.1. Temperature and photosynthetic photon flux density (PPFD) in the greenhouse during establishment and K fertilization period.**

**Table 2.3. Potassium (KCl) fertilizer concentration, application rate, and total amount of K applied during the 90 d fertilization period prior to simulated winter.**

| K Treatment Level | K Concentration (mmol $L^{-1}$) | Application Rate† (g $m^{-2}$) | Total K Applied (g $m^{-2}$) |
|---|---|---|---|
| 1 | 0.00 | 0.00 | 0.00 |
| 2 | 2.25 | 0.25 | 3.25 |
| 3 | 5.50 | 0.50 | 6.50 |
| 4 | 22.0 | 2.00 | 26.0 |
| 5 | 33.0 | 3.00 | 39.0 |

† K applied every 7 d for 90 d prior to simulated winter.

*2.3.2 Simulated Autumn, Winter, and Spring: Low Temperature Growth Chamber*

Following 180 days of growth in the greenhouse (90 d establishment + 90 d K treatments), EUs were moved into a 15 x 3 m refrigerated container car (reefer) located at the Bluegrass Lane Turf and Landscape Research Center in Ithaca, NY. The reefer was divided into 3- 4 x 3 m thermally isolated rooms allowing independent control of air temperatures (±0.5ºC) and light conditions within each room. Each of the 3 simulated 'seasons'; 1) incrementally decreasing temperature under illumination ('hardening'); 2) sub-zero constant temperature under darkness ('mid-winter'); and 3) near freezing, high humidity ('early-spring'), were conducted in separate rooms within the reefer. Climate conditions imposed during these three phases were meant to roughly represent seasonal conditions in Ithaca, NY.

During the 'hardening' period, EUs were randomly distributed within one 4 x 3 m room of the reefer. High pressure sodium lights provided an average plant-level photosynthetic photon flux density (PPFD) of 300 µmol $m^{-2}$ $s^{-1}$ and an 8 h day length. While a higher PPFD (400-800 µmol $m^{-2}$ $s^{-1}$) is commonly observed in the field during autumn months at northern latitudes, a PPFD of 300 µmol $m^{-2}$ $s^{-1}$ was used due to technical limitations of lighting equipment, and to

approximate ‘hardening’ conditions used in studies that evaluated overwintering carbohydrate dynamics and/or low temperature hardiness (Anderson et al., 1993; Dionne et al., 2001; Patton and Reicher, 2007; Patton et al., 2007; Wanner and Junttila, 1999). Over the course of 4 weeks, day/night temperatures decreased incrementally (10/4, 4/-2, 2/-4, -2/-6°C) every 7 d. Irrigation was applied (2 cm) using a hand held spray bottle during the daytime hours (ambient air temperature >0°C) of the first three weeks of hardening to prevent desiccation. Experimental unit position was randomized weekly.

After 28 d, EUs were moved to random locations within the second room of the reefer. Approximately 2 cm of chipped distilled $H_2O$ ice was placed over the foliage of each EU to prevent desiccation and they were held under darkness at -4°C for a 28 d ‘mid-winter’ period.

Experimental units were then moved to the third room of the reefer, randomly positioned on a 3 x 4 m slotted rack elevated above a catch basin, and were maintained under darkness and an ambient air temperature of 2°C for 40 d and then 4°C for another 40 d. Experimental units were misted every 1 h for 15 s, providing ~0.5 cm of precipitation every 7 d. These conditions were imposed to simulate the darkness, 24 h leaf wetness, ~99% relative humidity, and near 0°C temperatures that persist under snow cover during late winter and early spring. This is subsequently referred to as the ‘early spring’ period.

*2.3.3 Harvesting Tissue for Biochemical Analyses*

Five replicates of each K level were destructively sampled by harvesting all aerial tissues at the completion of the establishment, fertilization, hardening, mid-winter, and early spring experimental periods (5 replicates X 5 K levels X 5 sampling dates = 125 EUs) . Tissue was trimmed at the root/shoot interface, homogenized, split, and either frozen in liquid $N_2$ and stored at -80°C overnight or weighed and then placed in a forced air oven at 55ºC for 48 h. Dry weights were obtained and tissues were analyzed for K, Ca, Mg, Na, P, S, Fe, Mn, B, Cu, Zn, and Al using the microwave acid digestion method (Horneck and Miller, 1998) with tissue concentrations determined by inductively coupled plasma atomic emission spectroscopy. Tissue

N content was measured by combustion in a C/N analyzer (Horneck and Miller, 1998). Tissue Cl content was determined by hot water extraction (Ghosh and Drew, 1991) and detected with a Cl-specific electrode (Orion 961700, Fisher Scientific, Pittsburgh, PA). Tissue frozen in liquid $N_2$ was ground using a mortar and pestle in liquid $N_2$ and stored at -80°C until being analyzed for nonstructural carbohydrates and citric acid cycle metabolites.

*2.3.4 Determination of Glucose, Fructose, Sucrose, and Fructans*

Extraction of the major non-structural carbohydrates (NSCs) glucose (Glu), fructose (Fru), sucrose (Suc), and high/low degree of polymerization (DP) fructans was performed similarly to Zhao et al. (2010) and Ranwala and Miller (2008). While both of these authors derived their protocol from several older published articles, these papers present a very detailed description of reagent preparation and extraction.

Ethanol soluble NSCs (glucose, fructose, sucrose, low-DP fructans) were extracted by adding 2 mL of 80% (v/v) ethanol (EtOH) to a 4 mL polypropylene centrifuge tube containing 50 mg of liquid $N_2$ ground tissue and heating the samples in an 80°C water bath for 15 min. Each sample was extracted three times. Following each extraction, tubes were centrifuged (3000 x g) for 10 minutes and the supernatant from each repeated extraction was pooled into a 10 mL centrifuge tube. The three pooled supernatants were then brought to a 6 mL final volume with 80% EtOH. A 1.0 mL aliquot of each pooled extract was vacuum concentrated (Labconco Corp., Kansas City, MO) overnight in a 1.5 mL micro-centrifuge tube and resuspended with 1.0 mL of HPLC-grade water. Each resuspended sample was then transferred to a separate 1.2 mL tube within eight-tube, multichannel pipette compatible strips, and stored at -80°C until used for analysis.

The pellet remaining after EtOH extraction was vacuum concentrated overnight. The dried pellet was then extracted three times for 30 min at 80°C with 3 mL of HPLC grade water. Supernatants from each extraction were combined following centrifugation (3000 x g) and then brought to a final volume of 10 mL using HPLC grade water. Aliquots (1.0 mL) of each sample

extract were stored at -80°C in 1.2 mL multichannel pipette compatible tube strips. The purpose of the water extraction after 80% EtOH extraction was to extract high-DP fructans that were not soluble in 80% EtOH.

Acid hydrolysis of fructans results in depolymerization of the fructan chain into its individual Fru and Glu reducing sugars constituents which can then be quantified using colorimetric methods (Cairns, 1987) that are unable to quantify intact fructans. Acid hydrolysis of EtOH and water extracts was performed as follows. Aliquots (200 µL) of each sample were transferred to new eight-tube, multi-channel pipette compatible strips using an eight channel pipette. Two-hundred µL of 0.05 M HCl was added to each tube, and tube strips were then placed in a boiling water bath for 5 min. Once removed from the water bath, 200 µL of 0.05 M NaOH was added to each tube within 5 s. Samples were then stored at -80°C until being analyzed. Using a multi-channel pipette allows rapid neutralization of the reaction following boiling.

Glucose, fructose, and sucrose concentrations were measured in each of the four extract fractions (EtOH extract, $H_2O$ extract, acid hydrolyzed EtOH extract, acid hydrolyzed $H_2O$ extract) using a colorimetric assay modified from Cairns (1987), Chen and Setter (2003), and Zhao et al. (2010). The assay relies on the following coupled reactions. Glucose and Fru are converted to Glu-6-phosphate and Fru-6-phosphate in the presence of hexokinase (EC 2.7.1.1) and adenosine-5'- triphosphate (ATP), respectively. Glucose-6-phosphate dehydrogenase (EC 1.1.1.49) then reacts with Glu-6-phosphate resulting in the reduction of nicotinamide adenine dinucleotide ($NAD^+$) to NADH. Subsequent reduction of thiazolyl blue tetrazolium bromide (MTT) yields a blue formazan dye that can be readily quantified by measuring absorbance at $\lambda \sim$ 600 ηm using a spectrophotometer. Following the complete reaction of all Glu-6-phosphate contained in the sample, addition of phosphoglucose isomerase (PGI; EC 5.3.1.9) converts Fru-6-phosphate to Glu-6-phosphate which then participates in the reduction cascade resulting in a visible blue color change. Finally, sucrose is converted to Glu and Fru with the addition of invertase (EC 3.2.1.26). The Glu and Fru generated through the addition of invertase then

participates in the colorimetric reaction as described above. Essentially, this assay allows detection of Glu, Fru, and Suc sequentially by converting sugars to Glu-6-phosphate equivalents that can then participate in the reduction cascade. This assay was used to evaluate samples in 96-well microplates (BD Falcon 353915, BD Biosciences, Chicago, IL) in the following manner.

Two 20-µL aliquots of plant extracts were added to separate wells of a 96-well microplate. Two columns of each microplate were left empty for glucose, fructose, and sucrose standards, allowing the analysis of 40 samples (in duplicate) on each plate. Once samples were added, an additional 20 µL of distilled $H_2O$ was added to each sample well. Next, 6-Glu standards (0, 0.0125, 0.025, 0.05, 0.125, 0.25 mg $mL^{-1}$), a Fru check (0.25 mg $mL^{-1}$), and Suc check (0.25 mg $mL^{-1}$) were added to adjacent wells in the first two columns of each microplate. Absorbance at λ= 620 ηm ($A_{620}$) was measured (Beckman Coulter LD-400, Beckman Coulter, Brea, CA) and recorded for each well ( $A_{620}^{1^\circ}$ ). These values were later subtracted from total absorbance to account for variations in plate characteristics and absorbance of pigments contained in samples.

A master reagent was then formulated by mixing 2.0 mL of $H_2O$, 1.0 mL of bovine serum albumin (A8022, Sigma-Aldrich, St. Louis, MO) stock (20 g $L^{-1}$), 0.5 mL of MTT (M2128, Sigma) stock (20 mM), and 0.5 mL of phenazine methosulfate (PMS; P9625, Sigma) stock (60 mM) in that order. Phenazine methosulfate stock solution and the reagent mixture spontaneous change color in the light; therefore, it is essential to store PMS stocks in darkness, mix the assay reagent immediately before use, and minimize light exposure during the assay. Immediately after formulation, 40 µL of the master reagent was added to each well followed by the addition of 100 µL of glucose hexokinase reagent (1.5 mM NAD, 1.0 mM ATP, 1.0 U $mL^{-1}$ hexokinase, and 1.0 U $mL^{-1}$ Glu-6-phosphate dehydrogenase; G3293, Sigma). Microplates were then covered, placed in a dark incubator for 10 min at 30°C, removed, uncovered, and $A_{620}$ measured ( $A_{620}^{2^\circ}$ ). Color change of wells containing glucose standards provided visual confirmation that the reaction was proceeding appropriately. During the final minutes of the reaction, 1.0 mL of PGI (P5381, Sigma) enzyme reagent (20 U $mL^{-1}$) was mixed and kept on ice. Immediately after removing the

microplate from the plate reader, 10 µL of PGI reagent was added to each well (0.2 U PGI well$^{-1}$). Plates were then incubated and $A_{620}$ was measured ( $A_{620}^{3^\circ}$ ) as in the first step of the assay. Color change of wells containing a 0.25 mg mL$^{-1}$ Fru 'check' provided visual confirmation that the reaction was proceeding appropriately. During the final minutes of the PGI reaction, 1 mL of invertase (I4504, Sigma) enzyme reagent (800 U mL$^{-1}$) was mixed and kept on ice. Immediately after removing the microplate from the plate reader, 10 µL of invertase reagent was added to each well (8 U invertase well$^{-1}$). Plates were then incubated for 20 minutes at 30°C and $A_{620}$ was measured ( $A_{620}^{4^\circ}$ ) as in the first two steps of the assay. Color change of wells containing a 0.25 mg mL$^{-1}$ Suc 'check' provided visual confirmation that the reaction was proceeding appropriately.

A simple linear regression equation generated from duplicate mean $A_{620}$ values for each glucose standard was used to estimate Glu equivalent concentrations from adjusted $A_{620}$ at each measurement point. The equation was extremely stable ($\beta_0 = 0.000 \pm 0.004$; $\beta_1 = 0.25 \pm 0.02$) with $r^2 \geq 0.99$ in all cases. Within each plate, Glu, Fru, and Suc concentrations were calculated for each well using relevant regression equations and adjusted $A_{620}$ values for each unknown sample as described in Table 2.4. Each sample was run in duplicate on each plate, and assayed on three different plates; yielding a total of six replicate measurements for each extract fraction of each EU. Replicate measurements were averaged over EU.

**Table 2.4 Equations relating nonstructural carbohydrate concentrations in plant extracts to microplate well absorbance at λ= 620 ηm.**

| Carbohydrate (mg mL$^{-1}$) | | Adjusted $A_{620}$ † | | Slope‡ | | Intercept§ |
|---|---|---|---|---|---|---|
| Glucose | = | $A_{620}^{2^\circ} - A_{620}^{1^\circ}$ | x | $\beta_1^{2^\circ}$ | + | $\beta_0^{2^\circ}$ |
| Fructose | = | $A_{620}^{3^\circ} - A_{620}^{2^\circ}$ | x | $\beta_1^{3^\circ}$ | + | $\beta_0^{3^\circ}$ |
| Sucrose | = | $A_{620}^{4^\circ} - A_{620}^{3^\circ}$ | x | $\beta_1^{4^\circ}$ | + | $\beta_0^{4^\circ}$ |

†, $A_{620}^{x^\circ}$, absorbance at λ= 620 ηm at plate measurement time x (x=1,2,3,4).

‡ $\beta_1^{x^\circ}$, slope of regression relating $A_{620}$ and carbohydrate concentration, derived from glucose standards at plate measurement time x (x=2,3,4).

§ $\beta_0^{x^\circ}$, intercept of regression relating $A_{620}$ and carbohydrate concentration, derived from glucose standards at plate measurement time x (x=2,3,4).

Once Glu, Fru, and Suc concentrations of each extract fraction were calculated, sample totals of Glu, Fru, Suc, ethanol soluble low DP fructans (ESF), and water soluble high DP fructans (WSF) were calculated as outlined in Table 2.5.

**Table 2.5 Equations used to calculate sample totals of glucose, fructose, sucrose, and fructans using soluble carbohydrate concentrations in each extract fraction.**

| Type of Carbohydrate | Sample Total | | Constituents of Total† |
|---|---|---|---|
| Hexose & Oligosaccharide | | | |
| | Glucose | = | EtOH Glucose + $H_2O$ Glucose |
| | Fructose | = | EtOH Fructose + $H_2O$ Fructose |
| | Sucrose | = | EtOH Sucrose + $H_2O$ Sucrose |
| ESF‡ | | | |
| | Glucose Monomers | = | AH EtOH Glucose - EtOH Glucose |
| | Fructose Monomers | = | AH EtOH Fructose - EtOH Fructose |
| | Total ESF Fructan | = | Glucose Monomers +Fructose Monomers |
| WSF§ | | | |
| | Glucose Monomers | = | AH $H_2O$ Glucose - $H_2O$ Glucose |
| | Fructose Monomers | = | AH $H_2O$ Fructose - $H_2O$ Fructose |
| | Total WSF Fructan | = | Glucose Monomers +Fructose Monomers |

† EtOH, 80% ethanol extractant; $H_2O$, distilled water extractant; AH, acid hydrolyzed.

‡ ESF, 80% ethanol soluble low degree of polymerization fructan.

§ WSF, water soluble high degree of polymerization fructan.

*2.3.5 Determination of Metabolites and Minor Non-Structural Carbohydrates*

Fructose-6-phosphate, glucose-g-phosphate, raffinose, trehalose, myo-inositol, malate, citrate, α-ketoglutarate, succinate, fumarate, and shikimate were extracted, identified, and quantified following the procedures of Lisec et al. (2006) and Wang et al. (2010) with minor modification.

These compounds were extracted from liquid $N_2$ ground tissue (~100 mg) in 1.4 mL of 75% (v/v) methanol with 60 µL of ribitol (A5502, Sigma) stock (0.2 mg $mL^{-1}$) added to each sample as an internal standard. Samples were maintained at 30°C while being shaken for 30 min at 950 revolutions per minute (rpm) during the extraction. Samples were then centrifuged (10,000 x *g*) for 10 min, the supernatant was transferred to a tapered 5 mL glass centrifuge tube, 750 µL of chloroform (-20°C) and 1.5 mL of $H_2O$ (4°C) was added, tubes were vortexed for 10 s, and then centrifuged (2200 x *g*) for 15 min. An aliquot (100 µL) of the polar (upper) phase of each sample was then transferred to a 1.5 mL microcentrifuge tube and dried without heating in a vacuum concentrator for 6 h. Dried extracts were then derivatized by adding 40 µL of methoxyamine hydrochloride (M1139, Sigma) stock (20 mg $mL^{-1}$ in pyridine), shaking at 37°C for 2 h at 900 rpm, adding 60 µL of N-methyl-N-trimethylsilyl-trifluoroacetamide (MSTFA, CAS 24589-78-4, Macherey & Nagel, Düren, Germany), and shaking at 37°C for 30 min at 900 rpm. Derivatized samples were then transferred to 100 µL glass inserts (CTI-2410, Chromtech Inc., Apple Valley, MN) placed in 1.5 mL amber screw cap vials (CTV-4802(A), Chromtech), that were then sealed with septa containing screw caps (CTC-0956, Chromtech).

Samples were then analyzed with an Agilent 7890A GC/5795C MS (Agilent Technology, Palo Alto, CA, USA). Injection of a 1 µL aliquot of each sample was performed at 230°C in splitless mode with helium carrier gas flow set to 1 ml $min^{-1}$. Chromatography was performed on a DB-5MS custom capillary column (20 m length x 0.18 mm i.d. x 0.18 mm film thickness) with a 5 m Duraguard column (125-1334G5, Agilent Technology). The temperature program was isothermal at 70°C for 2.471 min, followed by a 10.119°C $min^{-1}$ ramp to 330°C and a final 2.471 min heating at 330°C. Cooling was performed as fast as possible. The system was then temperature equilibrated at 70°C for 5 min before subsequent sample injection. Mass spectra were collected at 5.6 scans $s^{-1}$ over an m/z 50–600 scanning range. The transfer line temperature and the ion source temperature were set to 250 and 230°C, respectively. Metabolites were identified by comparing fragmentation patterns with those in a mass spectral library generated on our GC/MS system and an annotated quadrupole GC–MS spectral library downloaded from the

Max Planck Institute of Molecular Plant Physiology (2010) and quantified based on standard curves generated for each metabolite and internal standard.

### *2.3.6 Monitoring Turfgrass Health*

Approximately every 14 d, all EUs were individually photographed under controlled light conditions using a Cannon PowerShot SX 110 IS camera (Cannon USA Inc., Lake Success, NY) mounted 30 cm above and perpendicular to the turfgrass surface. Lighting was provided by two 70 watt incandescent light bulbs. A white balance reference card (WhiBal G7, Michael Tapes Design, Melbourne, FL) was included within the field of view of each image. Because EUs lacked aerially visible indentifying marks, a written record of photo order and corresponding EU identity was maintained. Using the white balance reference card, white and grey balance of each image was normalized using Adobe Photoshop CS4 (Adobe Systems Inc., San Jose, CA). Images were also cropped to contain only turfgrass foliage within the 10 cm diam. i.d. of the PVC pot.

Once images were normalized and cropped, automated image analysis was performed in SigmaScan pro (v. 5.0, Systat Software Inc., San Jose, CA) using the 'turf analysis' macro presented by Karcher and Richardson (2005). Optimal hue and saturation thresholds (38-110 and 30-100, respectively) were established by starting with default levels outlined in Karcher and Richardson (2005) and iteratively making adjustments that maximized selection of green turfgrass and minimized interference caused by canopy shadow artifacts. Dark green color index (DGCI) of 'green' turfgrass was calculated as described in Karcher and Richardson (2003).

### *2.3.7 Statistical Analysis*

Treatments and observations were made on EUs arranged in a completely randomized design. All statistical analyses were conducted in JMP (version 8, SAS Institute, Cary, NC). Main treatment (K level) effects on DGCI for each observation date were analyzed as repeated measures using the REML method of the MANOVA personality. Main treatment (K level) effects on nonstructural carbohydrate and metabolite data were analyzed for each sampling date

using the REML method of the standard least squares personality in JMP, trial was considered a random effect (McIntosh, 1983). Single degree of freedom orthogonal contrasts were used to determine more specific treatment effects.

## 2.4 Results

### *2.4.1 Tissue Nonacid Cation Content Dynamics*

Following establishment under identical fertilization, there were no significant differences in major non-acid cation (K, Ca, Mg, Na) tissue concentrations across K treatment groups (data not shown). Significant differences in tissue K, Ca, and Mg content were observed among treatment groups 90 d after the initiation of K treatments and these trends largely persisted throughout the experiment (Table 2.6). On every sampling date following K treatment initialization, a positive linear association ($Pr>|t|<0.001$) between tissue K content and an inverse linear association ($Pr>|t|<0.001$) between tissue Ca content and K fertilization rate was observed. With the exception of the final sampling date, an inverse linear relationship ($Pr>|t|<0.001$) between tissue Mg content and K fertilization rate was also observed. Tissue K levels ranged across the recognized (Carrow et al., 2001) K sufficiency level of ~380 $mmol_c\ kg^{-1}$ (15 $g\ kg^{-1}$) on the final three sampling dates. It is important to note that although tissue K content in plants recieving less than 0.50 $g\ K\ m^{-2}\ 7\ d^{-1}$ fell below the recognized sufficiency level, there were no statistically significant differences in dark green color index (data not shown) on any date throughout both runs of the experiment. Clipping yields were not measured due to logistical difficulties of maintaining constant clipping heights while hand-mowing container grown grass; however, there were no obvious differences in clipping production between K treatment groups. Tissue Ca and Mg levels were within recognized 'sufficiency' levels in all cases (Carrow et al., 2001). Overall, there was an inverse relationship between tissue K and Na content. For each K treatment group, the total sum of tissue non-acid cations ($mmol_c\ kg^{-1}$) was not significantly different on any sampling date. Tissue concentrations of K, Ca, Mg and the total sum of tissue non-acid cations decreased once fertilization ceased and plants entered simulated winter

conditions. Tissue Na content increased markedly following plant hardening and remained relatively constant throughout the remainder of the experiment. The concentration of all other plant essential nutrients was not affected by K fertilization rate (data not shown).

**Table 2.6. Least square means of nonacid cation tissue concentrations by K fertilization rate following the fertilization, hardening, mid-winter and early spring experimental periods. Trial was considered a random variable. Mean seperations were conducted using Fisher's protected LSD (α = 0.05)**

| | | Tissue Nonacid Cation Content | | | | |
|---|---|---|---|---|---|---|
| Sample Date† | K Rate | $K^+$ | $Ca^{2+}$ | $Mg^{2+}$ | $Na^+$ | Total |
| | g $m^{-2}$ $7d^{-1}$ | | | $mmol_c$ $kg^{-1}$ | | |
| Fertilization | | | | | | |
| | 0.00 | 436 C‡ | 494 A | 321 A | 29.5 NS§ | 1281 NS |
| | 0.25 | 479 C | 491 A | 298 AB | 31.6 | 1300 |
| | 0.50 | 564 B | 428 B | 279 B | 27.1 | 1299 |
| | 2.00 | 704 A | 385 B | 256 C | 27.1 | 1373 |
| | 3.00 | 742 A | 334 C | 232 D | 25.7 | 1334 |
| Hardening | | | | | | |
| | 0.00 | 290 E | 423 A | 260 A | 97.9 A | 1071 NS |
| | 0.25 | 357 D | 401 A | 243 AB | 75.4 AB | 1078 |
| | 0.50 | 404 C | 369 B | 233 B | 66.4 B | 1073 |
| | 2.00 | 522 B | 321 C | 203 C | 54.6 C | 1101 |
| | 3.00 | 569 A | 302 C | 191 C | 41.6 D | 1105 |
| Mid-Winter | | | | | | |
| | 0.00 | 325 D | 399 A | 244 A | 78.3 A | 1047 NS |
| | 0.25 | 356 D | 374 AB | 223 B | 67.5 AB | 1022 |
| | 0.50 | 405 C | 358 B | 220 B | 63.8 B | 1047 |
| | 2.00 | 514 B | 323 C | 204 C | 56.5 C | 1099 |
| | 3.00 | 562 A | 285 D | 189 D | 50.6 C | 1088 |
| Early Spring | | | | | | |
| | 0.00 | 303 D | 362 A | 205 NS | 72.9 NS | 944 NS |
| | 0.25 | 355 C | 342 AB | 192 | 65.5 | 956 |
| | 0.50 | 405 B | 350 AB | 201 | 60.2 | 1017 |
| | 2.00 | 462 A | 317 BC | 197 | 57.6 | 1035 |
| | 3.00 | 482 A | 298 C | 184 | 56.8 | 1023 |

† Stage of experiment preceding harvest.
‡ Within columns and sampling dates, means not followed by a common letter are significantly different (Fisher's protected LSD; α=0.05).
§ NS, No significant differences between K treatment levels on that sampling date.

*2.4.2 Tissue Carbohydrate Content*

Following the fertilization period, an inverse linear relationship between K fertilization rate and both fructose ($Pr > |t| < 0.001$) and glucose ($Pr > |t| = 0.014$) was observed (Table 2.7). Fertilization rate significantly affected the concentration of both sugars ($\alpha=0.10$) on the final ('early spring') sampling date, with the lowest sugar concentrations associated with the highest two K fertilization rates. Tissue fructose and glucose were not affected by K fertilization rate following 'hardening' or mid-winter'.

Potassium fertilization rate did not affect tissue sucrose content on any sampling date. Raffinose content was not affected by K fertilization rate except following 'mid-winter', where an inverse linear relationship ($Pr > |t| < 0.001$) was observed. Potassium fertilization rate did not affect water soluble, high degree of polymerization fructan (WSF) content on any sampling date. Ethanol soluble, low degree of polymerization fructan (ESF) content was not affected by K fertilization rate except on the final ('early spring') sampling date, where an inverse linear relationship ($Pr > |t| < 0.001$) was observed. Potassium fertilization did not affect tissue trehalose content on any sampling date.

Following the fertilization period, tissue fructose-6-phosphate content was significantly greater in plants fertilized with 3.00 g K $m^{-2}$ 7 $d^{-1}$ than any other K fertilization rate. Fructose-6-phosphate content was not affected by K fertilization on any other sampling date. A positive linear association between tissue glucose-6-phosphate content ($Pr > |t| < 0.001$) and K fertilization rate was observed on every sampling date except following early spring, where no association was observed. Total non-structural carbohydrate content was not affected by K fertilization rate on any sampling date.

**Table 2.7. Mean non-structural carbohydrate content for each K fertilization rate following 'fertilization', 'hardening', 'mid-winter', and 'early spring' experimental phases. Carbohydrate concentrations are expressed on a fresh weight basis of pooled leaf and crown tissue. Mean separations of K treatment levels are reported only when K treatment level was a significant (α=0.05) source of analyte variability.**

| Sample Date† | Non-Structural Carbohydrates‡ | | | | | | | | | |
|---|---|---|---|---|---|---|---|---|---|---|
| g K $m^{-2}$ $7d^{-1}$ | Fructose | Glucose | Sucrose | Raffinose | WSF | ESF | Trehalose | F-6-P | G-6-P | Total |
| | mg $g^{-1}$ fresh wt. | | | | | | | | | |
| Fertilization | | | | | | | | | | |
| 0.00 | 0.89 A§ | 0.55 A | 2.46 NS¶ | 0.71 NS | 33.7 NS | 18.5 NS | 0.097 NS | 0.049 B | 0.051 BC | 57.3 NS |
| 0.25 | 0.69 B | 0.44 B | 2.54 | 0.73 | 31.5 | 16.9 | 0.096 | 0.049 B | 0.049 C | 53.4 |
| 0.50 | 0.63 BC | 0.44 B | 2.47 | 0.74 | 32.6 | 15.1 | 0.101 | 0.047 B | 0.049 C | 52.5 |
| 2.00 | 0.53 CD | 0.46 B | 2.44 | 0.73 | 30.7 | 15.6 | 0.092 | 0.049 B | 0.055 AB | 51.0 |
| 3.00 | 0.47 D | 0.39 B | 2.49 | 0.79 | 31.7 | 16.4 | 0.097 | 0.055 A | 0.058 A | 52.8 |
| Hardening | | | | | | | | | | |
| 0.00 | 4.65 NS | 2.97 NS | 11.4 NS | 2.15 NS | 80.1 NS | 48.0 NS | 0.228 NS | 0.055 NS | 0.053 C | 150 NS |
| 0.25 | 5.54 | 3.80 | 10.4 | 2.08 | 86.0 | 50.2 | 0.196 | 0.052 | 0.058 BC | 159 |
| 0.50 | 4.77 | 3.31 | 10.6 | 1.81 | 79.4 | 54.0 | 0.187 | 0.053 | 0.059 B | 155 |
| 2.00 | 3.71 | 2.67 | 9.19 | 1.94 | 82.4 | 48.6 | 0.163 | 0.055 | 0.067 A | 149 |
| 3.00 | 5.06 | 3.80 | 9.33 | 2.16 | 85.4 | 47.7 | 0.157 | 0.056 | 0.068 A | 154 |
| Mid-Winter | | | | | | | | | | |
| 0.00 | 6.72 NS | 3.83 NS | 7.72 NS | 1.16 AB | 89.4 NS | 47.8 NS | 0.141 NS | 0.045 NS | 0.047 C | 157 NS |
| 0.25 | 7.77 | 4.81 | 6.71 | 1.22 AB | 84.4 | 47.3 | 0.135 | 0.046 | 0.049 C | 153 |
| 0.50 | 7.46 | 4.69 | 7.79 | 1.24 AB | 90.9 | 47.8 | 0.139 | 0.046 | 0.054 B | 161 |
| 2.00 | 6.95 | 4.58 | 7.34 | 0.97 BC | 87.0 | 47.0 | 0.169 | 0.048 | 0.059 A | 155 |
| 3.00 | 7.45 | 4.74 | 6.64 | 0.87 C | 86.0 | 46.0 | 0.128 | 0.048 | 0.062 A | 152 |
| Early Spring | | | | | | | | | | |
| 0.00 | 1.98 NS | 0.77 NS | 1.74 NS | 0.23 NS | 32.9 NS | 16.5 A | 0.081 NS | 0.057 NS | 0.058 NS | 54.7 NS |
| 0.25 | 1.74 | 0.76 | 1.50 | 0.20 | 31.2 | 15.4 AB | 0.081 | 0.056 | 0.056 | 51.4 |
| 0.50 | 1.89 | 0.84 | 1.52 | 0.23 | 29.6 | 15.2 AB | 0.077 | 0.057 | 0.061 | 49.8 |
| 2.00 | 1.61 | 0.64 | 1.53 | 0.22 | 27.2 | 13.9 B | 0.073 | 0.052 | 0.056 | 45.5 |
| 3.00 | 1.61 | 0.65 | 1.57 | 0.21 | 30.9 | 14.1 B | 0.093 | 0.051 | 0.056 | 49.6 |

† Stage of experiment preceding harvest.

‡ WSF, Water soluble fructans; ESF, 80% ethanol soluble fructans; F-6-P, Fructose-6-Phosphate; G-6-P, Glucose-6-Phosphate.

§ Within columns and sampling dates, means not followed by a common letter are significantly different (Fisher's protected LSD; $\alpha$=0.05).

¶ NS, No significant differences between K treatment levels on that sampling date.

*2.4.3 Tissue Metabolite Content*

A positive linear association (Pr> | t | <0.001) between tissue citrate and malate content and K fertilization rate was observed on every sampling date (Table 2.8). A positive linear association (Pr> | t | <0.001) between α-ketoglutarate and K fertilization rate was observed following the fertilization period, but no significant association was observed on any other sampling date. A positive linear association (Pr> | t | <0.001) between succinate and fumarate content and K fertilization rate was observed following the fertilization and hardening periods, but not on any other sampling date. A positive linear association (Pr> | t | <0.001) between total TCA intermediate content and K fertilization rate was observed on every sampling date. A positive linear association (Pr> | t | <0.005) between tissue shikimate content and K fertilization rate was observed following the fertilization period but not on any other sampling date. Potassium fertilization rate did affect tissue myo-inositol content on any sampling date.

**Table 2.8. Mean tricarboxylic acid cycle intermediate, shikimate, and myo-inositol content for each K fertilization rate following ‘fertilization’, ‘hardening’, ‘mid-winter’, and ‘early spring’ experimental phases. Metabolite concentrations are expressed on a fresh weight basis of pooled leaf and crown tissue. Mean separations of K treatment levels are reported only when K treatment level was a significant ($\alpha$=0.05) source of analyte variability.**

| Sample Date† | Tricarboxylic Acid Intermediates | | | | | | Additional Metabolites | |
|---|---|---|---|---|---|---|---|---|
| g K $m^{-2}$ $7d^{-1}$ | Citrate | α-ketoglutarate | Succinate | Fumarate | Malate | Total | Shikimate | Myo-inositol |
| | mg $g^{-1}$ fresh wt. | | | | | | | |
| Fertilization | | | | | | | | |
| 0.00 | 3.77 B‡ | 0.091 B | 0.094 BC | 0.061 B | 1.52 C | 5.54 B | 0.241 AB | 0.286 NS§ |
| 0.25 | 3.44 B | 0.084 B | 0.089 C | 0.059 B | 1.48 C | 5.16 B | 0.226 B | 0.273 |
| 0.50 | 3.86 B | 0.087 B | 0.102 B | 0.059 B | 1.60 C | 5.72 B | 0.242 AB | 0.284 |
| 2.00 | 6.22 A | 0.119 A | 0.117 A | 0.073 A | 2.04 B | 8.58 A | 0.276 A | 0.296 |
| 3.00 | 6.81 A | 0.128 A | 0.128 A | 0.077 A | 2.40 A | 9.56 A | 0.278 A | 0.295 |
| Hardening | | | | | | | | |
| 0.00 | 1.71 D | 0.049 NS | 0.071 C | 0.058 C | 1.71 B | 3.61 D | 0.532 NS | 0.395 NS |
| 0.25 | 2.05 CD | 0.047 | 0.073 C | 0.054 C | 1.76 B | 4.11 CD | 0.581 | 0.398 |
| 0.50 | 2.39 BC | 0.049 | 0.078 BC | 0.059 BC | 2.12 A | 4.71 BC | 0.632 | 0.406 |
| 2.00 | 2.89 BC | 0.049 | 0.085 AB | 0.066 AB | 2.14 A | 5.24 B | 0.578 | 0.416 |
| 3.00 | 3.45 A | 0.051 | 0.092 A | 0.067 A | 2.42 A | 6.09 A | 0.575 | 0.425 |
| Mid-Winter | | | | | | | | |
| 0.00 | 1.75 C | 0.046 NS | 0.063 NS | 0.074 NS | 1.79 BC | 3.73 C | 0.449 NS | 0.579 NS |
| 0.25 | 1.91 C | 0.045 | 0.068 | 0.073 | 1.61 C | 3.72 C | 0.437 | 0.564 |
| 0.50 | 2.35 B | 0.045 | 0.069 | 0.073 | 1.85 AB | 4.39 B | 0.599 | 0.569 |
| 2.00 | 3.24 A | 0.047 | 0.071 | 0.077 | 2.07 AB | 5.51 A | 0.503 | 0.569 |
| 3.00 | 3.53 A | 0.044 | 0.072 | 0.078 | 2.03 AB | 5.77 A | 0.437 | 0.556 |
| Early Spring | | | | | | | | |
| 0.00 | 3.95 B | 0.125NS | 0.087 NS | 0.105 NS | 0.73 C | 5.01 C | 0.304 NS | 0.399 NS |
| 0.25 | 4.06 B | 0.125 | 0.085 | 0.104 | 0.79 C | 5.17 BC | 0.265 | 0.377 |
| 0.50 | 5.06 A | 0.127 | 0.091 | 0.112 | 0.89 BC | 6.29 AB | 0.264 | 0.413 |
| 2.00 | 5.78 A | 0.133 | 0.092 | 0.119 | 1.09 AB | 7.22 A | 0.386 | 0.431 |
| 3.00 | 5.94 A | 0.119 | 0.085 | 0.113 | 1.09 AB | 7.36 A | 0.275 | 0.391 |

† Stage of experiment preceding harvest.

‡ Within columns and sampling dates, means not followed by a common letter are significantly different (Fisher's protected LSD; α=0.05).

§ NS, No significant differences between K treatment levels on that sampling date.

## 2.5 Discussion

### *2.5.1 Tissue Nonacid Cation Dynamics*

Turfgrass scientists, as well as many agronomist and whole plant physiologists almost exclusively report tissue nutrient content on a dry mass basis. This convention may not be appropriate, particularly for K because cytosolic reactions affecting plant growth and metabolism are regulated by cytosolic K concentrations ($mmol_c\ L^{-1}$) , not a dry matter : K relationship (Leigh and Jones, 1984). Therefore, K content on the basis of tissue water ($K_W$) is a more physiologically meaningful parameter (Pitman, 1975). Other disciplines of plant science have reported $K_W$ for ryegrass, barley, and wheat; yet to my knowledge only Woods (2006) presents tissue K content of intensively managed turfgrass as both $K_W$ and $K_D$. In this abstract, tissue K content for creeping bentgrass [*Agrostis stolonifera* var. *palustris* (Huds.) Farw.] was reported between 5-25 g $kg^{-1}$ with corresponding $K_W$ values between 50 and 230 mmol $L^{-1}$. Furthermore, in samples with K concentrations below 15 g $kg^{-1}$, considered to be deficient on a dry mass basis, $K_W$ was often greater than 150 mmol $L^{-1}$, a biochemically sufficient K content (Leigh and Jones, 1984; Marschner, 1995). Tissue $K_W$ levels beyond the broadly defined sufficiency range (>150 mmol $L^{-1}$) may also have inhibitory effects on some enzymes (Preusser et al., 1981). Clearly turfgrass scientists need to diversify their methods of reporting and interpreting tissue K content.

Another useful convention for reporting tissue nutrient content is on a $mmol_c\ kg^{-1}$ basis (Woods, 2006). Even elements that fill a structural role in the plant and are largely electrochemically inactive (e.g. Ca, Mg) are initially taken up in accordance with the electrochemical composition of the soil solution and cell sap. Therefore, it is important to consider elemental electrochemical equivalents as well as tissue concentration on a mass basis. While this designation may seem entirely academic, it has significant implications to interpretation of experimental data. For example, we observed a positive linear association ($Pr>|t|<0.001$) between K fertilization rate and total tissue cation content when elements were

expressed as g $kg^{-1}$ but no association was observed when total cation content was expressed as mmolc $kg^{-1}$ (Table 2.6). As will be discussed in further detail, this changes the interpretation of relationships between nonacid cations and the composition of the nonacid cation pool. While this convention still does not address the fact that elemental composition of cellular compartments and structures is not determined on a dry matter basis, it does account for the electrochemical activities of nutrients upon ion uptake and storage. These results highlight the need to examine tissue nutrient composition using multiple units of measurement, as each convention has strengths, weaknesses, and situations of practical applicability.

Application of fertilizers or soil amendments containing K, Ca, or Mg is known to affect tissue nonacid cation composition of plants (Marschner, 1995; Pelletier et al., 2008a; Pelletier et al., 2008b; Woods et al., 2006). Interestingly, in this study the sum of cations ($mmol_c$ $kg^{-1}$) was not significantly affected by K fertilization rate, while the portion of the total nonacid cation pool occupied by each cation was (Table 2.6). This suggests that there is a conserved physiological limit on cation uptake, irrespective of fertilizer application rate. As such, the ratio of applied fertilizers can be critical determinant of nonacid cation pool composition. Monocots are proficient scavengers of K in soils, as the low cation exchange capacity of their root system (compared to dicots) preferentially excludes Ca and Mg affording them tremendous K uptake capabilities (Marschner, 1995). Therefore, it is likely that the reciprocal nature of nonacid cation uptake in this study was a function of Ca and Mg exclusion at the root/soil interface as well as electrochemical limitations on ion uptake and vacuolar capacity. Interestingly, tissue Ca content was more affected by K fertilization rate than Mg or Na.

The sum of tissue K and Ca ($mmol_c$ $kg^{-1}$) accounts for 92% of total cation content variability with ~85% of points falling between 800 and 1200 $mmol_c$ $kg^{-1}$ of total cations. When tissue Ca content ($mmol_c$ $kg^{-1}$) is plotted versus tissue K content ($mmol_c$ $kg^{-1}$), no statistically significant trend is observed. However, when the % of the total cation pool occupied by Ca is plotted versus the % of the total cation pool occupied by K, a strong inverse linear relationship is observed (Figure 2.2). These results highlight the reciprocal nature of tissue K and Ca content

and the profound effect of these cations on the composition of the total cation pool. No statistically significant correlation between dark green color index and any tissue nutrient parameters was observed; therefore, there is no clear 'optimal' base cation pool composition that affords maximal aesthetic performance. This nonconventional method of reporting tissue cations should be explored further under field conditions and varying nitrogen application rates.

**Figure 2.2. Relationship between tissue Ca and K when both are expressed as the percentage of the sum of nonacid cations ($Cation_{sum}$). Data from the two experimental runs was pooled.**

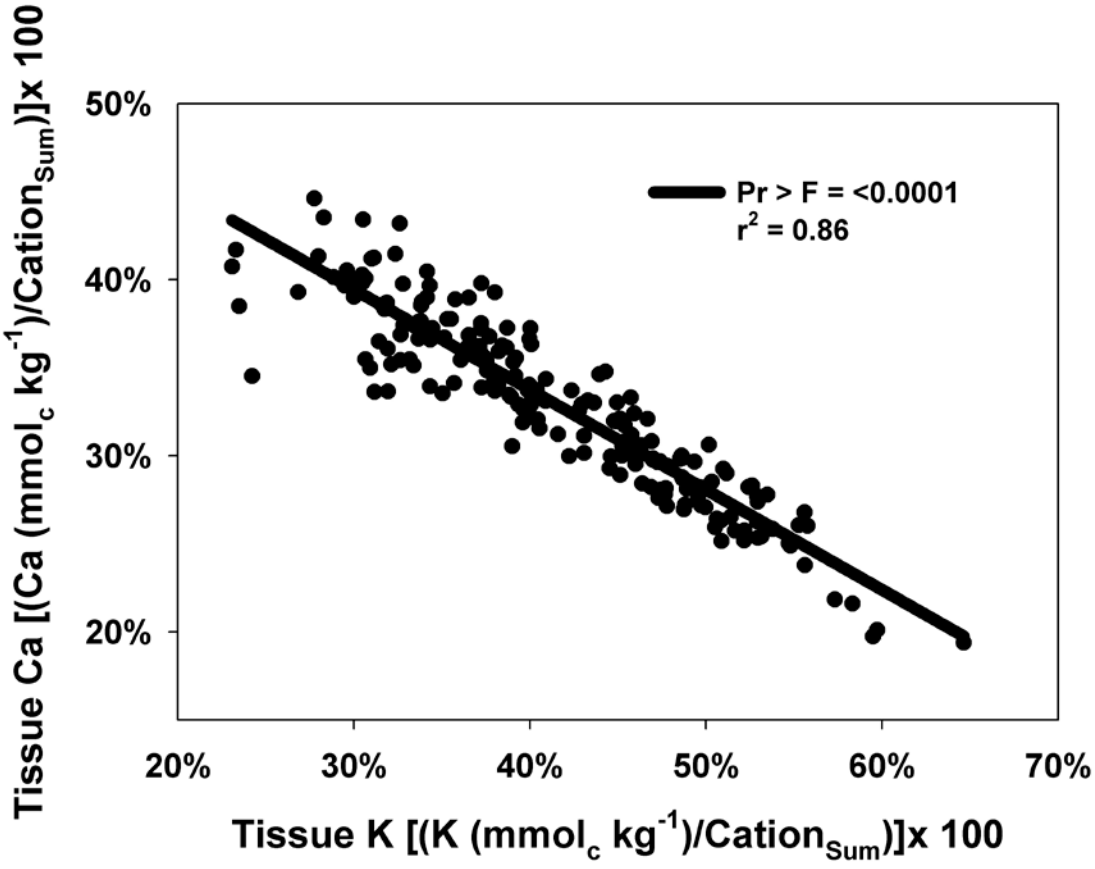

*2.5.2 Non-structural Carbohydrate Dynamics*

Fructose and glucose content following the fertilization period showed an inverse linear relationship with K fertilization rate (Table 2.7), likely due to the effects of plant K status on the speciation of osmotic pressure generating solutes within the vacuole (Evans and Sorger, 1966; Pitman et al., 1968; Wildes and Pitman, 1975). These differences were not apparent following plant hardening, potentially overshadowed by the ~10 fold increase in reducing sugar content following the onset of hardening conditions. Tissue sucrose content was not affected by K fertilization rate. Unlike glucose and fructose, the highest tissue sucrose levels were observed following 'hardening' and these values declined following the 'mid-winter' period. Correspondingly, glucose and fructose concentrations increased during this period, suggesting catabolism of sucrose (and potentially raffinose) to glucose and fructose. Bertrand et al. (2011) made similar observations in winter wheat.

The oligosaccharide raffinose has been shown to influence freezing tolerance of several grass species (Crowe et al., 1988; Koster and Lynch, 1992). Following the 'mid-winter' period, when the likelihood of experiencing killing temperatures in the field would be greatest, an inverse linear relationship between K fertilization rate and tissue raffinose content was observed. While not attributed to the effect of raffinose or other NSCs, Tyler et al. (1981) observed an inverse relationship between K fertilization rate and freezing tolerance of wheat. An inverse linear relationship between K fertilization rate and ethanol soluble-low degree of polymerization fructans (ESF) was observed following the final ('early-spring') sampling date only. Although usually associated with WSFs, spring fructan content has been linked to increased snow mold resistance, spring recovery, and seasonal yield of forage grasses (Bertrand et al., 2011; Lawton and Burpee, 1990; Sanada et al., 2010). The positive linear association between K fertilization rate and tissue glucose-6-phosphate and fructose-6-phosphate on several sampling dates (

Table 2.7) suggests that K fertilization increases the rate of carbon metabolism. These results are discussed further in the context of TCA metabolite dynamics.

### *2.5.3 Tricarboxylic Acid Intermediates*

The tricarboxylic acid (TCA) cycle is central to oxidative metabolism in nearly all organisms, where the oxidation of carbon fuels generates the bulk of reducing power yielded from carbon respiration. Furthermore, TCA cycle intermediates serve as carbon skeletons for nitrogen assimilation, amino acid synthesis, and a myriad of secondary metabolites. Not all TCA intermediates are found in the mitochondria. Beyond steady state concentrations involved in the mitochondrial TCA cycle, malate and citrate are accumulated in the vacuole and mobilized in response to homeostatic demands (Winter et al., 1994). As much as 95% of total malate is found within the vacuole even when whole leaf concentrations increase fourfold (Gerhardt et al., 1987). These organic acids participate in generating osmotic gradients (e.g. stomates), and maintenance of charge and pH homeostasis within cellular compartments (e.g. cytosol and vacuole). Malate transport into the vacuole is via an active transport mechanism (Boller and Wiemken, 1986; Martinoia et al., 1985) and there is considerable evidence that vacuolar malate and citrate transport are mediated by a shared transporter (Rentsch and Martinoia, 1991).

Experiments using $^{13}C$ have shown that citrate formed in the TCA cycle is not found in the cytoplasm, but is actively accumulated in the vacuole (Gout et al., 1993). Furthermore, citrate ions accumulated in the vacuole seem to remain there out of equilibrium with cytoplasmic enzymes even when intracellular carbohydrate pools are extremely low, making vacuolar citrate essentially metabolically inert (Genix et al., 1990; Gout et al., 1993). These features also suggest that citrate plays an important homeostatic roll, particularly in the vacuole.

The tendency of plants to absorb cations and anions at unequal rates depending on soil solution composition apparently violates the absolute principle that the total charge of ions within plant cells equals zero. However, disparate ion uptake ratios and compartmental charge

balance are buffered largely by the organic acids malate and citrate. As cation uptake exceeds anion uptake (the cation-anion difference; CAD), root cell cytosolic pH increases, largely due to extrusion of protons in order to drive K uptake. Consequently, organic acids (~90% malate) are mobilized in a corresponding fashion, maintaining pH homeostasis and serving as counter anions to maintain charge balance (Jacobson and Ordin, 1954). Cations in excess of cellular demands are then shuttled to the vacuole, where malate and citrate serve as charge balancing organic acid anions. This phenomenon has been demonstrated in several classic experiments (Hiatt, 1967; Jacobson and Ordin, 1954; Kirkby and Knight, 1977; Ulrich, 1941). In this experiment, CAD was calculated according to Goff et al. (2004), and mean CAD values were 64, 87, 106, 143, and 166 $mmol_c\ L^{-1}$ for turfgrass fertilized with 0.00, 0.25, 0.50, 2.00, or 3.00 g $K\ m^{-2}\ 7d^{-1}$, respectively. As would be expected, a significant ($Pr>F < 0.0001$), positive linear relationship between cation-anion difference and tissue malate ($r^2 = 0.68$) and citrate ($r^2 = 0.67$) was observed.

Potassium fertilization is an essential determinant of CAD, as tissue K content explains 94% of CAD variability when both parameters are expressed as $mmol_c\ L^{-1}$ and 80% of CAD variability when both parameters are expressed as $mmol_c\ kg^{-1}$. In a more applied sense, CAD is largely a function of tissue K content because nearly all cellular K is electrochemically active and CAD is scaled to account for the structural and therefore electrochemically inactive pool of Ca and Mg. It is important to note that fertilizing with potassium chloride only affected tissue K content. Total tissue cation content, total tissue anion content, and anion pool composition were unaffected by K fertilization rate; therefore, the influence of K fertilization on CAD is strictly due to an increased portion of the total cation pool being electrochemically active as K. As the percentage of the cation pool occupied by K increases, the overall electrochemical activity of cation pool increases, requiring additional organic acid anions to maintain charge homeostasis within the vacuole.

There is apparently no association between tissue malate and tissue K content until K concentrations reach ~125 $mmol_c\ L^{-1}$ (Figure 2.3 A) At tissue K concentration greater than ~125

$mmol_c\ L^{-1}$ a strong positive linear relationship with malate is observed. Interestingly, this value has been suggested as a generalized plant sufficiency level for affording the correct thermodynamic environment for optimal protein hydration, conformation, and function of K dependent enzymes (Leigh and Jones, 1984; Wyn Jones and Pollard, 1983). Furthermore, when tissue K concentrations are greater that ~200 $mmol_c\ L^{-1}$ there appears to be a significant increase in tissue citrate content (Figure 2.3 B)

Luxury K consumption has been described as the accumulation of tissue K to concentrations greater than the amount required to support adequate growth and cell maintenance (Hoagland and Martin, 1933; Wildes and Pitman, 1975). These important benchmarks of tissue K content may reflect the point of K sufficiency and 'luxury K consumption', respectively. These data suggest that malate synthesis increases in response to K uptake rates greater than those needed for maintaining adequate cytosolic K levels whereas citrate synthesis increases once cytosolic K pools are saturated and K begins to accumulate in the vacuole at high concentrations. The increased role of citrate as an organic acid anion at greater K concentrations may be because malate is a divalent organic acid anion whereas citrate is trivalent; therefore, the electrostatic buffering ability on a molar concentration basis is greater for citrate.

**Figure 2.3. Relationship between tissue K content ($mmol_c\ L^{-1}$) and tissue concentrations of the organic acids (A) malate and (B) citrate ($mmol\ L^{-1}$). Data from the two experimental runs is pooled.**

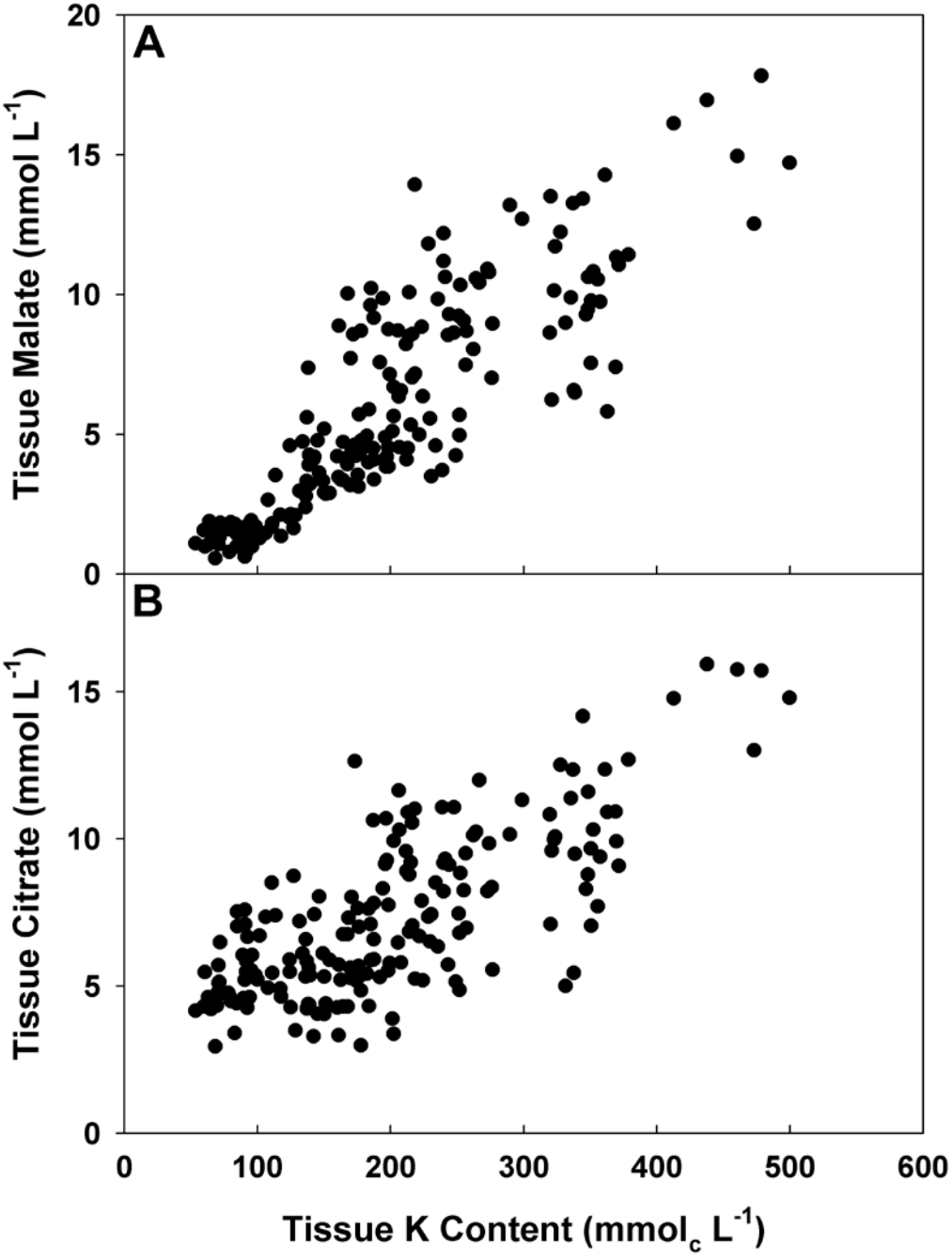
A
B
Tissue Malate (mmol L-1)
Tissue Citrate (mmol L-1)
Tissue K Content (mmolc L-1)
0
5
10
15
20
0
100
200
300
400
500
600

Averaged across all sampling dates, tissue K content was 140, 173, 187, 228, and 260 $mmol_c\ L^{-1}$ for turfgrass fertilized with 0.00, 0.25, 0.50, 2.00, or 3.00 g K $m^{-2}$ $7d^{-1}$, respectively. If ~200 $mmol_c$ K $L^{-1}$ truly represents the threshold designate of luxury K consumption, then fertilizing with K at a rate greater than 0.50 g $m^{-2}$ $7d^{-1}$ (1:1 N:K ratio) would promote luxury K consumption. These data also show that even with no supplemental K applications in a soil with low (6 mg $kg^{-1}$) exchangeable K, tissue K levels can remain at physiologically adequate levels. Without specific measurements of the location and concentrations of K and organic acids these statements are purely speculative; however, this model is logically supported by existing literature and bears further experimental consideration.

As tissue K content and CAD increases, a greater portion of organic acids are siphoned from metabolically active pools to fulfill homeostatic rolls. This represents a significant cost, in terms of the active transport of organic acids into the vacuole and subsequent redistribution in accordance with homeostatic demands, reduced availability of carbon skeletons for anabolic reactions, as well as unrealized ATP and reducing power that would be generated if these carbon resources were fully oxidized via oxidative respiration. The cost of unrealized chemical energy would be particularly pertinent for citrate, as K fertilization had the greatest effect on tissue citrate content and vacuolar citrate is known to be relatively metabolically inert even when carbon resources are low (Genix et al., 1990; Gout et al., 1993). Therefore, luxury K consumption has a real cost, at least on a biochemical level. The fact that malate and citrate are intermediates in multiple important metabolic pathways makes it nearly impossible to estimate a specific cost in terms of ATP, NADH, and/or carbon skeletons; however, it can be assumed with confidence that the utilization of organic acids strictly as homeostatic buffers represents an inefficient use of carbon resources. The positive linear relationship ($Pr>F <0.0001$) between K fertilization rate and other TCA intermediates following fertilization (α-ketoglutarate, succinate, and fumarate) and hardening (succinate, and fumarate) suggests an overall positive association between carbon metabolism and K fertilization rate. This is further supported by the positive

linear association between K fertilization rate and tissue glucose-6-phosphate content, suggestive of a higher rate of carbon flux through glycolysis and oxidative respiration. These findings are logical, as maintenance of pH and electrochemical homeostasis under increasing K fertilization would require greater metabolic carbon flux to satisfy organic acid buffer requirements. While the overall implications of this scenario are unclear, respiration of winter wheat decreases through the fall, and the rate of respiration at 0°C is inversely related to the degree of plant cold hardiness and dormancy (Newton and Anderson, 1931). Following this logic, increasing K fertilization would keep plants at a higher state of metabolic activity thereby compromising their cold hardiness and snow mold resistance. The inverse linear relationship between tissue raffinose content and K fertilization rate following mid-winter also implicates K fertilization in affecting plant cold tolerance. While the total flux of carbohydrates throughout simulated winter was not significantly different across K fertilization treatment groups, it is apparent that carbon resources were utilized differently depending on K fertilization rate. Clearly these topics deserve more attention with regards to plant winter hardiness.

### *2.5.4 Additional Considerations*

In addition to physiological impact of K fertilization on grasses, tissue potassium content is critically important when forages are grown as animal fodder. Fertilizing with adequate K to support maximal yields while preventing luxury uptake is critical, as forage elemental composition can predispose production animals to metabolic disorders associated with electrolyte imbalance. Homeostatic regulation of animal plasma Ca and Mg is greatly affected by electrolyte intake, largely a function of forage K, Ca, and Mg composition. The cation-anion difference (CAD), commonly referred to as dietary cation-anion difference (DCAD), is used to model the potential impact of forages on the manifestation of hypocalcaemia and hypomagnesaemia in dairy cows (Pelletier et al., 2008a). The risk of developing these disorders increases with DCAD, which significantly compromise animal health and farm profitability.

Forage organic acid composition also affects the nutritional quality and energy yield of ensiled crops. The purpose of ensiling grasses (including maize) is to preserve animal fodder resources that cannot be immediately used. Ensiling plant materials in an anaerobic environment promotes microbial fermentation of a portion of labile carbon fuels which lowers silage pH to where additional microbial decomposition of feed materials is inhibited. In doing so, the bulk of forage dry matter and digestible carbon fuels (e.g. carbohydrates, volatile fatty acids) are conserved to a greater extent than they would in an aerobic environment. An important component of efficient silage preservation is a precipitous drop in pH within several weeks of being ensiled. Extending this period can result in considerable dry matter loss through continued microbial decomposition. Malate and citrate contained in silage materials buffer against this pH decrease across the critical pH range of pH 4-6. Roughly 80% of silage buffering capacity comes from plant organic acids (Playne and McDonald, 1966).

Citrate and malate are degraded rapidly (~7 d) following ensiling (Hirst and Ramstad, 1957; Playne et al., 1967). While it is difficult to determine the fate of carbon contained in forage citrate and malate, they are rapidly fermented by microorganisms to organic acids with even greater buffering capacities, leading to delayed silage preservation (McDonald and Henderson, 1962). The overall impact of the buffering effects of malate, citrate, and/or their derivatives is that a larger portion of labile sugars are required to reduce silage pH to stable levels that support preservation. In fact, 50-80 times more hexose equivalents can be required to achieve silage preservation when the buffering capacity of organic acids is considered (Smith, 1962). Furthermore, the direct conversion of malate and citrate to pyruvate during fermentation results in 46 and 66% of dry matter loss as $CO_2$, respectively. This leads to greatly reduced efficiency in the conversion of plant biomass to suitable animal fodder. While organic acids may only represent ~1-2% of forage dry weight, this small percentage can significantly affect forage quality and preservation efficiency, particularly on larger farms where thousands of tons of silage are used annually.

In conclusion, the negative impact of excessive potassium fertilization on forage management is three-fold. The economic burden of K fertilization is significant, as potash costs have increased by ~300% over the past 10 years (USDA, 2010) making efficient use of fertilizers essential. Feeding animals high-potassium forages increases their likelihood of suffering from metabolic disorders associated with electrolyte imbalances. Finally, increased forage malate and citrate content at high K fertilization rates would result in less efficient conversion of resource intensive crop biomass to animal feed. These factors significantly impact production efficiency in a business were efficiency is paramount to economic viability, especially considering that feed represents ~75% of a dairy farms total operating cost (USDA, 2011).

## 2.6 Conclusions

As social awareness of environmental issues increases, a substantial amount of research is being directed towards reducing fertilizer and pesticide applications to agricultural and landscape crops while maintaining high productivity. In the past, K fertilizers were inexpensive and because K does not have any obvious detrimental impacts on plant performance or the environment, refining K fertilization strategies was not of practical or economic significance. In this study, we found that K fertilization rate has significant impacts on plant metabolism and on crop utility when used as animal feed. Results from a study run in parallel (Chapter 3) also demonstrated that K fertilization increases the risk of grey snow mold (*Typhula incarnata* Fr.) damage. While there is no doubt that K fulfills a critical role in plant function and utility, gratuitous applications of K fertilizers may be a costly, unnecessary, and wasteful allocation of resources with significant practical and economic consequences.

Besides affecting snow mold susceptibility, the relationship between K fertilization, plant utilization of carbon resources, and seasonal plant stresses remains unclear. However, the findings of this study provide a framework for devising new studies to examine the effects of K fertilization on carbon utilization of grasses under various stresses. A more robust data set taken from multiple environments where a greater number of ‘performance’ parameters were

monitored would provide more comprehensive information regarding whether increased diversion of carbon resources to organic acid anion production significantly affects plant performance. Understanding how fertilizer and soil chemical composition affect plant cation-anion balance, carbon utilization, and subsequent plant performance presents an interesting area of future research.

# CHAPTER 3: POTASSIUM FERTILIZATION AFFECTS PSYCHROPHILIC PATHOGEN SUSCEPTIBILITY OF ANNUAL BLUEGRASS

**3.1 Abstract**

*Typhula incarnata* (GSM) and *Microdochium nivale* (PSM) are important psychrophilic pathogens of cool-season turfgrasses. Existing field data suggests that K fertilization may affect disease severity, warranting additional experimentation under controlled conditions. In a greenhouse, annual bluegrass [*Poa annua* var. reptans (Hauskn) Timm.] was seeded into 120 – 30 x 10 cm diam. sand filled columns. Nitrogen (0.5 g $m^{-2}$ ), K (0.5 g $m^{-2}$), and all other essential nutrients were applied weekly for 90 d. Following establishment, weekly application rates of N and essential nutrients remained constant, yet 5 different K treatments (0, 0.25, 0.5, 2, 3 g $m^{-2}$) were imposed for 90 d. Columns were then moved to a refrigerated room, maintained under a photosynthetically active radiation flux of ~300 µmol $m^{-2}$ $s^{-1}$, and day/night air temperature incrementally decreased every 7 d over 28 d (10/4°C, 4/-2°C, 2/-4°C, -2/-6°C). Plants were then buried under 10 cm of snow and kept under darkness at -4°C for 28 d. After thawing at 2°C, 8 replicates of each K treatment were inoculated with a 5 mm agar disc taken from GSM, PSM, or sterile cultures. Columns were incubated at 2°C (40 d) then 4°C (40 d) under periodic misting and evaluated for % necrotic turf every 10 d. Survival analysis of days to 50% infection ($LI_{50}$) was used to quantify disease progression. Tissue harvested following each experimental phase was analyzed for nonacid cations, nonstructural carbohydrates, and several organic acids. The experiment was conducted twice and data was pooled. Potassium treatment significantly affected $LI_{50}$ in GSM ($Pr>\chi^2$ =0.007) but not PSM ($Pr>\chi^2$ =0.277) inoculated turf. While specific mechanisms remain unclear, several biochemical parameters (K, Ca, organic acid content) associated with GSM and PSM severity were impacted by K fertilization rate. In contrast to existing literature, nonstructural carbohydrate dynamics were not strongly correlated with disease severity.

## 3.2 Introduction

Winter cereals, perennial forages, ornamental turfgrasses, and conifers grown in northern locales are annually subjected to weather conditions that favor infection by *Microdochium nivale* [Fries] Samuel & Hallett (Pink snow mold, PSM), *Typhula spp.* (Grey snow mold, GSM), and other psychrophilic pathogens (Hartig, 1888; Hsiang et al., 1999). These pathogens can cause considerable crop damage during cool (0-15°C) wet weather (PSM) or following extended periods of continuous snow cover (PSM & GSM). These losses can affect the utility and spring recovery of amenity turfgrasses (Chang and Jung, 2009) and the spring recovery (Sanada et al., 2010) and seasonal yield of winter cereals (Lawton and Burpee, 1990).

Psychrophilic organisms, including pathogenic snow molds, have recently been identified as important contributors to carbon and nitrogen fluxes in subnivean environments (Larsen et al., 2007; Schmidt et al., 2008; Schmidt et al., 2009). Furthermore, snow mold disease pressure appears to be an important selective force in determining genetic diversity of amenity turfgrass (Bertrand et al., 2009; Wang et al., 2005) and forage grass populations (Hwang et al., 2002). The profound impact of these organisms on subnivean ecosystems has engendered growing interest in studying their biology and plant/snow mold interactions.

Snow molds caused by *Typhula spp.* develop exclusively under snow cover, and for this reason can only be treated preventatively with fall applications of fungicides that may loose efficacy through the winter. While PSM is often found in association with GSM, snow cover is not a strict prerequisite for PSM manifestation. The insulative properties of prolonged snow cover allows soil to thaw through geothermal heat flux, thereby maintaining soil temperatures near 0°C (Bruehl, 1982). These conditions facilitate growth of psychrophilic organisms and allow considerable depletion of plant storage carbohydrates, which are critical to affording plant resistance to snow molds and cold hardiness (Gaudet et al., 1999; Sanada et al., 2010). Furthermore, transcript levels of candidate plant defense and stress-related genes in winter wheat (*Triticum aestivum* L.) decrease over time when held at near-freezing temperatures (Gaudet et al., 2011).

The connection between cold hardiness and snow mold susceptibility is unclear, although both seem inseparably related to overwintering nonstructural carbohydrate (NSC) dynamics. Gaudet and Kozub (1991) did not observe a direct correlation between cold hardiness and resistance to most snow mold fungi; however, low temperature stress increases plants susceptibility to snow mold and snow mold infection may reduce cold hardiness (Gaudet and Chen, 1988). Recently, the combined work of Bertrand et al. (2011) and Dionne et al. (2010) demonstrated that cold hardiness and snow mold resistance are not always mutually exclusive traits, and that high degree of polymerization fructans are critical determinants of both. Furthermore, Gaudet et al. (2011) reports that antifreeze proteins isolated from winter rye (*Secale cereale* L.) apoplasts by Hon et al. (1994) and Griffith et al. (1992) are related to chitinases and β-1,3-glucanases, implicating their dual role in low temperature survival and pathogen defense. There is some evidence that a non-specific decline in cell water potential through the accumulation of osmotically active solutes (including NSCs) may contribute to cold hardiness and snow mold resistance as well (Tronsmo, 1986).

Snow mold resistance seems to be acquired within 1-2 weeks following the onset of 'hardening' conditions and is dependent on light (Nakajima and Abe, 1996); in contrast, cold hardiness seems to develop more slowly, over a period of 4-8 weeks (Dionne et al., 2001; Koster and Lynch, 1992; Levitt, 1980) and is light independent (Nakajima and Abe, 1996). More recent research presents a somewhat different timeline for the development of cold hardiness and snow mold resistance. Molecular characterization of cold hardiness genes suggests a more rapid (1-2 d) initiation of freezing tolerance (Sung and Amasino, 2005), while Gaudet et al. (2011) reports that maximum expression of genes associated with snow mold resistance is not realized until plants are exposed to low temperatures for a period of at least 21 days.

While molecular characterization of snow mold resistance is just beginning, several common themes have persisted in the literature for nearly 30 years. High polymeric sugar concentrations in autumn and winter as well as elevated fructan content in the spring are characteristic of snow mold resistant winter wheat varieties (Bertrand et al., 2011; Kiyomoto and

Bruehl, 1977; Sanada et al., 2010). Gaudet et al. (1999) suggest that exceptionally resistant varieties accumulate high levels of storage carbohydrates during the fall, affording their ability to maintain high concentrations of simple sugars throughout winter into spring. Bertrand et al. (2011) convincingly support this premise. These simple sugars may induce the expression of plant defense resistance genes though the hexokinase signal transduction pathway (Herbers et al., 1996). It has since been shown that several important pathogenesis related genes can be induced by soluble carbohydrates as well (Roitsch et al., 2003). There may also be a connection between the down regulation of photosynthesis, the accumulation of mono- and disaccharides during the onset of cold temperatures, and a concomitant up regulation of plant defense mechanisms (Herbers et al., 1996). Pociecha et al. (2010) observed differences in photosynthetic efficiency and carbohydrate storage between snow mold susceptible and resistant Festulolium genotypes, but the specific impacts of these phenomena on snow mold susceptibility is unclear.

Several cold-induced pathogenesis related proteins have also been associated with increased non-specific resistance to snow molds in winter wheat (Gaudet et al., 2003a; Gaudet et al., 2003b). Of these proteins, the monocot non-specific lipid transfer proteins have shown *in vitro* toxicity to pathogenic snow molds, apparently affecting fungal membrane permeability (Sun et al., 2008). Interestingly, transcripts of the defense related proteins γ-thionin and γ-purothionin were strongly upregulated during hardening yet were not detected following 1 d exposure to 20°C (Gaudet et al., 2003a). These results are in agreement with observations that overwintering plants can ‘deharden’ rapidly following exposure to warm temperatures, leaving them more susceptible to winter injury (Tompkins et al., 2000).

For many years turfgrass managers have been under the impression that increased seasonal or late-season K fertilization affords increased turfgrass resistance to snow molds, yet no peer reviewed literature supports this notion. This common ethos likely stems from the ubiquitous comprehensive review of turfgrass culture written by Beard (1973). Citing Goss and Gould (1968), Beard comments that higher potassium levels reduce the incidence of PSM. Closer inspection of Goss and Gould’s article reveals a less than convincing argument. Without

showing statistical analyses or data, the authors vaguely describe that increasing K applications from 0 to 400 kg $ha^{-1}$ $yr^{-1}$ reduced PSM disease severity, but not every year. They continued to comment that when N application rates were 1000 kg $ha^{-1}$ $yr^{-1}$, increasing K fertilization did not affect disease severity, and that this indicates proof that a 20:4:8 N:P:K ratio for the total season is in balance. Clearly our understanding of turfgrass fertility has advanced in the past 40 years, and the longstanding association between K fertilization and snow mold severity needs to be revisited. To the contrary of Goss and Gould (1968), both Woods et al. (2006) and Webster and Ebdon (2005) observed a positive, linear associated between snow mold severity and K fertilization. The physiological basis of these findings is unclear, yet K is directly and/or indirectly involved in many fundamental plant processes related to the aforementioned plant defense strategies.

The specific environmental conditions required for snow mold manifestation limits scientists ability to study the biology of these unique organisms and plant/pathogen interactions in the field. Furthermore, snow cover provides a physical barrier that precludes scouting of disease development and implementation of disease control options mid-winter, making it paramount to study pre-winter management strategies that may delay disease onset or improve spring recovery. Agricultural managers have a high level of control over seasonal crop fertilization, thus providing an opportunity to minimize the potential for overwintering crop losses. Therefore, the goal of this research was to confirm or refute the previously reported effects of K fertilization on snow mold severity in a controlled environment, and evaluate physiological parameters associated with the observed response.

## 3.3 Materials and Methods

### *3.3.1 Pathogen Isolation*

*Typhula incarnata* (GSM) was obtained from visually infected turfgrass (sclerotia present) at Portland Country Club (Falmouth, ME). The fungus was isolated and cultured

following the procedures of Chang et al. (2006b). Sclerotia from infected annual bluegrass leaves were surface sterilized with 10% bleach for 20 s, rinsed with $H_2O$, plated on 1.5% water agar (WA, Difco Laboratories, Detroit, MI), and incubated at 10°C for 14 d. Aided by a dissecting microscope, a sterile scalpel and forceps were used to extract one hyphal tip emanating from a single sclerotium. The hyphal tip was transferred to potato dextrose agar (PDA, Difco Laboratories, Detroit, MI) and incubated at 10°C. Once mycelia were present (~ 4 d), the culture was transferred to a 4°C incubator in the dark. After ~10 d, sclerotia were present and no fungal or bacterial contaminants were apparent.

Culture purity was confirmed in the following manner. Cellophane circles (150 mm diam.) were placed in a 150 x 15 mm glass Petri dish and covered with 10 mL of distilled water ($dH_2O$). The covered Petri dish was then autoclaved twice, waiting 24 h between each sterilization. The sterile cellophane disc was then placed on the surface of a PDA culture. A 5 mm cube was cut from the center of the presumed pure culture and placed on the surface of the cellophane disc (Hsiang and Wu, 2000). Following 14 d incubation at 10°C, mycelium was scrapped off of the cellophane using forceps, placed in a 2.2 mL microcentrifuge tube, and lyophilized. Fungal DNA was extracted from 100 mg of lyophilized mycelium using the Qiagen DNeasy Plant Mini Kit (Qiagen Inc., Valencia, CA, USA). Polymerase chain reaction (PCR) was then conducted using the extracted DNA and GSM specific primers (Chang et al., 2006b) designed from the internal transcribed spacer (ITS) of the nuclear ribosomal DNA (GSMF1:5'-AGGGCCGTCTGAGGCTCTCC-3'; GSMR1:5'-AGGGCCGTCTTTATAACGGT-3'), or a generic fungal primer set (ITS-1: 5'-TCCGTAGGTGAA CCTGCGG-3') and (ITS-4: 5'-TCCTCCGCTTATTGATATGC-3') (White et al., 1990). The 25 µL reactions were conducted with thermal cycling conditions of 91°C for denaturation (60 s for 1$^{st}$ cycle, 15 s thereafter), 61°C for annealing (15 s), and 72°C for elongation (70 s) for a total of 40 cycles. Products of each reaction were visualized in a 1.5% agarose gel impregnated with SYBR® safe DNA gel stain (invitrogen, Carlsbad, CA, USA). Reactions containing GSMF1/GSMR1 or ITS 1,4 primer

pairs yielded single ~750 kb or ~850 kb bands, respectively. These findings supported the visual determination of culture purity.

To further confirm the identity of the pure culture, PCR reaction products were purified using the QIAquick PCR Purification Kit (Qiagen Inc., Valencia, CA, USA) and the purified product was sequenced using an Applied Biosystems Automated 3730 DNA Analyzer (Applied Biosystems, Carlsbad, CA), at the Cornell University Life Sciences Core Laboratories Center.

The top match in the National Center for Biotechnology Information (NCBI) basic local alignment search tool (BLAST) (Altschul et al., 1990) is a *T. incarnata* strain (E value = $1x10^{-92}$) isolated from infected turfgrass in Cambridge, Ontario (Hsiang and Wu, 2000; NCBI, 1999). The top 15 matches are all *T. incarnata* isolates collected at The University of Wisconsin-Madison. These results confirmed the purity and identity of the isolated organism. This pure 'master culture' was propagated on fresh PDA media every 14 d and maintained under darkness at 4°C (Chang et al., 2007; Chang et al., 2006b).

*Microdochium nivale* (PSM) sampled from Portland Country Club was isolated and cultured similarly to Nicholson et al. (1996). Surface sterilized, visibly infected leaf tissue was plated on water agar media containing kanamycin, rifampicin, and penicillin (KWARP) and incubated in the dark at 10°C. Once mycelia were present (~4 d), a scalpel and forceps were used to remove and transfer a single hyphal tip to fresh KWARP media. Following 4 d of incubation, a single hyphal tip from this culture was removed and transferred to a PDA culture plate.

To confirm culture purity, six - 5 mm discs were removed from random positions within the presumed pure culture and placed in a 150 x 15 mm sterile glass Petri dish containing 40 mL of potato dextrose broth (PDB, Difco Laboratories, Detroit, MI). Following 14 d of incubation at 10°C, the mycelium was harvested and immediately lyophilized. Fungal DNA was extracted from 100 mg of homogenized lyophilized mycelium using the Qiagen DNeasy Plant Mini Kit (Qiagen Inc., Valencia, CA, USA). Polymerase chain reaction was then conducted using the extracted DNA and the generic, yet fungal specific ITS-1 and ITS-4 primer set (White et al., 1990). The 25 µL reaction was conducted with thermal cycling conditions of 95°C for

denaturation (180 s for 1st cycle, 30 s thereafter), 58°C for annealing (30 s), and 72°C for elongation (60 s) for a total of 30 cycles. Reaction products were visualized in a 1.5% agarose gel impregnated with SYBR® safe DNA gel stain. A single band ~550 kb was observed, confirming culture purity. To further confirm the identity of the pure culture, PCR reaction products were purified using the QIAquick PCR Purification Kit and the purified product was sequenced as described for GSM at the Cornell University Life Sciences Core Laboratories Center.

The top two matches in the NCBI BLAST database were *M. nivale* strain DSM62278 (E value = 0.0) isolated from 'sports grass courts' in Switzerland (NCBI, 2006) and an uncultured *Monographella nivalis* (teleomorph of *Microdochium nivale*) isolated from an Austrian grassland (E value = 0.0) (Klaubauf et al., 2010; NCBI, 2009). All of the top 20 matches are described as *Monographella nivalis* or *Microdochium nivale*, confirming the purity and identity of the isolated organism. This pure 'master culture' was propagated on fresh PDA media every 14 d and maintained under darkness at 4°C.

*3.3.2 Plant Establishment, Fertility Treatments, Simulated Winter, and Biochemical analyses.*

Experimental protocols were identical to those described in section 2.3.

*3.3.3 Inoculation of Experimental Units*

Once EUs were moved to the third room of the reefer, randomly positioned on a 3 x 4 m slotted rack elevated above a catch basin, and held at 2°C for 24 h under darkness, 8 replicate EUs of each K level were inoculated with a 5 mm disc obtained from the growing margin (Nicholson et al., 1996) of a 21 d old GSM PDA culture, a 14 d old PSM PDA culture, or from a random position within a sterile PDA culture (8 replicates x 5 K levels x 3 inoculum = 120 EUs). Once inoculated, EUs were maintained under darkness and an ambient air temperature of 2°C for the first 40 d and then 4°C for another 40 d. Experimental units were misted every 1 h for 15 s,

providing ~0.5 cm of precipitation every 7 d. These conditions were imposed to simulate the darkness, 24 h leaf wetness, ~99% relative humidity, and near 0°C temperatures that persist under snow cover during late winter and early spring. This is subsequently referred to as the 'early spring' period. These conditions were also chosen to provide near-optimal growth conditions for GSM and PSM (Remsberg, 1940; Wu and Hsiang, 1999).

*3.3.4 Monitoring Turfgrass Health*

Starting 30 d after inoculation, all EUs were photographed every 10 d under controlled light conditions using a Canon PowerShot SX 110 IS camera (Canon USA Inc., Lake Success, NY) mounted 30 cm above and perpendicular to the turfgrass surface. Lighting was provided by two 70 W incandescent light bulbs. A white balance reference card (WhiBal G7, Michael Tapes Design, Melbourne, FL) was included within the field of view of each image. Using the white balance reference card, white and grey balance of each image was normalized using Adobe Photoshop CS4 (Adobe Systems Inc., San Jose, CA). Images were also cropped to contain only turfgrass foliage within the 10 cm diam. of the pot.

Once images were normalized and cropped, visually symptomatic turfgrass cover (VSTC) was estimated. Furthermore, computed symptomatic turfgrass cover (CSTC) was determined by computer-automated image analysis (SigmaScan Pro v. 5.0, Systat Software Inc., San Jose, CA). During visual analysis, images were viewed in Adobe Photoshop CS4 and circles of known circumference were overlaid on the image to assist in accurate visual estimation of percent symptomatic turfgrass area in 5% intervals. Utilizing circles of known circumference to assist visual estimation of disease progress is particularly pertinent for evaluating snow molds, as these organisms grow in concentrically expanding hyphal mats both in culture and in the field (Schmidt et al., 2009). The lack of identifying marks on EUs ensured unbiased assessment of all images.

Automated image analysis was performed in SigmaScan pro using the 'turf analysis' macro presented by Karcher and Richardson (2005). Optimal hue and saturation thresholds (38-

110 and 30-100, respectively) were established by starting with default levels outlined in Karcher and Richardson (2005) and iteratively making adjustments that maximized selection of visually non-symptomatic turfgrass and minimized interference caused by the PDA inoculum disc, and canopy shadow artifacts. Computed symptomatic turfgrass area was determined by subtracting the area of 'green' turfgrass (as determined by preset thresholds) from the total area. Dark green color index (DGCI) of 'green' turfgrass was calculated as described in Karcher and Richardson (2003).

*3.3.5 Determination of Disease Severity*

Under field conditions, metrics of snow mold resistance or disease severity are limited to measurements of healthy or symptomatic turfgrass cover following snowmelt (Burpee et al., 1987; Sanada et al., 2010; Woods et al., 2006). This is particularly true for *Typhula* snow molds, as these organisms require prolonged snowcover to manifest in the field (Chang et al., 2006b; Hsiang et al., 1999). *Microdochium nivale* on the other hand has less stringent environmental requirements (Hsiang et al., 1999; Kaminski et al., 2004), allowing more thorough analysis of disease progression.

Several other snow mold severity metrics have been proposed, including the index of damage by snow mold (IDSM) (Sanada et al., 2010), average disease severity index (ASI) (Hartman et al., 1984), and PCR based methods for quantifying fungal DNA within infected plant tissues (Nicholson et al., 1996). While these methods can be useful in some studies, IDSM and ASI rely on a 'real-time' (no permanent image record), unaided, 0-9 visual rating scale. Ordinal data generated in this manner often shows considerable variability, can be difficult to reproduce by other evaluators, do not always provide adequate resolution to determine intermediate levels of disease severity, and can limit the power of statistical inference (Horst et al., 1984). More modern PCR based methods are extremely powerful in exploring pathogen growth dynamics within a single-plant; however, the extreme sensitivity inherent to PCR techniques precludes larger scale disease analysis. Visual estimation of disease progression on a

% symptomatic turfgrass scale is commonly used for evaluating snow mold severity (Chang et al., 2006a) and/or host resistance (Nakajima and Abe, 1996). Employing both computer automated and computer aided visual analysis techniques to rate EUs provides two methods of unbiased analysis with complementary strengths and weaknesses that will explored further during the discussion of results.

Crop researchers have long used the area under the disease progress curve (AUDPC) to evaluate patterns of disease severity in space/time and develop measures of quantitative plant resistance. A dizzying array of AUDPC variants exist in the literature (Jeger and Viljanen-Rollinson, 2001; Waggoner et al., 1986). Here, AUDPC was calculated from visual disease analysis data as described by Das et al. (1992) and Shaner and Finney (1977). In addition to AUDPC, days of incubation to 50% symptomatic turfgrass ($LI_{50}$) was estimated using visual disease analysis data in a manner similar to Nakajima and Abe (1996) and Hofgaard (2006).

*3.3.6 Turfgrass Recovery*

Maintaining EUs under 'optimal' conditions for several weeks following exposure to extreme abiotic conditions or disease epidemics and measuring healthy turfgrass cover is a common method for evaluating recuperative ability and longer-term implications of stresses (Hofgaard et al., 2006; Nakajima and Abe, 1996; Patton and Reicher, 2007; Webster and Ebdon, 2005; Yoshida et al., 1998). Here, following simulated winter in the reefer, all EUs were moved to a greenhouse and maintained at 25/10°C Day/Night temperatures and a 16 hr day length with average daily maximum PPFD of 1000 µmol $m^{-2}$ $s^{-1}$. Experimental units were photographed and evaluated as described above. From a practical standpoint, understanding the effects of prior K fertilization on turfgrass re-recovery from snow mold injury and overall winter decline was desirable. Therefore, the sensitivity of CSTC to quantifying both aspects of winter injury made it the most appropriate turfgrass recovery measurement protocol.

Several snow mold studies (Boulter et al., 2002; Chang and Jung, 2009) evaluate the percentage of symptomatic turfgrass remaining after a recovery period, or the total recovered

area as measures of turfgrass recovery from winter/snow mold injury. While these data provide useful information, the percentage of potential recovery realized and/or area under the crop recovery curve (Lawton and Burpee, 1990) provide a more thorough assessment of a stands recuperative ability for several reasons.

The percentage of symptomatic turfgrass remaining after a recovery period permits the relative ranking of treatment groups based on the final conditions of the turf stand, but does not account for the starting condition of the EU. Stand condition following recovery is inevitably correlated with stand condition following disease incubation (Boulter et al., 2002; Chang and Jung, 2009; Woods et al., 2006); therefore, this measure merely provides an additional metric of disease severity and not recovery *per se*.

The percentage of turfgrass improvement following recovery (% symptomatic turfgrass following incubation - % symptomatic turfgrass following recovery) is a poor measure of turfgrass recovery as it is inherently limited by the stand's potential for recovery. For example, if an EU starts the recovery period with 0% symptomatic turfgrass then by default total recovery will be 0%. This result could be erroneously interpreted as a lack of recovery, an undesirable situation. Both the percentage of potential recovery (total improvement following recovery/(100% - symptomatic turfgrass following winter)) and area under the crop recovery curve (Lawton and Burpee, 1990) account for stand status prior to recovery; therefore, providing a more appropriate metric of crop recuperative ability.

### *3.3.7 Statistical Analysis*

Treatments and observations were made on EUs arranged in a completely randomized design. All statistical analyses were conducted in JMP (version 8, SAS Institute, Cary, NC). Main treatment and interaction effects on AUDPC, AUCRC, and nonacid cation content data were analyzed using the REML method of the standard least squares personality in JMP, trial was considered a random effect (McIntosh, 1983). Main treatment and interaction effects on censored $LI_{50}$ data was analyzed first by the REML method of the proportional hazard

personality to specifically identify the effects of trial, fungus, and all interactions. Potassium level treatment effects on censored $LI_{50}$ data pooled across both trials was then analyzed separately for each fungus type (GSM and PSM) using Kaplan-Meier survival/reliability analysis.

## 3.4 Results

### *3.4.1 Tissue Nonacid Cation Content Dynamics*

See section 2.4.1 for nonacid cation content dynamics.

### *3.4.2 Metrics Used for Disease Progression Analysis*

Experimental units that were inoculated with sterile PDA discs showed no visual disease symptoms throughout the experiment (VSTC = 0); therefore, CSTC data from these samples provides a measure of turfgrass decline caused by factors other than snow mold infection. These data also provide a measure of how readily automated image analysis differentiated between turfgrass color change caused by seasonal decline or disease. Computed symptomatic turfgrass cover erroneously over-estimated symptomatic turfgrass by ~10% in trial #1 and ~20% in trial #2 (Table 3.1). Potassium level did not influence CSTC of sterile PDA inoculated EUs.

**Table 3.1. Computed symptomatic turfgrass cover of non-inoculated experimental units**

| Days of Incubation | Computed Symptomatic Turfgrass Cover† | |
|---|---|---|
| | Trial #1 | Trial #2 |
| 0 | 3.38 | 12.8 |
| 30 | 8.71 | 24.9 |
| 40 | 7.03 | 20.1 |
| 50 | 10.7 | 20.9 |
| 60 | 9.01 | 25.1 |
| 70 | 20.8 | 27.3 |
| 80 | 21.4 | 27.1 |
| Mean | 11.6 | 22.6 |

† Thresholds: Hue: 38-110; Saturation: 30-110)

There is considerable relative agreement between VSTC and CSTC (Figure 3.1 A, B); however, CSTC tends to be greater than the ideal 1:1 ratio below 20% and 30% VSTC (trial #1 and #2, respectively), and less than the 1:1 ratio above these values. In order for CSTC to be used as a valid surrogate measure of disease severity, CSTC values would need to be 'adjusted' to account for turfgrass decline caused by factors other than snow mold infection. If CSTC means from sterile PDA inoculated controls are subtracted from CSTC values for each inoculated EU at corresponding measurement dates, many 'adjusted' CSTC values fall below 0, even when VSTC is as high as 50% (Figure 3.1 C, D). Furthermore, adjusted CSTC values fall almost entirely below the 1:1 CSTC:VSTC ratio across the entire measurement range. The disparity between VSTC and both adjusted and non-adjusted CSTC at the lower and upper limits (0 and 100%) of the measurement scale is particularly concerning, because visual designation of 0% symptomatic turfgrass or 100% symptomatic turfgrass is quite absolute. Low adjusted CSTC values and the discrepancy between CSTC and VSTC is largely a function of significant decline in turfgrass green color (particularly trial #2) due to factors other than disease.

In conclusion, computer automated image analysis did not provide a valid measurement of disease severity in this study. While this technique has been used with considerable success to identify diseased turfgrass in a healthy/green sward (Karcher and Richardson, 2005) and quantify vegetation cover in a soil background (Richardson et al., 2001), the binary nature of digital image analysis (green or non-green) limits the applicability of this technique to situations where multiple factors contribute to turfgrass decline. As a result, snow mold severity metrics discussed in subsequent sections will rely on VSTC data.

**Figure 3.1. Computed symptomatic turfgrass cover vs. visually symptomatic turfgrass cover (A, B). Adjusted computed symptomatic turfgrass cover ($CSTC_{Adjusted} = CSTC_{Sample} - CSTC_{non\text{-}inoculated\ control}$) vs. visually symptomatic turfgrass cover (C, D). Trial #1 (A, C) and Trial #2 (B, D) are compared side to side. Data from inoculation 'day 0' and non-inoculated control experimental units were removed from the data set.**

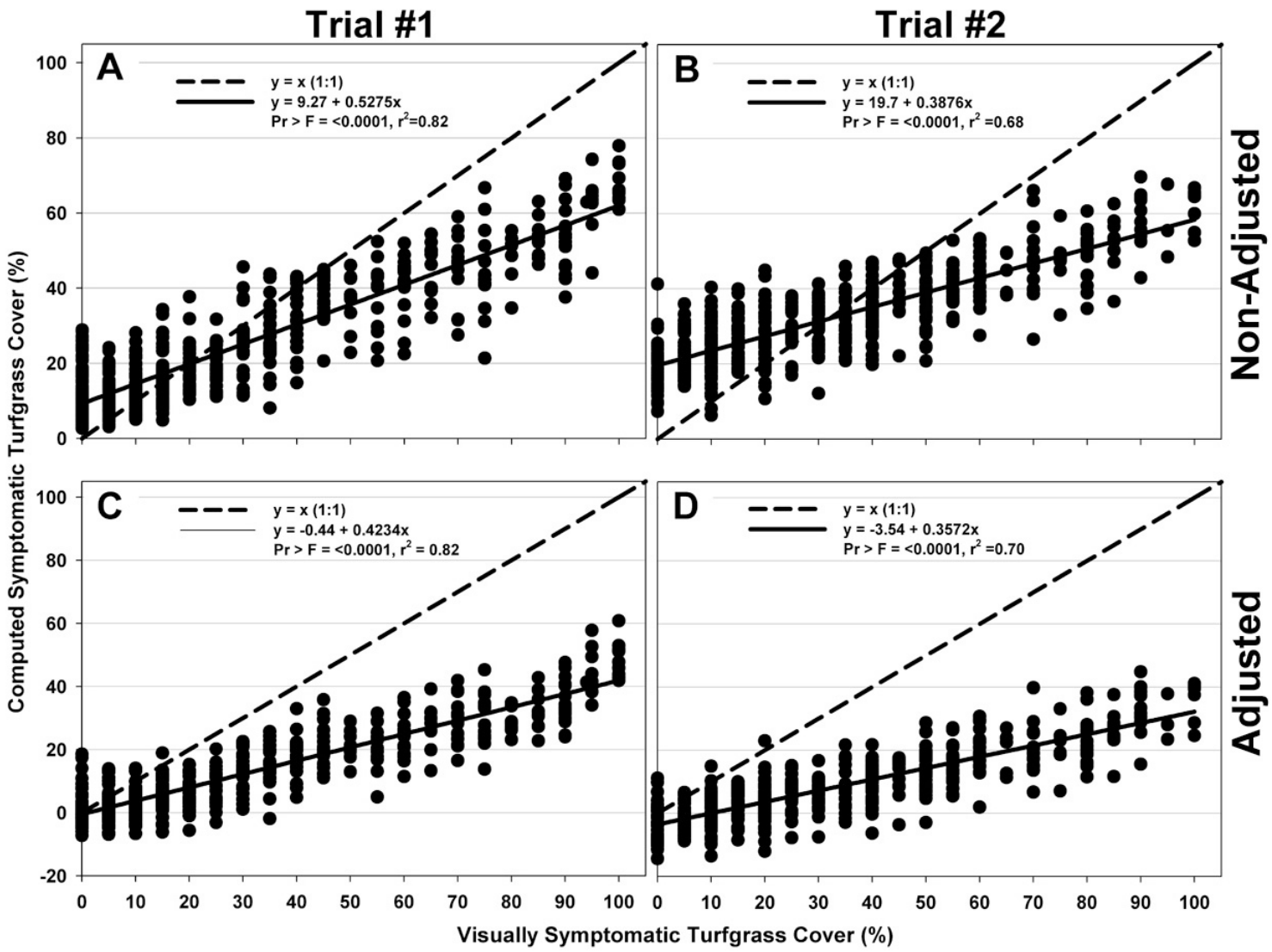
Trial #1
Trial #2
A
y = x (1:1)
y = 9.27 + 0.5275x
Pr > F = <0.0001, r2=0.82
B
y = x (1:1)
y = 19.7 + 0.3876x
Pr > F = <0.0001, r2 =0.68
C
y = x (1:1)
y = -0.44 + 0.4234x
Pr > F = <0.0001, r2 = 0.82
D
y = x (1:1)
y = -3.54 + 0.3572x
Pr > F = <0.0001, r2 =0.70
Non-Adjusted
Adjusted
Computed Symptomatic Turfgrass Cover (%)
Visually Symptomatic Turfgrass Cover (%)
100
80
60
40
20
0
-20
0
10
20
30
40
50
60
70
80
90
100

*3.4.3 Area Under the Disease Progress Curve*

The AUDPC provides a useful measure of disease severity, with high AUDPC values designating more severe disease conditions. Potassium treatment level significantly affected AUDPC at $\alpha = 0.1$ (Table 3.3) when data from GSM and PSM inoculated EUs were pooled. In this case a positive linear relationship between K fertilization rate and disease severity was observed. While there were no significant differences in AUDPC between K fertilization rates less than 0.5 g K $m^{-2}$ 7 $d^{-1}$; together, mean AUDPC for K fertilization rates less than 0.5 g K $m^{-2}$ 7 $d^{-1}$ were significantly lower than K fertilization rates greater than 0.5 g K $m^{-2}$ 7 $d^{-1}$. When data for each inoculum type is analyzed separately, these same trends hold for GSM but not PSM inoculated EUs. In fact, K level did not significantly affect AUDPC of PSM inoculated EUs (Table 3.2 & Table 3.3).

**Table 3.2. Mean area under the disease progress curve values by K fertilization level and inoculum type.**

| | | Mean AUDPC† | |
|---|---|---|---|
| K Level | Application Rate (g $m^{-2}$)‡ | Grey Snow Mold | Pink Snow Mold |
| 1 | 0.00 | 1788b§ | 1334NS¶ |
| 2 | 0.25 | 1719b | 1480 |
| 3 | 0.50 | 2113ab | 1385 |
| 4 | 2.00 | 2556a | 1304 |
| 5 | 3.00 | 2633a | 1706 |

† AUDPC, Area under the disease progress curve.

‡ Every 7 d for 90 d prior to simulated winter.

§ Within column, means not followed by a common letter are significantly different ($\alpha = 0.05$).

¶ NS, not significant ($\alpha$=0.05).

**Table 3.3. Analysis of variance for area under the disease progress curve, by source.**

| | | | Area Under the Disease Progress Curve (GSM and PSM)† | | | Area Under the Disease Progress Curve (GSM Only) | | | Area Under the Disease Progress Curve (PSM Only) | | |
|---|---|---|---|---|---|---|---|---|---|---|---|
| Source | Contrast | df | Estimate | Pr > \|t\| | Pr > F | Estimate | Pr > \|t\| | Pr > F | Estimate | Pr > \|t\| | Pr > F |
| K Level (KL)‡ | | 4 | | | 0.0804 | | | 0.0161 | | | NS§ |
| | Linear KL | 1 | 482.3 | 0.005 | | 773.1 | 0.001 | | NS | NS | |
| | Quadratic KL | 1 | NS | NS | | NS | NS | | NS | NS | |
| | KL 1,2, & 3 vs. KL 4 & 5 | 1 | 413.53 | 0.01 | | 721.6 | 0.001 | | NS | NS | |
| | KL 1 & 2 vs. KL 3 | 1 | NS | NS | | NS | NS | | NS | NS | |
| Fungus Type (F) | | 1 | | | *** | | | NA¶ | | | NA |
| KL x F | | 4 | | | NS | | | NA | | | NA |

***Significant at the 0.001 probability level.

† GSM, Grey snow mold (*Typhula incarnata*); PSM, Pink snow mold (*Microdochium nivale)*

‡ K level 1, 2, 3, 4, 5; 0.00, 0.25, 0.50, 2.00, and 3.00 g K $m^{-2}$ $7d^{-1}$ for 90 d prior to simulated winter, respectively.

§ NS, Not significant ($\alpha = 0.05$).

¶ NA, Not applicable.

*3.4.4 Days of Incubation to 50% Visually Symptomatic Turfgrass Cover*

Days of incubation to 50% visually symptomatic turfgrass cover ($LI_{50}$) was used as a measure of disease progression and severity in a manner similar to Nakajima and Abe (1990) and Hofgaard et al. (2006). Unlike AUDPC, low $LI_{50}$ values indicate more rapid disease onset. Cox proportional hazard analysis of $LI_{50}$ reveals that K level and inoculum fungus type (GSM vs. PSM) significantly affected $LI_{50}$, whereas trial and all source interactions did not (Table 3.4).

**Table 3.4. Cox proportional hazard analysis of days of incubation to 50% visually symptomatic turfgrass cover, by source.**

| Source | df | $Pr > \chi^2$ |
|---|---|---|
| K Level (KL) | 4 | 0.0103 |
| Inoculum Type (I) | 1 | 0.0002 |
| Trial (T) | 1 | NS† |
| KL x I | 4 | NS |
| KL x T | 4 | NS |
| I x T | 1 | NS |
| KL x I x T | 4 | NS |

† NS, not significant ($\alpha$=0.05).

Because $LI_{50}$ was not significantly affected by trial, data was pooled across trials and analyzed by inoculum fungus type using Kaplan-Meier survival analysis. Cox proportional hazard analysis of independent variable effects and their interactions was conducted first because Kaplan-Meier survival procedures only allow one independent variable in the model. Survival curves for K levels were significantly different for GSM ($Pr > \chi^2 = 0.0019$) but not PSM ($Pr > \chi^2 = 0.2780$) inoculated EUs. Mean $LI_{50}$ values for each inoculum type are reported in Table 3.5.

**Table 3.5. Mean days of incubation to 50% visually symptomatic turfgrass cover by K level and inoculum type.**

| | | Mean $LI_{50}$† (Standard Error) | |
|---|---|---|---|
| K Level | Application Rate (g $m^{-2}$)‡ | Grey Snow Mold | Pink Snow Mold |
| 1 | 0.00 | 77 (3) | 81 (3) |
| 2 | 0.25 | 74 (3) | 78 (2) |
| 3 | 0.50 | 71 (3) | 79 (2) |
| 4 | 2.00 | 64 (3) | 78 (3) |
| 5 | 3.00 | 58 (2) | 73 (3) |

† $LI_{50}$, Days of incubation to 50% visually symptomatic turfgrass cover

‡ Every 7 d for 90 d prior to simulated winter.

*3.4.5 Turfgrass Recovery Following Simulated Winter*

Inoculum type significantly ($\alpha = 0.05$) affected (Table 3.6) mean CSTC at 0 d recovery (GSM=PSM>Control), 28 d recovery (PSM>GSM>Control), the total percentage of recovered turfgrass area (GSM>PSM>Control), percentage of potential recovery realized after 28 d (Control=GSM>PSM) and area under the crop recovery curve (Control>GSM>PSM). Neither K fertilization rate nor a K fertilization rate x inoculum type interaction significantly affected any recovery parameter.

**Table 3.6. Mean computed symptomatic turfgrass cover (CSTC) at 0 and 28 d of greenhouse growth following simulated winter, the percent of recovered turfgrass area following 28 d, the percentage of potential recovery (% recovery / % CSTC at 0 d) realized during the recovery period, and area under the crop recovery curve (AUCRC).**

| | Recovery Time | | | | | | |
|---|---|---|---|---|---|---|---|
| | CSTC[†] ( 0 d) | | CSTC (28 d) | | | | |
| Inoculum[‡] | Range (%) | Mean (%) | Range (%) | Mean (%) | Recovery (%) | % of potential[§] | AUCRC[¶] |
| Control | 11.2 – 49.0 | 24.8b | 1.13 – 46.1 | 9.42c | 15.3c | 62.9a | 2287a |
| GSM | 15.7 – 77.9 | 44.8a | 1.05 – 55.6 | 16.8b | 28.0a | 62.9a | 1950b |
| PSM | 16.1 – 69.1 | 43.4a | 1.05 – 78.0 | 22.9a | 20.5b | 51.9b | 1832c |

† CSTC, Computed symptomatic turfgrass cover.

‡ Control, no inoculum; GSM, grey snow mold; PSM, pink snow mold.

§ % of potential = % Recovery / % CSTC (recovery time 0 d).

¶ AUCRC, Area under the crop recovery curve.

## 3.5 Discussion

Since the inception of this experiment in 2006, a considerable amount of progress has been made to understanding characteristics that afford plants snow mold resistance (Bertrand et al., 2011; Bertrand et al., 2009; Chang and Jung, 2009; Gaudet et al., 2011; Pociecha et al., 2010; Sanada et al., 2010; Sun et al., 2008). Whereas our previous understanding of snow mold resistance was largely based on presumed associations between NSC dynamics and the stimulation of plant defense systems (Gaudet et al., 1999) or overall robustness and recuperative ability (Bertrand et al., 2011; Sanada et al., 2010), we are rapidly gaining further insight into the molecular basis of snow mold resistance and cold hardiness thanks largely to ongoing research at The University of Guelph and Agri-Food Canada. This experiment was designed largely in the context of the NSC driven model of snow mold resistance, and is discussed as such.

### *3.5.1 The Effect of K Fertilization on Disease Severity*

For PSM inoculated samples, K fertilization rate did not affect disease severity in both the AUDPC and $LI_{50}$ scales of disease severity (Table 3.2 & Table 3.5). However, it is interesting to note that the lowest disease severity was observed at the 0.00 g K $m^2$ $7d^{-1}$ fertilization rate and the greatest disease severity was observed at the 3.00 g K $m^2$ $7d^{-1}$ fertilization rate in both measurement scales. For GSM inoculated samples, both AUDPC and $LI_{50}$ metrics of disease severity ranked K fertilization rate means in an identical ordinal fashion (Table 3.2 & Table 3.5). In both cases, an apparent positive linear relationship between K fertilization rate and disease severity/onset was observed. Within inoculum groups (e.g. PSM or GSM), AUDPC and $LI_{50}$ provide nearly identical trends in disease onset/severity; therefore, only $LI_{50}$ data are discussed in the context of other dependent variables for the remainder of the discussion.

Potassium fertilization clearly affected disease severity in GSM inoculated samples, while no statistically significant K treatment effects were observed in PSM inoculated EUs. However, the greatest PSM severity was observed in plants fertilized at the highest K fertilization rate. So why would we observe strikingly different trends for GSM and PSM progression at low to moderate K fertilization rates but similar results at a very high K fertilization rate? Gaudet et al. (2011) aptly describe snow mold resistance as quantitative rather than binary, as supported by the literature (Bertrand et al., 2011; Gaudet and Kozub, 1991; Kiyomoto and Bruehl, 1977; Sanada et al., 2010). Furthermore, following extended exposure to conditions favorable for snow mold development, even the most resistant winter wheat cultivars can suffer significant snow mold damage (Gaudet and Kozub, 1991). In fact, Gaudet et al. (2011) observed equal disease severity in 'snow mold resistant' and 'snow mold susceptible' winter wheat lines inoculated with PSM for eight weeks. Chang and Jung (2009) observed that PSM was able to infect and colonize three different creeping bentgrass cultivars more rapidly than six *Typhula spp.* isolates and that PSM infected turfgrass recovered more slowly, an indication of the pathogens 'aggressiveness'. This leaves the potential that innate snow mold defense systems and the physiological effects of K fertilization are subtle, and were overshadowed by the 'aggressiveness' of PSM and/or incubation conditions.

The question of how K fertilization affects snow mold resistance however, remains unanswered. In order to harvest enough tissue for all (nonacid cation, NSC, metabolite) biochemical analyses, entire EUs were destructively harvested following each experimental phase. Disease measurements were made on separate, inoculated EUs. Therefore, this study relies on comparing K fertilization treatment group means in order to identify parameters affecting snow mold severity. Conducting correlations between many independent variables greatly increases the risk of falsely assigning correlation when in fact a true correlation does not exist (type I error); that is, the correlation may exist simply by chance. This is one reason why 'shotgun' approaches to determining causative factors can be misleading. This can be particularly apparent when many autocorrelated factors are correlated to the same dependent

variable. In an effort to ascertain which biochemical parameters were associated with disease in this study, a multitude of such correlations were performed. However, the goal was not to apply causation to every statistically significant correlation, but rather identity parameters that were consistently and systematically correlated with disease across fungus types, sampling dates, and disease measurement metrics.

### *3.5.2 Tissue Nonacid Cation Dynamics and Snow Mold Severity*

The reciprocal nature of tissue nonacid cation composition (Table 2.6) complicates both statistical and practical interpretation of correlation coefficients listed in Table 3.7. That being said, some interesting trends regarding tissue nonacid cation composition and disease severity were observed. While correlation coefficients for all sampling dates and nonacid cation parameters are reported for thoroughness, the 'mid-winter' and 'early spring' sampling periods offer data that is arguably the most pertinent to disease severity as these reflect plant fertility conditions while inoculum were present. These data are therefore discussed in more detail.

Potassium tissue content following 'mid-winter' (time of inoculation) and 'early spring', when expressed on a dry matter ($mmol_c\ kg^{-1}$) or cell sap ($mmol_c\ L^{-1}$) basis, was inversely correlated with $LI_{50}$ of GSM inoculated plants ($\alpha$=0.05). Tissue K content ($mmol_c\ L^{-1}$) on these final two measurement dates was also inversely correlated with $LI_{50}$ of PSM inoculated plants ($\alpha$=0.10). The likelihood that these correlations are significant due to interactions with other physiological features is high; however, there is merit to exploring how K can directly affect plant susceptibility to snow molds and other diseases.

Local and systemic wound signaling and subsequent upregulation of healing and/or defense related genes is an important evolutionary advantage to plants. Their sessile nature precludes alternative avoidance mechanisms, leaving them dependent on preventing further damage and repair of wounded tissue. In their characterization of the K dependent *Arabidopsis* transcriptome, Armengaud et al. (2004) identified a very strong connection between plant K

status and the expression of genes linked to synthesis of jasmonic acid (JA) and other JA dependent gene pathways. Through synergistic or antagonistic interactions with other stress related plant hormones (e.g.. ethylene, salicylic acid, abscisic acid), these pathways are associated with a number of stress and defense responses to abiotic stress, wounding, and/or pathogenesis (Leon et al., 2001). Transcript levels of the first three JA biosynthesis enzymes lipoxygenase, allene oxide synthase, and allene oxide cyclase increased markedly during K starvation and rapidly declined follow resupply of K (Armengaud et al., 2004). Citing the fact that snow mold resistant winter wheat varieties maintained higher transcript levels of allene oxide synthase under winter-like conditions, Gaudet (2011) has implicated the importance of the jasmonic acid pathway to 'hardening' induced low-temperature and snow mold resistance. Leon et al. (2001) also reports that JA biosynthesis is limited by allene oxide synthase transcript/protein levels, which are very low in healthy plants and increase correspondingly with JA following a stress event. Maintaining plants under subclinical K stress may precondition them for rapid JA related responses to winter related stresses including pathogenesis by snow molds. This may be particularly beneficial when thermodynamic restrictions imposed by low temperatures precludes *de novo* synthesis of JA and rapid induction of JA related plant defense systems.

Tissue calcium content was the only predictor of $LI_{50}$ for both GSM and PSM inoculated samples that showed a statistically significant ($\alpha$=0.05) correlation (positive) on both of the final two measurement dates. The systematic and statistically significant nature of these results suggests that the depression of tissue Ca content by K fertilization may play an important role in disease dynamics. Calcium is an important component of secondary messenger systems for a multitude of plant cell signaling pathways, including JA-dependent and JA-independent wound signaling/response pathways (Leon et al., 1998). The distribution of Ca within the cell is complex, with pronounced electrochemical gradients across the plasma membrane, tonoplast, endoplasmic reticulum, and even within the cytoplasm (Bush, 1995). Vacuolar $Ca^{2+}$ has been implicated in maintaining homeostatic cytosolic $Ca^{2+}$ concentrations as well as providing a

source of $Ca^{2+}$ during signal transduction (Bush, 1995). The regulatory effect of $Ca^{2+}$ is modulated through the activation of $Ca^{2+}$ binding proteins including calmodulin and calmodulin-related proteins and the interaction of Ca-bound proteins with a plethora of enzymes and regulatory proteins (Klee and Vanaman, 1982). In addition to discovering that JA biosynthesis genes and related pathways were strongly down-regulated following re-supply of K, Armengaud et al. (2004) also observed strong down-regulation of several genes associated $Ca^{2+}$ binding proteins including calmodulin. These research findings provide an interesting theoretical framework for the observed positive correlation between $LI_{50}$ and tissue Ca content. While it is difficult to assume the cellular distribution of $Ca^{2+}$, it is likely that $Ca^{2+}$ homeostasis of cellular structures/compartments would be maintained at the expense of vacuolar $Ca^{2+}$ stores. Therefore, the combined effect of reduced transcript levels of $Ca^{2+}$ binding secondary messenger proteins, JA biosynthetic and wound/defense related proteins, and reduced $Ca^{2+}$ stores could have hindered the plants ability to elicit plant defense systems in response to pathogen attack.

The ionic environment of the apoplast is known to affect cell wall extensibility and expansion. Specifically, increased concentrations of polyvalent cations (e.g. $Ca^{2+}$) restricts enzymatic modification of pectin and subsequent arrangement of other cell wall components (Wehr et al., 2004). While it would be attractive to attribute increased disease severity to reduced tissue Ca content and subsequent cell wall integrity at increased K fertilization rates, speculating the fraction of the total $Ca^{2+}$ pool residing in the cell wall under these conditions would be impossible. Furthermore, a considerable amount of research has shown that when calcium is taken up from the soil solution, there is a rapid, initial enrichment of the cell wall ‘free space’ and then a slow linear progression of uptake into the cell (Demarty et al., 1984). Therefore, it seems logical that even under conditions where Ca uptake is restricted by heavy K fertilization, cell wall Ca content would be less affected by mild Ca starvation. Of course, this ignores the likely possibility that Ca can be remobilized from cell wall structures to other cellular compartments through reciprocal regulation of cell wall modifying enzymes.

Seling et al. (2000) observed that a greater portion of total tissue Ca was localized to the cell wall under low Ca conditions and that significant differences in cell wall Ca content were only observed in conjunction with visual deficiency symptoms in potato leaves. Furthermore, their data suggest that increased enzymatic degradation of pectin was only observed under obvious Ca deficiency symptoms. None of the EUs used in our experiment showed any visual symptoms of Ca deficiency, and the lowest tissue Ca value observed was 4.3 g $kg^{-1}$. This value is within the accepted range for turfgrass tissue (3.0-12.5 g $kg^{-1}$) and very close to the tissue Ca content (4.5 g $kg^{-1}$) above which no deficiency symptoms were observed by Seling et al. (2000).

Microscopic observation of mycelial invasion of creeping bentgrass (Oshiman et al., 1995) and winter wheat (Takenaka and Yoshino, 1989) inoculated with *Typhula* snow molds suggested that infection occurs initially through stomata and then through the cuticle and epidermal cells. This suggests that cell wall integrity would not be a major determinant of snow mold infection, as stomata would provide a path of least resistance for mycelial invasion of leaf tissues. Therefore, there is insufficient evidence to support the notion that the observed inverse correlation between tissue Ca content and disease severity was a function of compromised cell wall integrity under increasing K fertilization.

**Table 3.7. Simple correlation coefficients (r) relating turfgrass tissue non-acid cation parameters measured following each experimental phase and days to 50% infection for grey snow mold (GSM) and pink snow mold (PSM) inoculated experimental units. Correlations were performed using means for different potassium fertilization rate treatment groups. Negative correlation coefficients designate a trend toward greater disease severity (fewer days to 50% infection).**

| Turfgrass Tissue | Stage of Experiment Preceding Harvest | | | | | | | |
|---|---|---|---|---|---|---|---|---|
| | 'K Treatment' | | 'Hardening' | | 'Mid-Winter' | | 'Early Spring' | |
| Nonacid Cation Parameter† | GSM† | PSM‡ | GSM | PSM | GSM | PSM | GSM | PSM |
| | Correlation Coefficient (r) | | | | | | | |
| K $mmol_c$ $kg^{-1}$ | -0.98** | NS§ | -0.98** | -0.83¶ | -0.99*** | -0.82 | -0.96** | NS |
| K $mmol_c$ $L^{-1}$ | -0.99*** | -0.81 | -0.96** | -0.89* | -0.99*** | -0.85 | -0.91* | -0.84 |
| Ca $mmol_c$ $kg^{-1}$ | 0.99*** | 0.81 | 0.98** | 0.80 | 0.99*** | 0.89* | 0.96** | 0.92* |
| Mg $mmol_c$ $kg^{-1}$ | 0.99*** | 0.86 | 0.98** | 0.81 | 0.97** | 0.89* | NS | 0.95* |

*,**,*** Statistically significant at the 0.05, 0.01, and 0.001 probability level, respectively.

† GSM, Mean days to 50% infection of grey snow mold inoculated experimental units.

‡ PSM, Mean days to 50% infection of pink snow mold inoculated experimental units.

§ NS, Not significant (α=0.10).

¶ Correlation coefficients not followed to *,**. or *** are significant at the 0.10 probability level.

*3.5.3 Non-structural Carbohydrate Dynamics and Snow Mold Severity*

Resistance to snow molds has been attributed to leaf water potential (Tronsmo, 1986), 'strategic' catabolism of storage carbohydrates (Gaudet et al., 1999), and light conditions during the 'hardening' period (Nakajima and Abe, 1996). Common to all of these findings is the importance of non-structural carbohydrates (NSCs), and as a result, NSC dynamics have long been the focus of efforts to understand snow mold resistance. The potential interactions between plant K status and NSCs made this an attractive focus for this study as well. Overall, K fertilization did not appreciably affect NSC dynamics (Table 2.7).

The correlation coefficients (Table 3.8) generated from NSC data contained in Table 2.7 suggest very little correlation between NSCs and disease severity. In fact, the only NSC parameter significantly correlated with both GSM and PSM severity was ESF content on the date of inoculation. Similarly, Bertrand et al. (2011) observed that snow mold resistant annual bluegrass genotypes accumulated greater concentration of low degree of polymerization fructans than snow mold sensitive types. Citing plant defense activation by fungal and cell wall oligosaccharides (Ryan and Farmer, 1991), Bertrand et al. (2011) suggest that fructans having a low degree of polymerization (8-16 monomers) may elicit plant defense systems in a similar manner. While an interesting hypothesis, structural differenced between fructans (β- linked fructose) and dominant plant/fungal cell wall oligosaccharides (β- linked glucose) complicates the direct transfer of this mechanism. Particularly because high-affinity receptors for β-glucan elicitors show considerable binding specificity (Ryan and Farmer, 1991). Furthermore, ESF fructans are present throughout the growing season and constant stimulation of plant defense mechanisms by a ubiquitous storage carbohydrate presents an avoidable non-sequitor.

We observed no correlation between WSF or total NSC content and disease severity (Table 3.8) or recuperative ability (data not shown). High WSF content in the later stages of winter has been observed in snow mold resistant varieties of winter wheat (Yoshida et al., 1998),

orchardgrass (Sanada et al., 2010), and annual bluegrass (Bertrand et al., 2011). Greater total NSC content following winter (real or simulated) has also been ubiquitously associated with snow mold resistance (Bertrand et al., 2011; Kiyomoto and Bruehl, 1977; Pociecha et al., 2008; Pociecha et al., 2010; Sanada et al., 2010; Yoshida et al., 1998). In all of these experiments, NSC dynamics of resistant and susceptible varieties were compared and from these comparisons it was inferred that NSC storage and/or utilization is a critical component of snow mold resistance. However, as pointed out by Bertrand et al. (2011), it is unclear whether fructans actually confer greater snow mold resistance or whether accumulating and maintaining greater concentrations of fructans is an independent trait commonly associated with snow mold resistant varieties. Our results would suggest the latter, but the systematic association between NSC dynamics and snow mold severity across species, years, and continents cannot be ignored. Clearly the quantitative nature of snow mold resistance is multifaceted.

The author would be remiss to not address features of our experimental design that may partially explain differences between previously published results and our findings. Most studies that have linked NSC dynamics with snow mold resistance measured NSCs at their primary site of accumulation in crown tissue (Bertrand et al., 2011; Kiyomoto and Bruehl, 1977; Sanada et al., 2010), whereas whole plant (aerial tissue) NSC measurements were made in our study. That being said, the total and individual NSC (except sucrose) concentrations observed in whole leaf samples in this study closely matched those observed in crowns of 42 annual bluegrass ecotypes (Dionne et al., 2010) and crowns of annual bluegrass ecotypes assayed under similar conditions in two other studies (Bertrand et al., 2011; Dionne et al., 2001). Therefore, it seems as though the potential ‘dilution effect’ of including leaf tissue did not appreciably affect our results. Sucrose content was considerably lower in this experiment than in the other aforementioned studies, it is unclear whether this is a turfgrass varietal effect or other experimental artifact.

**Table 3.8. Simple correlation coefficients (r) relating turfgrass tissue non-structural carbohydrates measured following each experimental phase and days to 50% infection for grey snow mold (GSM) and pink snow mold (PSM) inoculated experimental units. Correlations were performed using means for different potassium fertilization rate treatment groups. Negative correlation coefficients designate a trend toward greater disease severity (fewer days to 50% infection).**

| | Stage of Experiment Preceding Harvest | | | | | | | |
|---|---|---|---|---|---|---|---|---|
| | 'K Treatment' | | 'Hardening' | | 'Mid-Winter' | | 'Early Spring' | |
| Non-structural Carbohydrate† | GSM‡ | PSM§ | GSM | PSM | GSM | PSM | GSM | PSM |
| —— mg $g^{-1}$ fresh wt. —— | —— Correlation Coefficient (r) —— | | | | | | | |
| Fructose | 0.92* | NS ¶ | NS | NS | NS | NS | NS | NS |
| Glucose | NS | NS | NS | NS | NS | NS | NS | NS |
| Sucrose | NS | NS | 0.90* | NS | NS | NS | NS | NS |
| Raffinose | NS | -0.93* | NS | NS | 0.88* | NS | NS | NS |
| WSF | NS | NS | NS | NS | NS | NS | NS | NS |
| ESF | NS | NS | NS | NS | 0.90* | 0.97** | 0.91* | NS |
| Total Fructan | NS | NS | NS | NS | NS | NS | NS | NS |
| Total NSCs | NS | NS | NS | NS | NS | NS | NS | NS |

*,**,*** Statistically significant at the 0.05, 0.01, and 0.001 probability level, respectively.

† WSF, water soluble fructans; ESF, 80% ethanol soluble fructans; NSCs, non-structural carbohydrates.

‡ GSM, Mean days to 50% infection of grey snow mold inoculated experimental units.

§ PSM, Mean days to 50% infection of pink snow mold inoculated experimental units.

¶ NS, Not significant (α=0.10).

*3.5.4 Tricarboxylic Acid Intermediates and Snow Mold Resistance*

The correlation coefficients (Table 3.9) generated from metabolite data contained in Table 2.8 suggests very little correlation between organic acid content and $LI_{50}$. Where a significant correlation did exist, there was an inverse relationship between TCA parameters and $LI_{50}$. There are some indications that plant TCA metabolite status may truly influence disease severity, particularly malate and citrate content following 'hardening'. However, strong correlations between organic acid content and nonacid cation dynamics complicate interpretation of these data.

Although there is no clear association between disease severity and tissue metabolite content, organic acid dynamics may be another component of the overall 'subtle' effect of K fertilization on plant susceptibility to snow molds. Potassium fertilization is an essential determinant of CAD, as $K^+$ is the greatest single ion contributor to total CAD. Furthermore, plants grown in media supplying sufficient K generally accumulate greater tissue K than the amount required to support adequate growth and cell maintenance, termed 'luxury consumption' (Hoagland and Martin, 1933; Wildes and Pitman, 1975). As tissue K content and CAD increases, a greater portion of organic acids are siphoned from metabolically active pools to fulfill homeostatic rolls, representing a significant biochemical cost. The cost of unrealized chemical energy would be particularly pertinent for citrate, as K fertilization had the greatest effect on tissue citrate content and vacuolar citrate is known to be relatively metabolically inert (Genix et al., 1990; Gout et al., 1993). Therefore, vacuolar storage of K has a tangible biochemical cost, which may effect snow mold severity.

**Table 3.9. Simple correlation coefficients (r) relating turfgrass tissue tricarboxylic acid intermediates measured following each experimental phase and days to 50% infection for grey snow mold (GSM) and pink snow mold (PSM) inoculated experimental units. Correlations were performed using means for different potassium fertilization rate treatment groups. Negative correlation coefficients designate a trend toward greater disease severity (fewer days to 50% infection).**

| | Stage of Experiment Preceding Harvest | | | | | | | |
|---|---|---|---|---|---|---|---|---|
| | 'K Treatment' | | 'Hardening' | | 'Mid-Winter' | | 'Early Spring' | |
| TCA Cycle Intermediate† | GSM‡ | PSM§ | GSM | PSM | GSM | PSM | GSM | PSM |
| ——— mmol $L^{-1}$ ——— | ——— Correlation Coefficient (r) ——— | | | | | | | |
| Malate | -0.97** | -0.89* | -0.95* | -0.93* | NS¶ | NS | -0.96** | NS |
| Citrate | -0.95* | NS | -0.99*** | -0.93* | -0.98** | NS | -0.98** | NS |
| Total | -0.96** | NS | -0.99*** | NS | -0.96** | NS | -0.96** | NS |

*,**,*** Statistically significant at the 0.05, 0.01, and 0.001 probability level, respectively.

† TCA, Tricarboxylic acid.

‡ GSM, Mean days to 50% infection of grey snow mold inoculated experimental units.

§ PSM, Mean days to 50% infection of pink snow mold inoculated experimental units.

¶ NS, Not significant (α=0.10).

### *3.5.5 Turfgrass Recovery Following Simulated Winter*

Potassium fertilization rate did not affect turfgrass recovery following simulated winter and/or inoculation with snow molds; however, fungus type (GSM vs. PSM) did significantly affect turfgrass recuperative ability (Table 3.6). Specifically, samples inoculated with PSM recovered to a lesser extent than non-inoculated and GSM inoculated EUs. These data support anecdotal field observations and are in agreement with Chang and Jung (2009). Bruehl (1982) describes that *Typhula* snow molds tend to infect older leaves and then progress slowly towards the crown as snow cover persists; in contrast, PSM progresses from the roots and lower leaf sheaths immediately to the crown. Infecting crown tissue during disease progression makes PSM a particularly destructive pathogen, as plant recuperative potential is severely compromised.

### *3.5.6 Practical Application of Data*

Snow molds (particularly GSM) are 'threshold diseases', in that their manifestation depends almost exclusively on the duration of continuous snow cover during winter. In this context, $LI_{50}$ provides a particularly meaningful measure of disease as it represents the number of days to an 'unacceptable' threshold (50% infection). Statistically significant differences between $LI_{50}$ means provided grounds for scientific interpretation of K fertilization affects, but the true practical significance of these findings is best analyzed in the context of climatological data. Table 3.10 shows the percentage of winters from 1940 to 2006 in Madison, WI where days of continuous snow cover (>2.54 cm) were greater than or equal to $LI_{50}$ for each K fertilization rate. Madison, WI was chosen as the example site due to the availability of a complete data set and because this region experiences significant snow mold disease pressure. Data were obtained from the Wisconsin State Climatology Office (Young, 2010). These data show that on any given year, the probability of experiencing winter conditions that would facilitate 'unacceptable' GSM damage would be 36% for turfgrass fertilized with 0.00 g K $m^{-2}$ $7d^{-1}$ and 69% for turfgrass

fertilized with 3.00 g K $m^{-2}$ $7d^{-1}$. The nearly two-fold increase in 'seasonal risk' associated with K fertilization at 3.00 g K $m^{-2}$ $7d^{-1}$ represents a tremendous practical disadvantage to growers. Furthermore, even though $LI_{50}$ for GSM inoculated turfgrass fertilized with 0.00 g K $m^{-2}$ $7d^{-1}$ differed from turfgrass fertilized with 0.50 g K $m^{-2}$ $7d^{-1}$ by only 6 d, this represents a seasonal risk increase of 18%. For PSM inoculated turfgrass, the seasonal risk for turfgrass fertilized with 3.00 g K $m^{-2}$ $7d^{-1}$ was 14% greater than that for turfgrass fertilized with 0.00 g K $m^{-2}$ $7d^{-1}$. While these interpretations assume a 1:1 relationship between $LI_{50}$ and days of continuous snow cover, meaningful trends can be taken from this discussion even if this assumption is not perfect. These data provide a more practical interpretation of $LI_{50}$, and highlight the greatly increased seasonal risk of snow mold damage associated with increased K fertilization.

**Table 3.10. Percentage of winters from 1940 to 2006 in Madison, Wisconsin where days of continuous snow cover (>2.54 cm) were greater than or equal to days of incubation to 50% visually symptomatic turfgrass cover ($LI_{50}$) for each K fertilization rate.**

| | Grey Snow Mold | | Pink Snow Mold | |
|---|---|---|---|---|
| Application Rate (g $m^{-2}$)† | $LI_{50}$‡ | Winters (%)§ | $LI_{50}$ | Winters (%) |
| 0.00 | 77 | 36% | 81 | 34% |
| 0.25 | 74 | 43% | 78 | 37% |
| 0.50 | 71 | 54% | 79 | 36% |
| 2.00 | 64 | 62% | 78 | 37% |
| 3.00 | 58 | 69% | 73 | 48% |

† Every 7 d for 90 d prior to simulated winter.

‡ $LI_{50}$, Days of incubation to 50% visually symptomatic turfgrass.

§ Percentage of winters between 1940 and 2006 with continuous snow cover ≥ $LI_{50}$.

*3.5.7 Additional Considerations*

This experiment, like most other published snow mold studies, distinguishes levels of disease severity based on the linear growth rate of a point source inoculum under controlled conditions favorable for disease development. This system provides a viable method for evaluating relative disease severity, but differs from natural systems in several important ways.

Most notably, it assumes that there are no plant/snow mold interactions prior to early spring and that the near linear growth of snow molds at constant temperatures and high humidity is reflective of actual growth dynamics under snow cover.

While penetration of artificially inoculated grasses by *Typhula* snow molds has been characterized (Oshiman et al., 1995; Takenaka and Yoshino, 1989), natural disease progression dynamics are largely unknown. Although rare, germination of *Typhula* sclerotia during cool, wet periods prior to snowfall has been observed (Hsiang et al., 1999). Furthermore, interactions between seasonal fungicide applications and snow mold severity the following spring have been observed (Reicher and Throssell, 1997). These findings suggest significant plant/snow mold interactions prior to macro-scale mycelial production and/or visible tissue necrosis. Therefore, the precise timing of infection, disease progression, and mycelial growth in natural systems remains unclear, compromising the applicability of data obtained in controlled environment studies.

While mycelial production of snow molds held at constant temperatures is near linear, casual observations of pathogenic snow molds in the field suggests exponential growth of mycelial blooms following the transition from sub-zero to near 0°C temperatures at the edges of a receding snow pack (Remsberg, 1940). These observations are supported by studies that monitor subnivean ecosystem respiration rates (Monson et al., 2006), and more recently, growth rate analyses of snow molds isolated from sub-alpine forests of Colorado (Schmidt et al., 2009). The $Q_{10}$ of growth rates exhibited by snow molds can be as high as 330 across the temperature range of -2 to -0.3°C (Schmidt et al., 2009), supporting the notion of rapid mycelial growth just prior to complete snow melt. Therefore, it is conceivable that snow molds infect the plant during fall, progress slowly through plant tissues under the humid, dark, near freezing conditions that persist under snow cover, and then rapidly produce mycelium when soil temperatures rapidly warm above 0 in the final ~48 hrs preceding complete snow melt. Again, these features may complicate the applicability of results obtained via controlled environment studies to field scenarios.

### 3.6 Conclusions

The complex nature of quantitative snow mold resistance and the temporal scale of plant/snow mold interactions make it difficult to draw strong conclusions from controlled environment snow mold studies. Strong correlations between dependent variables also made it difficult if not impossible to determine with great confidence which parameters were important components of disease resistance. That being said, snow mold severity and other correlated biochemical parameters were significantly affected by K fertilization. While specific mechanisms discussed were largely speculative, these findings broaden our understanding of snow mold resistance to include biochemical parameters other than nonstructural carbohydrates (e.g. mineral nutrient composition, TCA intermediates). The results of this study also illustrate the importance of considering 'seasonal risk' when devising snow mold control strategies or making practical interpretations of data.

In reviewing much of the published literature on snow molds, this study also highlights the importance of developing conventional methods for studying quantitative snow mold resistance. Variations in type/age of plant materials, pathogen isolates, and experimental protocol make it difficult to make comparisons across studies and allow for a tremendous amount of speculation. Greater consensus among researchers on these topics would facilitate a more integrated and directed approach to studying plant/snow mold interactions. Furthermore, until researchers develop novel methods for monitoring disease dynamics in the field, the true nature of snow mold disease cycles and host resistance will remain elusive.

## CHAPTER 4: REFERENCES


Altschul, S.F., W. Gish, W. Miller, E.W. Myers, D.J. Lipman. 1990. Basic Local Alignment Search Tool. Journal of Molecular Biology 215:403-410.

Amtmann, A., J.P. Hammond, P. Armengaud, P.J. White. 2006. Nutrient Sensing and Signalling in Plants: Potassium and Phosphorus. pp. 209-257. *In*, Advances in Botanical Research, Vol 43.

Anderson, J.A., C.M. Taliaferro, D.L. Martin. 1993. Evaluating Freeze Tolerance of Bermudagrass in a Controlled Environment. Hortscience 28:955-955.

Armengaud, P., R. Breitling, A. Amtmann. 2004. The Potassium-Dependent Transcriptome of Arabidopsis Reveals a Prominent Role of Jasmonic Acid in Nutrient Signaling. Plant Physiology 136:2556-2576.

Aurisano, N., A. Bertani, M. Mattana, R. Reggiani. 1993. Abscisic-Acid Induced Stress-Like Polyamine Pattern in Wheat Seedlings, and Its Reversal by Potassium-Ions. Physiologia Plantarum 89:687-692.

Bancal, P., C.A. Henson, J.P. Gaudillere, N.C. Carpita. 1991. Fructan Chemical-Structure and Sensitivity to an Exohydrolase. Carbohydrate Research 217:137-151.

Beard, J.B. 1973. Turfgrass: Science and Culture. Prentice Hall, Upper Saddle River, New Jersey.

Bertrand, A., Y. Castonguay, A. Azaiez, T. Hsiang, J. Dionne. 2011. Cold-Induced Responses in Annual Bluegrass Genotypes with Differential Resistance to Pink Snow Mold (Microdochium Nivale). Plant Science 180:111-119.

Bertrand, A., Y. Castonguay, J. Cloutier, L. Couture, T. Hsiang, J. Dionne, S. Laberge. 2009. Genetic Diversity for Pink Snow Mold Resistance in Greens-Type Annual Bluegrass. Crop Science 49:589-599.

Boller, T., A. Wiemken. 1986. Dynamics of Vacuolar Compartmentation. Annual Review of Plant Physiology and Plant Molecular Biology 37:137-164.

Boulter, J.I., G.J. Boland, J.T. Trevors. 2002. Assessment of Compost for Suppression of Fusarium Patch (Microdochium Nivale) and Typhula Blight (Typhula Ishikariensis) Snow Molds of Turfgrass. Biological Control 25:162-172.

Bruehl, G.W. 1982. Developing Wheats Resistant to Snow Mold in Washington State. Plant Disease 66:1090-1095.

Burpee, L.L., L.M. Kaye, L.G. Goulty, M.B. Lawton. 1987. Suppression of Gray Snow Mold on Creeping Bentgrass by an Isolate of Typhula-Phacorrhiza. Plant Disease 71:97-100.

Bush, D.S. 1995. Calcium Regulation in Plant-Cells and Its Role in Signaling. Annual Review of Plant Physiology and Plant Molecular Biology 46:95-122.

Cairns, A.J. 1987. Colorimetric Microtiter Plate Assay of Glucose and Fructose by Enzyme-Linked Formazan Production - Applicability to the Measurement of Fructosyl Transferase-Activity in Higher-Plants. Analytical Biochemistry 167:270-278.

Carrow, R.N., D.V. Waddington, P.E. Rieke. 2001. Turfgrass Soil Fertility and Chemical Problems. Ann Arbor Press, Chelsea, MI.

Chang, S.W., G. Jung. 2009. Aggressiveness of Three Snow Mold Fungi on Creeping Bentgrass Cultivars under Controlled Environment Conditions. Plant Pathology Journal 25:6-12.

Chang, S.W., T.H. Chang, L. Tredway, G. Jung. 2006a. Aggressiveness of Typhula Ishikariensis Isolates to Cultivars of Bentgrass Species (Agrostis Spp.) under Controlled Environment Conditions. Plant Disease 90:951-956.

Chang, S.W., T.H. Chang, R.A.B. Abler, G. Jung. 2007. Variation in Bentgrass Susceptibility to Typhula Incarnata and in Isolate Aggressiveness under Controlled Environment Conditions. Plant Disease 91:446-452.

Chang, S.W., E. Scheef, R.A.B. Abler, S. Thomson, P. Johnson, G. Jung. 2006b. Distribution of Typhula Spp. And Typhula Ishikariensis Varieties in Wisconsin, Utah, Michigan, and Minnesota. Phytopathology 96:926-933.

Chatterton, N.J., P.A. Harrison, J.H. Bennett, K.H. Asay. 1989. Carbohydrate Partitioning in 185 Accessions of Gramineae Grown under Warm and Cool Temperatures. Journal of Plant Physiology 134:169-179.

Chen, C.T., T.L. Setter. 2003. Response of Potato Tuber Cell Division and Growth to Shade and Elevated Co2. Annals of Botany 91:373-381.

Cherney, J.H., Q.M. Ketterings, J.L. Orloski. 2004. Plant and Soil Elemental Status as Influenced by Multi-Year Nitrogen and Potassium Fertilization. Journal of Plant Nutrition 27:991-1014.

Crowe, J.H., L.M. Crowe, J.F. Carpenter, A.S. Rudolph, C.A. Wistrom, B.J. Spargo, T.J. Anchordoguy. 1988. Interactions of Sugars with Membranes. Biochimica et Biophysica Acta (BBA) - Reviews on Biomembranes 947:367-384.

DaCosta, M., B.R. Huang. 2006. Changes in Carbon Partitioning and Accumulation Patterns During Drought and Recovery for Colonial Bentgrass, Creeping Bentgrass, and Velvet Bentgrass. Journal of the American Society for Horticultural Science 131:484-490.

Das, M.K., S. Rajaram, C.C. Mundt, W.E. Kronstad. 1992. Inheritance of Slow-Rusting Resistance to Leaf Rust in Wheat. Crop Science 32:1452-1456.

Demarty, M., C. Morvan, M. Thellier. 1984. Calcium and the Cell-Wall. Plant Cell and Environment 7:441-448.

Demmig, B., H. Gimmler. 1983. Properties of the Isolated Intact Chloroplast at Cytoplasmic K+ Concentrations .1. Light-Induced Cation Uptake into Intact Chloroplasts Is Driven by an Electrical Potential Difference. Plant Physiology 73:169-174.

Dest, W.M., K. Guillard. 2001. Bentgrass Response to K Fertilization and K Release Rates from Eight Sand Rootzone Sources Used in Putting Green Construction. Int. Turfgrass Soc. Res. J. 9:375-381.

Dionne, J., Y. Castonguay, P. Nadeau, Y. Desjardins. 2001. Freezing Tolerance and Carbohydrate Changes During Cold Acclimation of Green-Type Annual Bluegrass (Poa Annua L.) Ecotypes. Crop Science 41:443-451.

Dionne, J., S. Rochefort, D.R. Huff, Y. Desjardins, A. Bertrand, Y. Castonguay. 2010. Variability for Freezing Tolerance among 42 Ecotypes of Green-Type Annual Bluegrass. Crop Science 50:321-336.

Epstein, E. 1980. pp. 32. *In* R. M. Spanswick, et al. (Eds.), Plant Membrane Transport: Current Conceptual Issues. Elsevier/North Holland Biomedical Press, Amsterdam.

Evans, H.J., G.J. Sorger. 1966. Role of Mineral Elements with Emphasis on Univalent Cations. Annual Review of Plant Physiology 17:47-&.

Fisher, J.D., D. Hansen, T.K. Hodges. 1970. Correlation between Ion Fluxes and Ion-Stimulated Adenosine Triphosphatase Activity of Plant Roots. Plant Physiology 46:812-814.

Fry, J., B.R. Huang. 2004. Applied Turfgrass Science and Physiology. John Wiley and Sons, Hoboken, NJ.

Gaudet, D.A., T.H.H. Chen. 1988. Effect of Freezing Resistance and Low-Temperature Stress on Development of Cottony Snow Mold (Coprinus-Psychromorbidus) in Winter-Wheat. Canadian Journal of Botany-Revue Canadienne De Botanique 66:1610-1615.

Gaudet, D.A., G.C. Kozub. 1991. Screening Winter-Wheat for Resistance to Cottony Snow Mold under Controlled Conditions. Canadian Journal of Plant Science 71:957-965.

Gaudet, D.A., A. Laroche, M. Yoshida. 1999. Low Temperature-Wheat-Fungal Interactions: A Carbohydrate Connection. Physiologia Plantarum 106:437-444.

Gaudet, D.A., A. Laroche, M. Frick, R. Huel, B. Puchalski. 2003a. Cold Induced Expression of Plant Defensin and Lipid Transfer Protein Transcripts in Winter Wheat. Physiologia Plantarum 117:195-205.

Gaudet, D.A., A. Laroche, M. Frick, R. Huel, B. Puchalski. 2003b. Plant Development Affects the Cold-Induced Expression of Plant Defence-Related Transcripts in Winter Wheat. Physiological and Molecular Plant Pathology 62:175-184.

Gaudet, D.A., Y. Wang, M. Frick, B. Puchalski, C. Penniket, T. Ouellet, L. Robert, J. Singh, A. Laroche. 2011. Low Temperature Induced Defence Gene Expression in Winter Wheat in Relation to Resistance to Snow Moulds and Other Wheat Diseases. Plant Science 180:99-110.

Genix, P., R. Bligny, J.B. Martin, R. Douce. 1990. Transient Accumulation of Asparagine in Sycamore Cells after a Long Period of Sucrose Starvation. Plant Physiology 94:717-722.

Gerhardt, R., M. Stitt, H.W. Heldt. 1987. Subcellular Metabolite Levels in Spinach Leaves - Regulation of Sucrose Synthesis During Diurnal Alterations in Photosynthetic Partitioning. Plant Physiology 83:399-407.

Ghosh, G., M.C. Drew. 1991. Comparison of Analytical Methods for Extraction of Chloride from Plant-Tissue Using Cl-36 as Tracer. Plant and Soil 136:265-268.

Goff, J.P., R. Ruiz, R.L. Horst. 2004. Relative Acidifying Activity of Anionic Salts Commonly Used to Prevent Milk Fever. Journal of Dairy Science 87:1245-1255.

Goss, R.L., C.J. Gould. 1968. Turfgrass Diseases: The Relationship to Potassium. USGA Green Section Record. 5:10-13.

Gout, E., R. Bligny, N. Pascal, R. Douce. 1993. C-13 Nuclear-Magnetic-Resonance Studies of Malate and Citrate Synthesis and Compartmentation in Higher-Plant Cells. Journal of Biological Chemistry 268:3986-3992.

Gregory, F.G., E.C.D. Baptiste. 1936. Physiological Studies in Plant Nutrition. V. Carbohydrate Metabolism in Relation to Nutrient Deficiency and to Age in Leaves of Barley. Annals of Botany 50:579-619.

Griffith, M., P. Ala, D.S.C. Yang, W.C. Hon, B.A. Moffatt. 1992. Antifreeze Protein Produced Endogenously in Winter Rye Leaves. Plant Physiology 100:593-596.

Han, S., T.W. Fermanian, J.A. Juvik, L.A. Spomer. 2004. Total Nonstructural Carbohydrate Storage in Creeping Bentgrass Treated with Trinexapac-Ethyl. Hortscience 39:1461-1464.

Hartig, R. 1888. *Herpotrichia Nigra* N. Sp. Allgem. Forst Jagdzeit 64:15-17.

Hartman, C.L., T.J. McCoy, T.R. Knous. 1984. Selection of Alfalfa (Medicago-Sativa) Cell-Lines and Regeneration of Plants Resistant to the Toxin(S) Produced by Fusarium-Oxysporum F-Sp Medicaginis. Plant Science Letters 34:183-194.

Hawker, J.S., H. Marschner, A. Krauss. 1979. Starch Synthesis in Developing Potato-Tubers. Physiologia Plantarum 46:25-30.

Herbers, K., P. Meuwly, W.B. Frommer, J.P. Metraux, U. Sonnewald. 1996. Systemic Acquired Resistance Mediated by the Ectopic Expression of Invertase: Possible Hexose Sensing in the Secretory Pathway. Plant Cell 8:793-803.

Hiatt, A.J. 1967. Relationship of Cell Sap Ph to Organic Acid Change During Ion Uptake. Plant Physiology 42:294-298.

Hirst, E.L., S. Ramstad. 1957. Changes in Organic Acid Content of Perennial Rye-Grass During Conservation. Journal of the Science of Food and Agriculture 8:727-732.

Hoagland, D.R., J.C. Martin. 1933. Absorption of Potassium by Plants in Relation to Replaceable, Non-Replaceable, and Soil Solution Potassium. Soil Science 36:1-33.

Hofgaard, I.S., L.A. Wanner, G. Hageskal, B. Henriksen, S.S. Klemsdal, A.M. Tronsmo. 2006. Isolates of Microdochium Nivale and M-Majus Differentiated by Pathogenicity on Perennial Ryegrass (Lolium Perenne L.) and in Vitro Growth at Low Temperature. Journal of Phytopathology 154:267-274.

Hon, W.C., M. Griffith, P.L. Chong, D.S.C. Yang. 1994. Extraction and Isolation of Antifreeze Proteins from Winter Rye (Secale-Cereale L) Leaves. Plant Physiology 104:971-980.

Horneck, D.A., R.O. Miller. 1998. Determination of Total Nitrogen in Plant Tissue. pp. 75-85. *In* Y. P. Kalra (Ed.), Handbook of Reference Methods for Plant Analysis. CRC Press, Boca Raton, FL.

Horst, G.L., M.C. Engelke, W. Meyers. 1984. Assessment of Visual Evaluation Techniques. Agronomy Journal 76:619-622.

Housley, T.L., C.J. Pollock. 1985. Photosynthesis and Carbohydrate-Metabolism in Detached Leaves of Lolium-Temulentum L. New Phytologist 99:499-507.

Housley, T.L., C.S.T. Daughtry. 1987. Fructan Content and Fructosyltransferase Activity During Wheat Seed Growth. Plant Physiology 83:4-7.

Hsiang, T., C.R. Wu. 2000. Genetic Relationships of Pathogenic Typhula Species Assessed by Rapd, Its-Rflp and Its Sequencing. Mycological Research 104:16-22.

Hsiang, T., N. Matsumoto, S.M. Millett. 1999. Biology and Management of Typhula Snow Molds of Turfgrass. Plant Disease 83:788-798.

Hull, R. 1992. Energy Relations and Carbohydrate Partitioning in Turfgrass. pp. 175-205. *In* D. V. Waddington, et al. (Eds.), Turfgrass Agronomy Monograph. ASA, CSSA, SSSA, Madison, WI.

Hwang, S.F., D.A. Gaudet, G.D. Turnbull, K.F. Chang, R.J. Howard, H. Najda. 2002. Effect of Plant Age and Cottony Snow Mold on Winter Survival of Forage Grasses. Canadian Journal of Plant Science 82:701-708.

Jacobson, L., L. Ordin. 1954. Organic Acid Metabolism and Ion Absorption in Roots. Plant Physiology 29:70-75.

Janssen, G., R.P. Bartholomew. 1930. The Influence of Potash Concentration in the Culture Medium on the Production of Carbohydrates in Plants. Journal of Agricultural Research 40:243-261.

Jeger, M.J., S.L.H. Viljanen-Rollinson. 2001. The Use of the Area under the Disease-Progress Curve (Audpc) to Assess Quantitative Disease Resistance in Crop Cultivars. TAG Theoretical and Applied Genetics 102:32-40.

Jones, J.B. 1980. Turf Analysis. Golf Course Management 48:29-32.

Kaminski, J.E., P.H. Dernoeden, C.A. Bigelow. 2004. Soil Amendments and Fertilizer Source Effects on Creeping Bentgrass Establishment, Soil Microbial Activity, Thatch, and Disease. Hortscience 39:620-626.

Karcher, D.E., M.D. Richardson. 2003. Quantifying Turfgrass Color Using Digital Image Analysis. Crop Science 43:943-951.

Karcher, D.E., M.D. Richardson. 2005. Batch Analysis of Digital Images to Evaluate Turfgrass Characteristics. Crop Science 45:1536-1539.

Kirkby, E.A., A.H. Knight. 1977. Influence of Level of Nitrate Nutrition on Ion Uptake and Assimilation, Organic-Acid Accumulation, and Cation-Anion Balance in Whole Tomato Plants. Plant Physiology 60:349-353.

Kiyomoto, R.K. 1987. Carbon-Dioxide Exchange and Total Nonstructural Carbohydrate in Soft White Winter-Wheat Cultivars and Snow Mold Resistant Introductions. Crop Science 27:746-752.

Kiyomoto, R.K., G.W. Bruehl. 1977. Carbohydrate Accumulation and Depletion by Winter Cereals Differing in Resistance to Typhula-Idahoensis. Phytopathology 67:206-211.

Klaubauf, S., E. Inselsbacher, S. Zechmeister-Boltenstern, W. Wanek, R. Gottsberger, J. Strauss, M. Gorfer. 2010. Molecular Diversity of Fungal Communities in Agricultural Soils from Lower Austria. Fungal Diversity 44:65-75.

Klee, C.B., T.C. Vanaman. 1982. Calmodulin. Advances in Protein Chemistry 35:213-321.

Koster, K.L., D.V. Lynch. 1992. Solute Accumulation and Compartmentation During the Cold-Acclimation of Puma Rye. Plant Physiology 98:108-113.

Lambers, H., A. van der Werf, H. Konings. 1991. Respiratory Patterns in Roots in Relation to Their Functioning. pp. 229-263. *In* Y. Waisel, et al. (Eds.), Plant Roots, the Hidden Half. Marcel Dekker, New York, New York.

Larsen, K.S., P. Grogan, S. Jonasson, A. Michelsen. 2007. Respiration and Microbial Dynamics in Two Subarctic Ecosystems During Winter and Spring Thaw: Effects of Increased Snow Depth. Arctic, Antarctic, and Alpine Research 39:268-276.

Lawton, M.B., L.I. Burpee. 1990. Seed Treatments for Typhula Blight and Pink Snow Mold of Winter-Wheat and Relationships among Disease Intensity, Crop Recovery, and Yield. Canadian Journal of Plant Pathology-Revue Canadienne De Phytopathologie 12:63-74.

Leigh, R.A., A.E. Johnston. 1983a. The Effects of Fertilizers and Drought on the Concentrations of Potassium in the Dry-Matter and Tissue Water of Field-Grown Spring Barley. Journal of Agricultural Science 101:741-748.

Leigh, R.A., A.E. Johnston. 1983b. Concentrations of Potassium in the Dry-Matter and Tissue Water of Field-Grown Spring Barley and Their Relationships to Grain-Yield. Journal of Agricultural Science 101:675-685.

Leigh, R.A., R.G.W. Jones. 1984. A Hypothesis Relating Critical Potassium Concentrations for Growth to the Distribution and Functions of This Ion in the Plant-Cell. New Phytologist 97:1-13.

Leon, J., E. Rojo, J.J. Sanchez-Serrano. 2001. Wound Signalling in Plants. Journal of Experimental Botany 52:1-9.

Leon, J., E. Rojo, E. Titarenko, J.J. Sanchez-Serrano. 1998. Jasmonic Acid-Dependent and -Independent Wound Signal Transduction Pathways Are Differentially Regulated by Ca2+/Calmodulin in Arabidopsis Thaliana. Molecular and General Genetics 258:412-419.

Levitt, J. 1980. Response of Plants to Environmental Stress. 2nd ed. Academic Press, New York, New York.

Lisec, J., N. Schauer, J. Kopka, L. Willmitzer, A.R. Fernie. 2006. Gas Chromatography Mass Spectrometry-Based Metabolite Profiling in Plants. Nat. Protocols 1:387-396.

Liu, X.Z., B.R. Huang. 2000. Carbohydrate Accumulation in Relation to Heat Stress Tolerance in Two Creeping Bentgrass Cultivars. Journal of the American Society for Horticultural Science 125:442-447.

Marschner, H. 1995. Mineral Nutrition of Higher Plants. 2nd ed. Academic Press, San Diego, CA.

Martinoia, E., U.I. Flugge, G. Kaiser, U. Heber, H.W. Heldt. 1985. Energy-Dependent Uptake of Malate into Vacuoles Isolated from Barley Mesophyll Protoplasts. Biochimica Et Biophysica Acta 806:311-319.

Max Planck Institute of Molecular Plant Physiology. 2010. The Golm Metabolome Database. http://gmd.mpimp-golm.mpg.de/ (verified December 16, 2010). Max Planck Institute of Molecular Plant Physiology, Golm, Germany.

McDonald, P., A.R. Henderson. 1962. Buffering Capacity of Herbage Samples as a Factor in Ensilage. Journal of the Science of Food and Agriculture 13:395-400.

McIntosh, M.S. 1983. Analysis of Combined Experiments. Agronomy Journal 75:153-155.

Mengel, K. 1980. Potassium in Crop Production. Advances in Agronomy 33:59-110.

Mengel, K., H.E. Haeder. 1977. Effect of Potassium Supply on Rate of Phloem Sap Exudation and Composition of Phloem Sap of Ricinus-Communis. Plant Physiology 59:282-284.

Mengel, K., D. Steffens. 1985. Potassium Uptake of Rye-Grass (*Lolium-Perenne*) and Red-Clover (*Trifolium-Pratense*) as Related to Root Parameters. Biology and Fertility of Soils 1:53-58.

Monson, R.K., D.L. Lipson, S.P. Burns, A.A. Turnipseed, A.C. Delany, M.W. Williams, S.K. Schmidt. 2006. Winter Forest Soil Respiration Controlled by Climate and Microbial Community Composition. Nature 439:711-714.

Nagaraj, V.J., D. Altenbach, V. Galati, M. Luscher, A.D. Meyer, T. Boller, A. Wiemken. 2004. Distinct Regulation of Sucrose: Sucrose-1-Fructosyltransferase (1-Sst) and Sucrose: Fructan-6-Fructosyltransferase (6-Sft), the Key Enzymes of Fructan Synthesis in Barley Leaves: 1-Sst as the Pacemaker. New Phytologist 161:735-748.

Nair, K.P.P. 1996. The Buffering Power of Plant Nutrients and Effects on Availability. Advances in Agronomy 57:237-287.

Nakajima, T., J. Abe. 1990. A Method for Assessing Resistance to the Snow Molds Typhula-Incarnata and Microdochium-Nivale in Winter-Wheat Incubated at the Optimum Growth Temperature Ranges of the Fungi. Canadian Journal of Botany-Revue Canadienne De Botanique 68:343-346.

Nakajima, T., J. Abe. 1996. Environmental Factors Affecting Expression of Resistance to Pink Snow Mold Caused by Microdochium Nivale in Winter Wheat. Canadian Journal of Botany-Revue Canadienne De Botanique 74:1783-1788.

National Center for Biotechnology Information. 1999. Accession Af134709. http://www.ncbi.nlm.nih.gov/nucleotide/4894807?report=genbank&log$=nucltop&blast_rank=1&RID=G1X84WRR015 (verified 12/9/10). National Center for Biotechnology Information, Bethesda, MD.

National Center for Biotechnology Information. 2006. Accession Ef 187912. http://www.ncbi.nlm.nih.gov/nucleotide/122892467?report=genbank&log$=nucltop&blast_rank=1&RID=G1YM4XBT015 (verified 12/9/10). National Center for Biotechnology Information, Bethesda, MD.

National Center for Biotechnology Information. 2009. Accession Gu055586. http://www.ncbi.nlm.nih.gov/nucleotide/261871832?report=genbank&log$=nucltop&blast_rank=2&RID=G1YM4XBT015 (verified 12/9/10). National Center for Biotechnology Information, Bethesda, MD.

Newton, R., J.A. Anderson. 1931. Respiration of Winter Wheat Plants at Low Temperatures. Can J. Res. 5:337-354.

Nicholson, P., A.K. Lees, N. Maurin, D.W. Parry, H.N. Rezanoor. 1996. Development of a Pcr Assay to Identify and Quantify Microdochium Nivale Var Nivale and Microdochium Nivale Var Majus in Wheat. Physiological and Molecular Plant Pathology 48:257-271.

Nie, Z., G.F. Tremblay, G. Bélanger, R. Berthiaume, Y. Castonguay, A. Bertrand, R. Michaud, G. Allard, J. Han. 2009. Near-Infrared Reflectance Spectroscopy Prediction of Neutral Detergent-Soluble Carbohydrates in Timothy and Alfalfa. Journal of Dairy Science 92:1702-1711.

Nowakowski, T.Z., J. Bolton, M. Byers. 1974. Effect of Replacing Potassium by Sodium on Growth and on Inorganic and Organic Composition of Italian Ryegrass. Journal of the Science of Food and Agriculture 25:271-283.

Obenland, D.M., U. Simmen, T. Boller, A. Wiemken. 1991. Regulation of Sucrose-Sucrose-Fructosyltransferase in Barley Leaves. Plant Physiology 97:811-813.

Olien, C.R., J.L. Clark. 1993. Changes in Soluble Carbohydrate-Composition of Barley, Wheat, and Rye During Winter. Agronomy Journal 85:21-29.

Oshiman, K.-I., I. Kobayashi, H. Shigemitsu, H. Kunoh. 1995. Studies on Turfgrass Snow Mold Caused by *Typhula Ishikariensis*. Ii. Microscopical Observation of Infected Bentgrass Leaves. Mycoscience 36:179-185.

Patton, A.J., Z.J. Reicher. 2007. Zoysiagrass Species and Genotypes Differ in Their Winter Injury and Freeze Tolerance. Crop Science 47:1619-1627.

Patton, A.J., S.M. Cunningham, J.J. Volenec, Z.J. Peicher. 2007. Differences in Freeze Tolerance of Zoysiagrasses: Ii. Carbohydrate and Proline Accumulation. Crop Science 47:2170-2181.

Pavis, N., J. Boucaud, M.P. Prud'homme. 2001. Fructans and Fructan-Metabolizing Enzymes in Leaves of Lolium Perenne. New Phytologist 150:97-109.

Pelletier, S., G. Belanger, G.F. Tremblay, P. Virkajarvi, G. Allard. 2008a. Timothy Mineral Concentration and Derived Indices Related to Cattle Metabolic Disorders: A Review. Canadian Journal of Plant Science 88:1043-1055.

Pelletier, S., R.J. Simpson, R.A. Culvenor, G. Belanger, G.F. Tremblay, G. Allard, J. Braschkat, P.J. Randall. 2008b. Dietary Cation-Anion Differences in Some Pasture Species, Changes During the Season and Effects of Soil Acidity and Lime Amendment. Australian Journal of Experimental Agriculture 48:1143-1153.

Pitman, M.G. 1975. Whole Plants. pp. 267-308. *In* D. A. Baker and J. L. Hall (Eds.), Ion Transport in Plant Cells and Tissues. North Holland Publishing Company, Amsterdam.

Pitman, M.G., A.C. Courtice, B. Lee. 1968. Comparison of Potassium and Sodium Uptake by Barley Roots at High and Low Salt Status. Australian Journal of Biological Sciences 21:871-881.

Playne, M.J., P. McDonald. 1966. Buffering Constituents of Herbage and of Silage. Journal of the Science of Food and Agriculture 17:264-&.

Playne, M.J., A.C. Stirling, P. McDonald. 1967. Changes in Organic Acid Composition During Incubation of Aseptically-Grown Grass. Journal of the Science of Food and Agriculture 18:19-&.

Pociecha, E., A. Plazek, F. Janowiak, A. Janeczko, Z. Zwierzykowski. 2008. Physiological Basis for Differences in Resistance to Microdochium Nivale (Fr.) Samuels and Hallett in Two Androgenic Genotypes of Festulolium Derived from Tetraploid F1 Hybrids of Festuca Pratensis X Lolium Multiflorum (Festulolium). Journal of Phytopathology 156:155-163.

Pociecha, E., A. Plazek, M. Rapacz, E. Niemczyk, Z. Zwierzykowski. 2010. Photosynthetic Activity and Soluble Carbohydrate Content Induced by the Cold Acclimation Affect Frost Tolerance and Resistance to Microdochium Nivale of Androgenic Festulolium Genotypes. Journal of Agronomy and Crop Science 196:48-54.

Pollock, C.J. 1984. Sucrose Accumulation and the Initiation of Fructan Biosynthesis in *Lolium-Temulentum* L. New Phytologist 96:527-534.

Pollock, C.J., N.J. Chatterton. 1988. Fructans. pp. 109-140. *In* J. Priess (Ed.), The Biochemistry of Plants. Academic Press, San Diego, CA.

Pollock, C.J., A.J. Cairns. 1991. Fructan Metabolism in Grasses and Cereals. Annual Review of Plant Physiology and Plant Molecular Biology 42:77-101.

Pontis, H.G., E. del Campillo. 1985. Fructans. *In* P. M. Dey and R. A. Dixon (Eds.), Biochemistry of Storage Carbohydrates in Green Plants. Academic Press, London.

Pratt, P.F. 1965. Potassium. pp. 1022-1030. *In* C. A. Black (Ed.), Methods of Soil Analysis. ASA, ASTM, Madison, WI.

Preusser, E., F.A. Khalil, H. Goring. 1981. Regulation of Activity of the Granule-Bound Starch Synthetase by Mono-Valent Cations. Biochemie Und Physiologie Der Pflanzen 176:744-752.

Ranwala, A.P., W.B. Miller. 2008. Analysis of Nonstructural Carbohydrates in Storage Organs of 30 Ornamental Geophytes by High-Performance Anion-Exchange Chromatography with Pulsed Amperometric Detection. New Phytologist 180:421-433.

Reggiani, R., N. Aurisano, M. Mattana, A. Bertani. 1993. Influence of K+ Ions on Polyamine Level in Wheat Seedlings. Journal of Plant Physiology 141:136-140.

Reicher, Z.J., C.S. Throssell. 1997. Effect of Repeated Fungicide Applications on Creeping Bentgrass Turf. Crop Science 37:910-915.

Remsberg, R. 1940. Studies in the Genus Typhula. Mycologia 32:52-96.

Rentsch, D., E. Martinoia. 1991. Citrate Transport into Barley Mesophyll Vacuoles - Comparison with Malate-Uptake Activity. Planta 184:532-537.

Rich, C.I. 1968. Minerology of Soil Potassium. pp. 79-108. *In* V. J. Kilmer (Ed.), Role of Potassium in Agriculture. ASA, CSSA, SSSA, Madison, WI.

Richardson, M.D., D.E. Karcher, L.C. Purcell. 2001. Quantifying Turfgrass Cover Using Digital Image Analysis. Crop Science 41:1884-1888.

Roitsch, T., M.E. Balibrea, M. Hofmann, R. Proels, A.K. Sinha. 2003. Extracellular Invertase: Key Metabolic Enzyme and Pr Protein. Journal of Experimental Botany 54:513-524.

Ryan, C.A., E.E. Farmer. 1991. Oligosaccharide Signals in Plants - a Current Assessment. Annual Review of Plant Physiology and Plant Molecular Biology 42:651-674.

Sanada, Y., K. Tamura, T. Yamada. 2010. Relationship between Water-Soluble Carbohydrates in Fall and Spring and Vigor of Spring Regrowth in Orchardgrass. Crop Science 50:380-390.

Schmidt, S., K. Wilson, A. Meyer, M. Gebauer, A. King. 2008. Phylogeny and Ecophysiology of Opportunistic “Snow Molds” from a Subalpine Forest Ecosystem. Microbial Ecology 56:681-687.

Schmidt, S.K., K.L. Wilson, R.K. Monson, D.A. Lipson. 2009. Exponential Growth Of "Snow Molds" At Sub-Zero Temperatures: An Explanation for High beneath-Snow Respiration Rates and Q (10) Values. Biogeochemistry 95:13-21.

Seling, S., A.H. Wissemeier, P. Cambier, P. Van Cutsem. 2000. Calcium Deficiency in Potato (Solanum Tuberosum Ssp. Tuberosum) Leaves and Its Effects on the Pectic Composition of the Apoplastic Fluid. Physiologia Plantarum 109:44-50.

Shaner, G., R.E. Finney. 1977. Effect of Nitrogen-Fertilization on Expression of Slow-Mildewing Resistance in Knox Wheat. Phytopathology 67:1051-1056.

Shearman, R.C., J.B. Beard. 2002. Potassium Nutrition Effects on *Agrostis Stolonifera* Wear Stress Tolerance. pp. 667-675. *In* E. Thain (Ed.), Science and Golf Iv. Routledge, London.

Smeekens, S., F. Rook. 1997. Sugar Sensing and Sugar-Mediated Signal Transduction in Plants. Plant Physiology 115:7-13.

Smiley, R.W., P.H. Dernoeden, B.B. Clarke. 2007. Compendium of Turfgrass Diseases. 3rd ed. APS Press, St. Paul, MN.

Smith, D. 1967. Carbohydrates in Grasses 2. Sugar and Fructosan Composition of Stem Bases of Bromegrass and Timothy at Several Growth Stages and in Different Plant Parts at Anthesis. Crop Science 7:62-67.

Smith, D. 1972. Carbohydrate Reserves of Grasses. pp. 318-333. *In* C. M. McKell (Ed.), The Biology and Utilization of Grasses. Academic Press, New York, NY.

Smith, D., R.D. Grotelueschen. 1966. Carbohydrates in Grasses 1. Sugar and Fructosan Composition of Stem Bases of Several Northern-Adapted Grasses at Seed Maturity. Crop Science 6:263-266.

Sparks, D.L. 1987. Potassium Dynamics in Soils. Advances in Soil Science 6:1-63.

Sun, J.Y., D.A. Gaudet, Z.X. Lu, M. Frick, B. Puchalski, A. Laroche. 2008. Characterization and Antifungal Properties of Wheat Nonspecific Lipid Transfer Proteins. Molecular Plant-Microbe Interactions 21:346-360.

Sung, S., R.M. Amasino. 2005. Remembering Winter: Toward a Molecular Understanding of Vernalization. Annual Review of Plant Biology 56:491-508.

Takenaka, S., R. Yoshino. 1989. Development of Suitable Technique for Testing Resistance of Wheat Cultivars to 3 Snow Mold Diseases. Jarq-Japan Agricultural Research Quarterly 22:284-289.

Tompkins, D.K., J.B. Ross, D.L. Moroz. 2000. Dehardening of Annual Bluegrass and Creeping Bentgrass During Late Winter and Early Spring. Agronomy Journal 92:5-9.

Tronsmo, A.M. 1986. Host Water Potentials May Restrict Development of Snow Mold Fungi in Low Temperature-Hardened Grasses. Physiologia Plantarum 68:175-179.

Turner, T.R., N.W. Hummel. 1992. Nutritional Requirements and Fertilization. pp. 385-439. *In* D. V. Waddington, et al. (Eds.), Turfgrass Agronomy Monograph. ASA, CSSA, SSSA, Madison, WI.

Tyler, N.J., L.V. Gusta, D.B. Fowler. 1981. The Influence of Nitrogen, Phosphorus and Potassium on the Cold-Acclimation of Winter-Wheat (Triticum-Aestivum L). Canadian Journal of Plant Science 61:879-885.

Ulrich, A. 1941. Metabolism of Non-Volatile Organic Acids in Excised Barley Roots as Related to Cation-Anion Balance During Salt Accumulation. American Journal of Botany 28:526-537.

Ulrich, A., F.J. Hills. 1967. Principles and Practices of Plant Analysis. *In* G. W. Hardy (Ed.), Soil Testing and Plant Analysis. ASA, CSSA, SSSA, Madison, WI.

USDA - Economic Research Service. 2010. Fertilizer Use and Price. http://www.ers.usda.gov/Data/FertilizerUse/ (verified December 1, 2010). USDA - Economic Research Service, Washington, D.C.

USDA - Economic Research Service. 2011. Commodity Costs and Returns: Data. http://www.ers.usda.gov/Data/CostsAndReturns/TestPick.htm (verified March 15, 2011). USDA - Economic Research Service, Washington, D.C.

Waddington, D.V., T.L. Zimmerman. 1972. Growth and Chemical Composition of Eight Grasses Grown under High Water Table Conditions. Commun. Soil Sci. Plant Anal. 3:329-337.

Waddington, D.V., E.L. Moberg, J.M. Duich. 1972. Effect of Nitrogen Source, Potassium Source, and Potassium Rate on Soil Nutrient Levels and Growth and Elemental Composition of Penncross Creeping Bentgrass, *Agrostis-Palustris* Huds. Agronomy Journal 64:562-566.

Wade, L.G. 1999. Organic Chemistry. 4th ed. Prentice Hall, Upper Saddle River, NJ.

Waggoner, P.E., C.L. Campbell, L.V. Madden. 1986. Disease Progress Curves. pp. 3-55. *In* K. J. Leonard and W. E. Fry (Eds.), Plant Disease Epidemiology. Macmillan Publishing Company, New York, New York.

Wagner, W., A. Wiemken. 1987. Enzymology of Fructan Synthesis in Grasses - Properties of Sucrose-Sucrose-Fructosyltransferase in Barley Leaves (Hordeum-Vulgare-L Cv Gerbel). Plant Physiology 85:706-710.

Wagner, W., A. Wiemken, P. Matile. 1986. Regulation of Fructan Metabolism in Leaves of Barley (*Hordeum Vulgare* L. Cv Gerbel). Plant Physiology 81:444-447.

Wang, H.C., F.F. Ma, L.L. Cheng. 2010. Metabolism of Organic Acids, Nitrogen and Amino Acids in Chlorotic Leaves of 'Honeycrisp' Apple (Malus Domestica Borkh) with Excessive Accumulation of Carbohydrates. Planta 232:511-522.

Wang, Z., M.D. Casler, J.C. Stier, J.S. Gregos, S.M. Millett. 2005. Genotypic Variation for Snow Mold Reaction among Creeping Bentgrass Clones. Crop Science 45:399-406.

Wanner, L.A., O. Junttila. 1999. Cold-Induced Freezing Tolerance in Arabidopsis. Plant Physiology 120:391-399.

Webster, D.E., J.S. Ebdon. 2005. Effects of Nitrogen and Potassium Fertilization on Perennial Ryegrass Cold Tolerance During Deacclimation in Late Winter and Early Spring. Hortscience 40:842-849.

Wehr, J.B., N.W. Menzies, F.P.C. Blamey. 2004. Inhibition of Cell-Wall Autolysis and Pectin Degradation by Cations. Plant Physiology and Biochemistry 42:485-492.

White, T.J., T. Bruns, S. Lee, J.W. Taylor. 1990. Amplification and Direct Sequencing of Fungal Ribosomal Rna Genes for Phylogenetics. pp. 315-322. *In* M. A. Innis, et al. (Eds.), P C R Protocols: A Guide to Methods and Applications. Academic Press, New York, New York.

Wildes, R.A., M.G. Pitman. 1975. Pyruvate-Kinase Activity in Roots of Barley Seedlings in Relation to Salt Status. Zeitschrift Fur Pflanzenphysiologie 76:69-75.

Winter, H., D.G. Robinson, H.W. Heldt. 1994. Subcellular Volumes and Metabolite Concentrations in Spinach Leaves. Planta 193:530-535.

Woodhouse, P.J., A. Wild, C.R. Clement. 1978. Rate of Uptake of Potassium by 3 Crop Species in Relation to Growth. Journal of Experimental Botany 29:885-894.

Woods, M.S. 2006. Nonacid Cation Bioavailability in Sand Rootzones. Ph.D. Diss. Cornell University, Ithaca, NY.

Woods, M.S., Q.M. Ketterings, F.S. Rossi. 2005. Effectiveness of Standard Soil Tests for Assessing Potassium Availability in Sand Rootzones. Soil Science 170:110-119.

Woods, M.S., Q.M. Ketterings, F.S. Rossi, A.M. Petrovic. 2006. Potassium Availability Indices and Turfgrass Performance in a Calcareous Sand Putting Green. Crop Science 46:381-389.

Wu, C., T. Hsiang. 1999. Mycelial Growth, Sclerotial Production and Carbon Utilization of Three Typhula Species. Canadian Journal of Botany-Revue Canadienne De Botanique 77:312-317.

Wyn Jones, R.G., A. Pollard. 1983. Proteins, Enzymes, and Inorganic Ions. pp. 528-562. *In* A. Läuchli and R. L. Bieleski (Eds.), Encyclopedia of Plant Physiology. Springer-Verlag, Berlin.

Wyn Jones, R.G., C.J. Brady, J. Speirs. 1979. Ionic and Osmotic Relations in Plant Cells. pp. 63-103. *In* D. L. Laidman and R. G. Wyn Jones (Eds.), Recent Advances in the Biochemistry of Cereals. Academic Press, London.

Yoshida, M., J. Abe, M. Moriyama, T. Kuwabara. 1998. Carbohydrate Levels among Winter Wheat Cultivars Varying in Freezing Tolerance and Snow Mold Resistance During Autumn and Winter. Physiologia Plantarum 103:8-16.

Young, J. 2010. Madison Climate Data. http://www.aos.wisc.edu/~sco/clim-history/7cities/madison.html#Snow (verified February 7, 2011). Young, J., Madison, WI.

Yukawa, T., Y. Watanabe, S. Yamamoto. 1994. Studies on Fructan Accumulation in Wheat (Triticum-Aestivum L) 2. Changes in Degree of Polymerization of Fructan under Treatment at 1-Degrees-C in Dark. Japanese Journal of Crop Science 63:430-435.

Zhao, D., C.T. MacKown, P.J. Starks, B.K. Kindiger. 2010. Rapid Analysis of Nonstructural Carbohydrate Components in Grass Forage Using Microplate Enzymatic Assays. Crop Science 50:1537-1545.